REGULATORY ROLE OF APOE AND APOER2 IN

SYNAPTIC ACTIVITY:

A NEW INSIGHT INTO ALZHEIMER'S DISEASE

APPROVED BY SUPERVISORY COMMITTEE

Joachim Herz, M.D.

Lisa M. Monteggia, Ph.D.

Philip W. Shaul, M.D.

Ilya Bezprozvanny, Ph.D.

Mark J. Henkemeyer, Ph.D.

DEDICATION

This thesis is dedicated to my parents and my husband, who have supported me with their unconditional love.

REGULATORY ROLE OF APOE AND APOER2 IN SYNAPTIC ACTIVITY: A NEW INSIGHT INTO ALZHEIMER'S DISEASE

by

YING CHEN

DISSERTATION

Presented to the Faculty of the Graduate School of Biomedical Sciences

The University of Texas Southwestern Medical Center at Dallas

In Partial Fulfillment of the Requirements

For the Degree of

DOCTOR OF PHILOSOPHY

The University of Texas Southwestern Medical Center at Dallas

Dallas, Texas

June, 2008

ACKNOWLEDGMENTS

Firstly, I would like to gratefully acknowledge my mentor, Dr. Joachim Herz, for giving me this exciting project to work on for my graduate study. He has provided enthusiastic supervision and helpful instructions not only on experimental strategies and methods, but also on skills to develop research project as an independent scientist. I thank him for his consistent encouragement and assistance throughout my graduate study.

I am grateful to my supervisory committee, Dr. Lisa Monteggia, Dr. Philip Shaul, Dr. Ilya Bezprozvanny, and Dr. Mark Henkemyer, for their sincere support and scientific advices.

I thank members of the Herz lab, past and present, for the technical supports and for providing a stimulating and fun environment to work in, especially Dr. Peggy Stolt-Bergner, Dr. Uwe Beffert, Wenling Niu, Huichuan Reyna, Dr. Li Zhou, Irene Bowen, and Priscilla Rodriguez.

I thank everyone in the Department of Molecular Genetics and elsewhere on campus who has helped me with reagents, equipments, techniques or advices, especially Lisa Beatty, Angela Carroll, Dr. Tiina Kotti, Dr. Tie-Shan Tang, Dr. Ilya Bezprozvanny, Dr. Ege Kavalali, Dr. Kim Huber, and Dr. Kate Luby-Phelps. I also thank the staffs of Integrative Biology Graduate Program, especially Dr. Yi Liu and Priyarama Sen, for their excellent administrative work and assistance.

Finally, I am forever indebted to my family. I am deeply grateful to my parents for raising me, educating me important values in life and giving me endless love and support when it was most needed. I thank my father who has always put education as a first priority in my life and encouraged me to set high goals for myself. Last but not least, I wish to extend the special thanks to my beloved husband, Chiyuan Chen. His constant support, assistance and companionship have turned my graduate school journey pleasant and productive. For all his endeavor, and for all the love from my parents, I dedicate this thesis to them.

REGULATORY ROLE OF APOE AND APOER2 IN SYNAPTIC ACTIVITY: A NEW INSIGHT INTO ALZHEIMER'S DISEASE

Ying Chen, Ph.D.

The University of Texas Southwestern Medical Center at Dallas, 2008

Supervising Professor: Joachim Herz, M.D.

Apolipoprotein E (ApoE) genotype is the major genetic modifier of late-onset Alzheimer's disease (AD), the most common neurodegenerative disease in the elderly. By unknown mechanisms, ApoE4 isoform is strongly associated with a substantially earlier age of onset of AD. A synaptic ApoE receptor, Apoer2, activates Dab1 and Src family tyrosine kinases (SFKs) upon binding to the extracellular ligand Reelin.

Here, we show that this Reelin-Apoer2-Dab1-SFKs signaling complex greatly enhances the tyrosine phosphorylation as well as the calcium conductance of NMDA receptor, a calcium-permeable postsynaptic glutamate receptor that is critical for synaptic plasticity. The simultaneous interaction of Apoer2 with both Dab1 and postsynaptic scaffolding protein PSD-95 is required for Apoer2 to activate NMDA receptor in response to Reelin. Through this NMDAR-dependent mechanism, Reelin also stimulates the phosphorylation of CREB, a transcription factor that is necessary for neuronal survival and synaptic plasticity. In addition, Reelin can potently counteract the surpression of surface NMDA receptor expression induced by Aβ peptide, the accepted causative factor in the pathogenic process of AD. These results indicate that Apoer2-mediated signaling, by counteracting depressive effect on synapses, is critical for proper function of synaptic network. Last, we show that ApoE4 impairs the trafficking and reduces the surface expression of Apoer2. Consequently, ApoE4 critically diminishes the ability of Reelin to enhance NMDA receptor activity or CREB phosphorylation in primary neurons. As a result, the ability of Reelin to enhance long-term potentiation (LTP), a form of synaptic plasticity involved in learning and memory formation, is significantly impaired in the hippocampus of mice expressing the human ApoE4 isoform.

Taken together, in this thesis, we identified a novel synaptic function of Apoer2, which is to enhance NMDA receptor activity, and thereby to enhance

synaptic plasticity and maintain the integrity of synaptic network. ApoE4 impairs the function of synapses by suppressing the synaptic function of Apoer2. These findings suggest a novel rational mechanism by which ApoE4 may accelerate the destabilization of synaptic network, neuronal degeneration, and eventually the progression of AD.

TABLE OF CONTENTS

Title Fly ..... **i**

Dedication ..... **ii**

Title Page ..... **iii**

Copyright ..... **iv**

Acknowledgements ..... **v**

Abstract ..... **vii**

Table of Contents ..... **x**

Prior Publications ..... **xiii**

List of Figures ..... **xiv**

List of Tables ..... **xvi**

List of Abbreviations ..... **xvii**

CHAPTER ONE: Introduction……..... **1**

Synaptic transmission and plasticity……1

NMDA receptor and postsynaptic signaling.....3

The LDLR gene family.....8

Reelin signaling mediated by lipoprotein receptors.....10

Alzheimer's disease and apolipoprotein E.....14

CHAPTER TWO: Studying the Functional Role of PI Binding by Dab1.....19

Abstract……..……19

Introduction.....19

Results and Discussion 23

Materials and Methods.....26

CHAPTER THREE: Reelin Signaling Modulates NMDA Receptor Activity in Primary Neurons…….…....31

Abstract……..31

Introduction.....32

Results and Discussion 33

Materials and Methods.....53

CHAPTER FOUR: Role of the Intracellular Domain of Apoer2 in NMDA Receptor Regulation…….….61

Abstract……..61

Introduction.....62

Results and Discussion 65

Materials and Methods.....75

CHAPTER FIVE: Opposing Effects of Reelin and β-Amyloid on NMDA Receptor Phosphorylation and Trafficking……..77

Abstract……..77

Introduction.....78

Results and Discussion 80

Materials and Methods.....87

CHAPTER SIX: ApoE4 Selectively Impairs ApoE Receptor-Mediated Modulation of NMDA Receptor Function and Synaptic Plasticity……..89

Abstract……89

Introduction.....90

Results and Discussion 92

Materials and Methods.....106

CHAPTER SEVEN: Discussion.....111

Bibliography……...…….....135

PRIOR PUBLICATIONS

Ying Chen, Murat Durakoglugil, Patrick M. Sullivan, Nobuyo Maeda, and Joachim Herz. ApoE4 selectively impairs ApoE receptor modulation of NMDA receptor function and synaptic plasticity. 2008 Submitted.

Murat Durakoglugil, **Ying Chen**, Ege T. Kavalali, and Joachim Herz. Signal amplification by ApoE receptors reverses β-amyloid induced synaptic depression. 2008 Submitted.

Joachim Herz, and **Ying Chen.** Reelin, lipoprotein receptors and synaptic plasticity. *Nature Review Neuroscience*. (2006) 11, 850-859

Ying Chen, Uwe Beffert, Mert Ertunc, Tie-Shan Tang, Ege T. Kavalali, Ilya Bezprozvanny, and Joachim Herz. Reelin modulates NMDA receptor activity in cortical neurons. *The Journal of Neuroscience*. (2005) 25(36), 8209-8216

Peggy C. Stolt, **Ying Chen**, Pingsheng Liu, Hans H. Bock, Stephen C. Blacklow, and Joachim Herz. Phosphoinositide binding by the disabled-1 PTB domain is necessary for membrane localization and Reelin signal transduction. *The Journal of Biological Chemistry*. (2005) 280(10), 9671-9677

LIST OF FIGURES

Figure 1.1 Illustration of an excitatory glutamatergic synapse and postsynaptic signaling. 6
Figure 1.2 Schematic representation of the mammalian LDLR family members. ..9
Figure 1.3 Reelin-initiated signaling events in neurons..... 13
Figure 2.1 The Dab1 mutants..... 22
Figure 2.2 Fractionation of primary neurons expressing Dab1 mutants..... 25
Figure 2.3 Tyrosine phosphorylation of Dab1 mutants upon Reelin stimulation..26
Figure 3.1 Representative images of Reelin-induced enhancement of Ca^{2+} influx in cortical neurons. 43
Figure 3.2 Reelin enhances glutamate stimulated Ca^{2+} influx through NMDA receptor in wild type cortical neurons..... 44
Figure 3.3 RAP, a ligand for LDLR family members, blocks Reelin-mediated enhancement of glutamate stimulated Ca^{2+} influx. 45
Figure 3.4 Dab1 is required for Reelin-induced enhancement of Ca^{2+} influx. 46
Figure 3.5 Src family tyrosine kinases are required for Reelin-induced enhancement of Ca^{2+} influx. 47
Figure 3.6 Reelin-Dab1 signal increases the tyrosine phosphorylation of NR2B. 48
Figure 3.7 Reelin potentiates synaptically evoked NMDA currents 49
Figure 3.8 Reelin increases glutamate-induced CREB Ser^{133} phosphorylation. ...51
Figure 3.9 Model of Reelin-induced modulation of NMDA receptor function.....52
Figure 4.1 Schematic illustration of the four receptor mutants. 64
Figure 4.2 Apoer2, but not Vldlr, is required for Reelin-induced enhancement of Ca^{2+} influx through NMDA receptor. 68

Figure 4.3 Reelin-stimulated tyrosine phosphorylation of NR2A and NR2B requires Apoer2.....69
Figure 4.4 C-terminus of Apoer2 is required for Reelin to enhance NMDA receptor-mediated Ca^{2+} influx.....70
Figure 4.5 C-terminus of Apoer2 is required for Reelin-stimulated NMDA receptor phosphorylation. 71
Figure 4.6 Ex19 of Apoer2 is required for Reelin-induced regulation of NMDA receptor activity. 73
Figure 4.7 Direct interaction of Apoer2 and Dab1 is necessary for Reelin-induced regulation of NMDA receptor activity.....74
Figure 5.1 Reelin prevents amyloid-β-induced NMDA receptor endocytosis 83
Figure 5.2 Amyloid-β peptide blocks Reelin-enhanced NMDA receptor phosphorylation.....85
Figure 5.3 Model of Reelin and ApoE receptor-mediated regulation of synaptic function 86
Figure 6.1 ApoE4 suppresses surface expression of Apoer2 in primary neurons. 99
Figure 6.2 ApoE4 disrupts Reelin-induced enhancement of NMDA receptor-mediated Ca^{2+} influx. 101
Figure 6.3 ApoE4 inhibits Reelin-induced CREB Ser133 phosphorylation.....103
Figure 6.4 ApoE4 inhibits Reelin-induced increase of long-term potentiation. ..105
Figure 7.1 Model for the physical and functional coupling of Reelin signaling complex with NMDA receptor at the synapse. 116
Figure 7.2 Model for ApoE isoform-selective regulation of synaptic function...134

LIST OF TABLES

Table 3.1 Activation of the Reelin signaling pathway enhances the response of cortical neurons to glutamate 55

LIST OF ABBREVIATIONS

ACSF	artificial cerebrospinal fluid
AD	Alzheimer's disease
ADDL	amyloid β derived diffusible ligand
AMPA	α-amino-3-hydroxy-5-methyl-4-isozazolepropionic acid
ApoE	apolipoprotein E
Apoer2	apolipoprotein E receptor 2
APP	β-amyloid precursor protein
BCL-2	B-cell CLL/lymphoma 2
BDNF	brain-derived neurotrophic factor
BSA	bovine serum albumin
CaM	calmodulin
CaMKII	Ca^{2+}/Calmodulin-dependent protein kinase II
C/EBP	CCAAT/enhancer binding protein
CNQX	6-cyano-7-nitroquinoxaline-2,3-dione
CNS	central nervous system
CREB	cAMP-response-element-binding-protein
CSF	cerebrospinal fluid
Dab1	Disabled-1
D-APV	2-amino-5-phosphonovalerate

DIV	days *in vitro*
DMEM	Dulbecco's modified Eagle's medium
EAAT	excitatory amino-acid transporter
EDTA	ethylenediaminetetraacetic acid
EGF	epidermal growth factor
EGTA	ethylene glycol tetraacetic acid
EPSP	excitatory postsynaptic potential
ER	endoplasmic reticulum
FCS	fetal calf serum
FH	familial hypercholesterolemia
GSK3β	glycogen synthase kinase 3β
IACUC	Institutional Animal Care and Use Committee
ICD	Intracellular domain
HBSS	Hanks' Balanced Salt Solution
HEK293	human embryonic kidney cell line
LDLR	low-density lipoprotein receptor
LRP1	LDLR related protein 1
LTD	long term depression
LTP	long term potentiation
Megf7/Lrp4	multiple EGF domain protein 7
NMDA	N-methyl-D-aspartate

NPxY	Asp-Pro-any amino acid-Tyr
PI	phosphoinositide
PI3K	phosphatidylinositol-3-kinase
PKB	protein kinase B
PS1	presenilin 1
PS2	presenilin 2
PSD	postsynaptic density
PTB	phosphotyrosine biding
RAP	receptor-associated protein
ROS	reactive oxygen species
SD	standard deviation
SEM	standard error of the mean
SFKs	Src family kinases
STEP	striatal enriched tyrosine phosphatase
TRL	triglyceride-rich lipoprotein
Vldlr	very low-density lipoprotein receptorr

CHAPTER ONE

Introduction

Alzheimer's disease (AD) is the most common neurodegenerative disease currently. Apolipoprotein E (ApoE) is the major genetic risk factor for late-onset AD. The isoform ApoE4 predisposes its carrier to late-onset AD through unknown mechanism. A few years ago, the evidence that indicates a regulatory role of ApoE receptors in the synapse began to emerge. This thesis will explore the mechanism by which ApoE receptors regulate synaptic strength, and reveal a novel synaptic function of ApoE which may serve as a mechanism for ApoE-mediated pathogenesis of AD.

Synaptic transmission and plasticity

During development and adulthood, the capacity of the nervous system experiences constant change, a phenomenon commonly referred as neural plasticity. Neural plasticity is necessary for the formation of neural circuits, learning, and establishing memories. Despite that the mechanisms underlining the neural plasticity remain to be fully elucidated, the plasticity in the adult brain is believed to rely primarily on delicately regulated changes in the strength of the existing synapses.

Synapse is the specialized junction through which neurons communicate with each others. In chemical synapse, the most abundant type of synapse in the

nervous system, the information is carried by neurotransmitter molecules from presynaptic to postsynaptic neuron. When action potential reaches the presynaptic terminal, neurotransmitter is released to the synaptic cleft. The released neurotransmitter binds to and activates its receptors that locate at the postsynaptic specialization and subsequently opens or closes the ion channels in the postsynaptic membrane. Altered current flow results in the change in membrane potential and thus the excitability of the postsynaptic neuron. Synaptic transmission is terminated by either the breakdown or reuptake of neurotransmitters. In the mammalian central nervous system (CNS), glutamate is the major excitatory neurotransmitter. Glutamate is cleared from the extracellular space by glial cells through excitatory amino-acid transporters (EAATs). Glial cells convert glutamate to glutamine, which is transported back into neurons and then converted back to glutamate by glutaminase.

In the aforementioned synaptic transmission process, the change in membrane potential of postsynaptic neuron is defined as synaptic strength. The change in synaptic strength, or synaptic plasticity, can be short-term, lasting seconds to minutes, or long-term, which persists for months or even years. By the direction of change in synaptic strength, two types of long-term synaptic plasticity are designated. Long-term potentiation (LTP) is a long-lasting increase in synaptic strength, whereas long-term depression (LTD) is the long-lasting decrease in synaptic efficacy. Synaptic plasticity can occur through presynaptic mechanisms,

such as changes in neurotransmitter release, or postsynaptic mechanisms, such as altered abundance and/or activity of the receptors.

Multiple literatures on the lesion or pharmacological inactivation of hippocampus suggest that hippocampus is essential for the formation of memories (Zola-Morgan and Squire 1993). The properties of LTP suggest it as the cellular correlate of learning and memory (Bliss and Collingridge 1993). Experimentally, LTP can be readily induced by certain patterns of electric stimulation and recorded from the transverse hippocampal slices. Together with pharmacological and genetic tools, this *in vitro* system has greatly advanced our understanding of the molecular mechanisms of synaptic plasticity.

NMDA receptor and postsynaptic signaling

In the mammalian central nervous system (CNS), glutamate is the major excitatory neurotransmitter. On the postsynaptic side of most synapses, two principal ionotropic glutamate receptors are the α-amino-3-hydroxy-5-methyl-4-isozazolepropionic acid (AMPA) - type glutamate receptor and the N-methyl-D-aspartate (NMDA) – type glutamate receptor. AMPA receptor is mostly permeable to sodium and potassium ions in the CNS. It opens and rapidly depolarizes the cell membrane once it binds to glutamate. Thus AMPA receptor mediates the majority of the excitatory postsynaptic potentials (EPSPs).

NMDA receptor is a tetramer, consisting of two NR1 and two NR2 subunits (NR2A-D). The composition of NR2 subunits determines the physiological characteristic and function of NMDA receptors (Cull-Candy and Leszkiewicz 2004). The NR1 subunit is expressed ubiquitously in the brain, whereas the expression of NR2 subunits is regulated spatially and temporally. NR2A and NR2B are mainly expressed in the forebrain (Kutsuwada, Kashiwabuchi et al. 1992). At most excitatory synapses, NR2B predominates in early developmental stages and is gradually replaced by NR2A (Monyer, Burnashev et al. 1994; Sheng, Cummings et al. 1994).

At resting membrane potentials, the pore of NMDA receptor is blocked by Mg^{2+} ion, which is repelled when membrane is depolarized (Nowak, Bregestovski et al. 1984). As a result, NMDA receptor opens only when presynaptic release of glutamate and the depolarization of postsynaptic cell occur simultaneously. NMDA receptor is permeable to both sodium and calcium ions (Ascher and Nowak 1988). Thus, activation of NMDA receptor can increase the concentration of Ca^{2+} in the postsynaptic neuron, which triggers NMDA-dependent synaptic plasticity, the major form of plasticity in the CA1 region of the hippocampus. When Ca^{2+} is buffered pharmacologically, both LTP and LTD are abolished (Lynch, Larson et al. 1983; Mulkey and Malenka 1992).

Ca^{2+}/Calmodulin-dependent protein kinase II (CaMKII) is a Ca^{2+}-activated kinase required for NMDA receptor-dependent LTP (Lisman, Schulman et al.

2002). The activation of CaMKII following the opening of NMDA receptor causes its association with the cytoplasmic tail of NMDA receptor subunit NR2B (Bayer, De Koninck et al. 2001). The mechanisms by which activation of CaMKII increases synaptic transmission and induces LTP likely involve that CaMKII enhances the activity and synaptic distribution of AMPA receptor through phosphorylating AMPA receptor subunit GluR1 (Barria, Muller et al. 1997; Lisman and Zhabotinsky 2001).

NMDA receptor activation promotes neuronal survival and synaptic plasticity, but also cell death in many pathological conditions (Hardingham and Bading 2003). This dual effect is likely determined by the distinct gene expression profiles activated under different conditions (Zhang, Steijaert et al. 2007). Ca^{2+} influx through synaptic NMDA receptors activates Ras-ERK1/2 pathway as well as the nuclear calmodulin (CaM) kinase pathway, both of which can phosphorylate and activate transcription factor cAMP-response-element-binding-protein (CREB) (Hardingham, Arnold et al. 2001; Hardingham, Arnold et al. 2001). Activated CREB then turns on the transcription of target genes that are important for the neuronal development, survival, and synaptic plasticity (Shaywitz and Greenberg 1999). For instance, target genes brain-derived neurotrophic factor (BDNF) and B-cell CLL/lymphoma 2 (BCL-2) are involved in neuronal survival (Shieh, Hu et al. 1998; Tao, Finkbeiner et al. 1998), and

CCAAT/enhancer binding protein (C/EBP) is involved in long-term memory formation (Taubenfeld, Milekic et al. 2001).

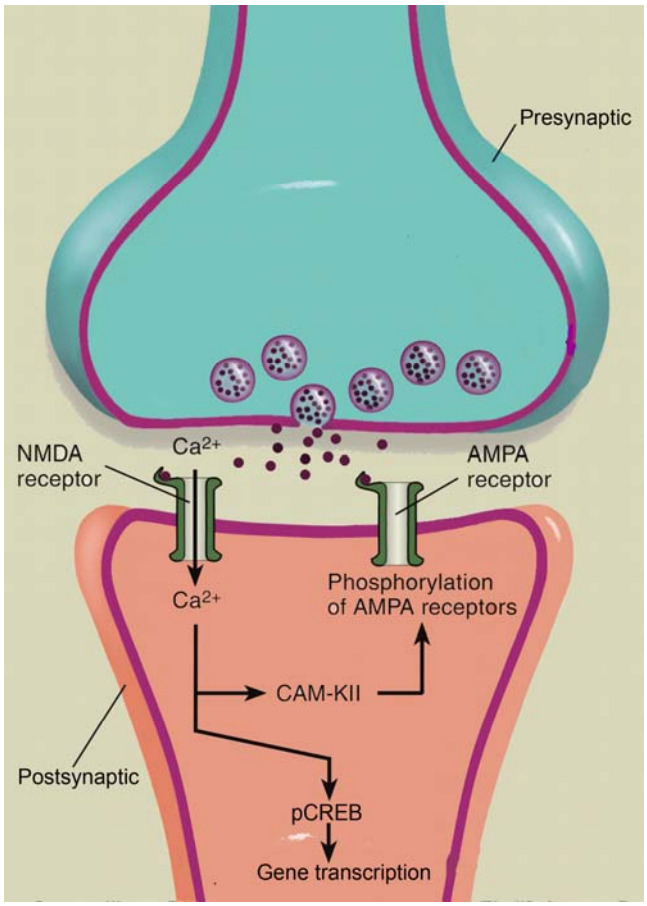

Figure 1.1. Illustration of an excitatory glutamatergic synapse and postsynaptic signaling. Glutamate released from presynaptic terminal can bind and open AMPA receptor and NMDA receptor on the postsynaptic side. Ca^{2+} influx through NMDA receptor activates signaling events leading to increased phosphorylation of AMPA receptor as well as increased transcription activity of CREB.

In the postsynaptic density (PSD), NMDA receptor forms a large protein complex with a number of scaffolding proteins, such as PSD-95, and signaling proteins, such as Src tyrosine kinase (Kennedy 2000). These scaffolding proteins

are important for the intracellular trafficking, synaptic delivery of NMDA receptor, and the stabilization of NMDA receptor in the PSD (Kutsuwada, Kashiwabuchi et al. 1992). The function of NMDA receptor is strongly upregulated by the tyrosine phosphorylation events occurred in NR2 subunits (Wang and Salter 1994; Salter and Kalia 2004). Increased phosphorylation can increase NMDA receptor channel opening probability and stabilize NMDA receptor on the cell surface; whereas dephosphorylation reduces NMDA receptor activity (Wang, Yu et al. 1996; Roche, Standley et al. 2001; Vissel, Krupp et al. 2001). Src is suggested to be the crucial endogenous tyrosine kinase responsible for NMDA receptor regulation (Yu, Askalan et al. 1997). The dephosphorylation of NMDA receptor is performed by the striatal enriched tyrosine phosphatase (STEP), which is also localized at the PSD of glutamatergic synapse (Boulanger, Lombroso et al. 1995; Pelkey, Askalan et al. 2002). Multiple signaling pathways are able to regulate the activity of Src family tyrosine kinases (SFKs), such as G-protein-coupled receptor pathway, EphB receptor kinase pathway, and Ras pathway. Therefore, SFKs serve as a point of convergence for these signaling pathways that enhance NMDA receptor activity and NMDA receptor-dependent synaptic plasticity (Marino, Rouse et al. 1998; Manabe, Aiba et al. 2000; Takasu, Dalva et al. 2002; Yaka, He et al. 2003).

The LDLR gene family

The low-density lipoprotein receptor (LDLR) family is a gene family of cell-surface receptors sharing similar structures. In mammals, seven members of gene family have been identified: *Ldlr*, Apolipoprotein E Receptor 2 (*Apoer2*), Very Low-Density Lipoprotein Receptor (*Vldlr*), Multiple EGF Domain protein 7 (*Megf7/Lrp4*), LDLR related protein 1 (*Lrp1*), *Lrp1b*, and Megalin (*gp330*). All of LDLR gene family members contain ligand-binding repeats and epidermal growth factor (EGF) precursor homology domains in the extracellular compartment and NPxY (Asp-Pro-any amino acid-Tyr) motif in the cytoplasmic domain (Figure 1.2). All the receptors in LDLR gene family bind receptor-associated protein (RAP), which functions as a chaperone for the receptors in the endoplasmic reticulum (ER) and assists their folding (Herz, Goldstein et al. 1991; Bu, Geuze et al. 1995; Willnow 1998).

All the core members of LDLR gene family are expressed in the CNS. The functions of these receptors range from lipoprotein transport, neural signaling, membrane receptor signal modulation, etc. LDLR binds and internalizes LDL, the major cholesterol-carrying lipoprotein in plasma. Mutation in *Ldlr* results in high plasma cholesterol levels and underlies the genetic defect of an inherited human disease familial hypercholesterolemia (FH) (Brown and Goldstein 1986). Therefore LDLR is critical for cholesterol homeostasis. Apoer2 and Vldlr

transmit signaling essential for brain development, which is discussed in detail in next section.

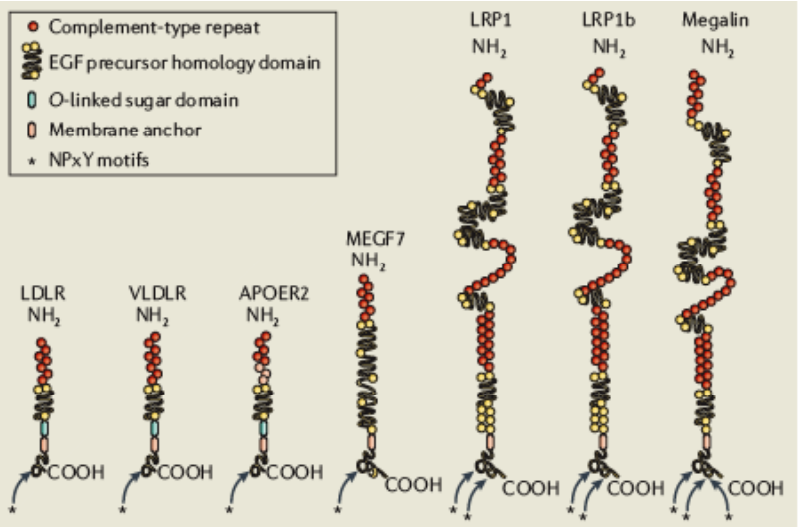

Figure 1.2. Schematic representation of the mammalian LDLR family members. The receptor members share the common structural organization. Ligand Binding Repeats- Red; EGF Precursor Homology Domains- Yellow; O-linked Sugar Domain- Green (adapted from (Herz and Chen 2006)).

Megf7 is essential for proper development of limb, kidney and neuromuscular junction as observevd in mice genetic studies ((Johnson, Hammer et al. 2005); Johnson et al. unpublished observations). The function of LRP1b is largely unknown, since the LRP1b knockout mice appear to be normal upon gross examination (Marschang, Brich et al. 2004). Megalin is mostly expressed in the proximal tubules in kidney where it mediates the resorption of multiple proteins (Zheng, Bachinsky et al. 1994; Christensen, Moskaug et al. 1999). Megalin knockout mice display midline defects including cleft palates, absence of

olfactory bulbs and holoprosencephly, which is a malformation of the forebrain. However, the molecular mechanisms underlying these defects are not clear (Willnow, Hilpert et al. 1996).

LRP1 has critical function during early embryonic development that leads to early embryonic lethality of knockout embryos. LRP1 also plays an important regulatory role in the proliferation and migration of smooth muscle cells and the onset of atherosclerotic lesions (Boucher, Gotthardt et al. 2003). Mice that lacked LRP1 selectively in neurons had multiple neurological defects, including hyperactivity, tremor, and abnormalities in muscle tone, whereas the gross anatomy of their brains were normal. LRP1 co-immunoprecipitated with PSD-95 and NMDA receptor from neuronal cell lysates, suggesting that LRP1 is closely associated with NMDA receptor in the synapse (Strasser, Fasching et al. 2004). LRP1 could also evoke Ca^{2+} influx through NMDA receptor in response to its ligand, activated α(2)-macroglobulin, in primary neurons (Bacskai, Xia et al. 2000), which strongly indicates a role for LRP1 in synaptic plasticity.

Reelin signaling mediated by lipoprotein receptors

In order to study the physiological function of the receptors in LDLR family, our lab has generated knockout mice that are deficient in these receptors. Strikingly, mice that lack both Apoer2 and Vldlr show a severe neurological

developmental disorder that includes cerebellar ataxia, inverted lamination of neocortex, and ectopic localization of neurons in hippocampus (Trommsdorff, Gotthardt et al. 1999). This phenotype is identical to mutant mice that lack either the extracellular signaling protein Reelin or the intracellular adaptor protein Disabled-1 (Dab1) (D'Arcangelo, Miao et al. 1995; Howell, Hawkes et al. 1997; Sheldon, Rice et al. 1997), suggesting that Reelin and Dab1 function in a linear pathway, and that Apoer2 and Vldlr are receptors which transmit the signal from Reelin to Dab1. This hypothesis is further supported by biochemical evidence that Apoer2 and Vldlr bind Reelin with high affinity on their extracellular domains and Dab1 through the cytoplasmic NPxY motifs (Trommsdorff, Borg et al. 1998; D'Arcangelo, Homayouni et al. 1999; Hiesberger, Trommsdorff et al. 1999).

Reelin is a large signaling protein secreted by Cajal-Retzius cells at the surface of neocortex during embryonic development (Alcantara, Ruiz et al. 1998). Independent studies from several research groups have revealed the signaling pathway initiated by Reelin (Figure 1.3). Reelin binding to Apoer2 and Vldlr on the neuronal surface induces tyrosine phosphorylation of Dab1 through clustering Apoer2 and Vldlr (D'Arcangelo, Homayouni et al. 1999; Hiesberger, Trommsdorff et al. 1999; Strasser, Fasching et al. 2004). Receptor clustering also brings SFKs to this signaling complex in which Dab1 and SFKs mutually activate each other (Bock and Herz 2003). Tyrosine phosphorylation of Dab1 is essential

for signal propagation, since mice in which these tyrosine residues were mutated to phenylalanine had indistinguishable phenotype from Reelin-deficient mice (Howell, Herrick et al. 2000). Activated SFKs then activates phosphatidylinositol-3-kinase (PI3K) and subsequently protein kinase B (PKB), which inhibits the activity of kinase glycogen synthase kinase 3β (GSK3β) (Beffert, Morfini et al. 2002). GSK3β is one of the major kinases that phosphotylate the microtubule stabilizing protein tau (τ). Consistently, tau phosphorylation is increased in mutant mice with defects in Reelin signaling pathway (Hiesberger, Trommsdorff et al. 1999). Dab1 also recruits CRK-like (CRKL) and promotes the formation of RAP1-GTP, which controls actin cytoskeleton rearrangement (Ballif, Arnaud et al. 2004). Lissencephaly 1 (LIS1) is another binding partner of tyrosine-phosphorylated Dab1, and it regulates microtubule dynamics (Assadi, Zhang et al. 2003).

After developmental stage, Reelin is mainly secreted by GABA-ergic interneurons throughout the neocortex and hippocampus (Ramos-Moreno, Galazo et al. 2006). The expression of Apoer2, Vldlr and Dab1 also persist in the adulthood. Although either Apoer2 or Vldlr alone is able to induce Dab1 phosphorylation in response to Reelin in primary neurons, mice lacking either receptor showed deficits in contextual fear-conditioned learning, a generally accepted behavioral test for hippocampus dependent learning and memory (Weeber, Beffert et al. 2002). Consistently, hippocampal LTP was moderately

defective in mice lacking either receptor, whereas baseline synaptic transmission was unaltered. To test whether the LTP defects in receptor knockout mice might result from impaired Reelin signaling, Weeber et al. performed reverse experiment in which Reelin was applied to hippocampal slices. Applying Reelin to wild type hippocampal slices greatly enhanced LTP, which was abolished in either Apoer2 or Vldlr knockout slices. These results indicate that the receptor-mediated Reelin signaling can physiologically regulate the synaptic plasticity, learning and memory.

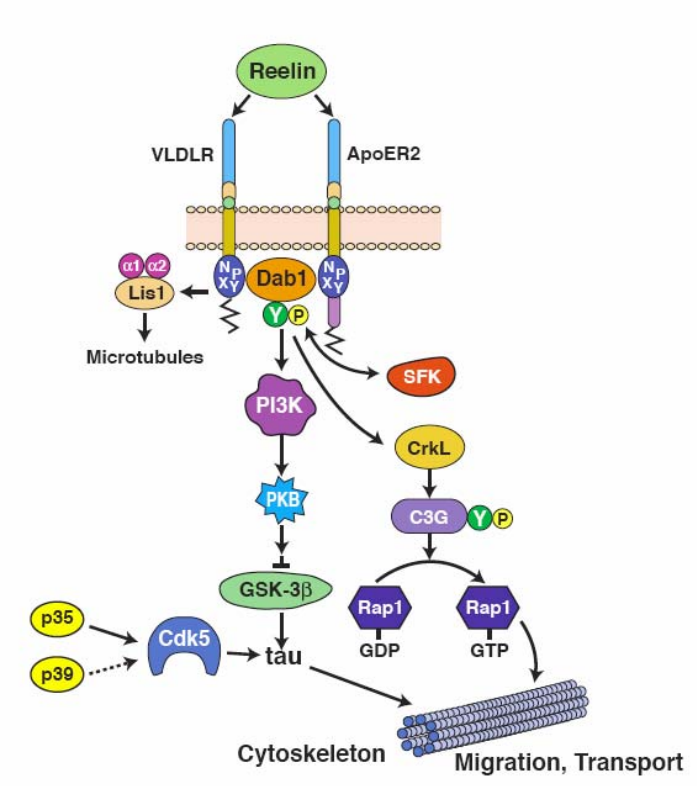

Figure 1.3. Reelin-initiated signaling events in neurons.

Alzheimer's disease and apolipoprotein E

Alzheimer's disease (AD) is the most common form of dementia and neurodegenerative disease in the elderly. It afflicts up to 24 million people worldwide, and is the seventh-leading cause of death in the United States. Clinical symptoms of AD include progressive memory loss, cognitive impairment and personality changes. At a macroscopic level, brains of AD patients display severe atrophy in multiple regions of cerebral cortex, such as temporal lobe and frontal cortex, due to the loss of neurons and synapses in these regions. Histologically, brains of AD patients are characterized by extracellular deposit of senile plaques and intraneuronal neurofibrillary tangles. The main component of the plaques is β-amyloid peptide (Aβ), the proteolytic product of β-amyloid precursor protein (APP) by β- and γ-secretase. Neurofibrillary tangles are made of hyperphosphorylated tau proteins. Currently there is no cure for AD; understanding and preventing AD remain a big challenge for the neuroscientists.

AD usually begins with a pure impairment of cognitive function in the absence of any other clinical signs of brain injury. Brain biopsies from patients within 2 to 4 years of the onset of AD revealed a significant decrease in the density of synapses (Davies, Mann et al. 1987). Even in late-stage AD brains, synapse loss correlates more robustly with cognitive deficits than the numbers of plaques or tangles (Terry, Masliah et al. 1991). In the rodent model for AD, loss of synapses occurs prior to the formation of plaques and the loss of whole neurons

(Hsia, Masliah et al. 1999). These studies strongly suggest that synapses are the initial target in AD.

There are two basic types of AD: early-onset familial AD (FAD) and late-onset AD. Patients of FAD are usually diagnosed with the disease before age 60. FAD only accounts for 5 to 10 percent of the total AD cases. Genetic studies have identified three genes whose mutations are linked to FAD in an autosomal dominant manner: APP, presenilin 1 (PS1), and presenilin 2 (PS2). Most of these mutations cause increased production of $A\beta_{1-42}$, an amyloidogenic form of Aβ, suggesting that the production of $A\beta_{1-42}$ may be an initial event in AD development.

The concept that the accumulation of Aβ triggers the deficits in memory and cognition observed in AD cases is supported by multiple evidences showing that Aβ impairs synaptic function. Young mice transgenic for human APP with AD-causing mutations have significant deficits in basal synaptic transmission and LTP in hippocampus (Chapman, White et al. 1999; Hsia, Masliah et al. 1999; Moechars, Dewachter et al. 1999; Fitzjohn, Morton et al. 2001). In these mice, synaptic dysfunction occurs well before the development of detectable amyloid plaques, suggesting that the synaptic dysfunction is caused by a diffusible form of Aβ. Cerebral microinjection of cell medium containing natural oligomers of human Aβ potently suppressed hippocampal LTP in rats *in vivo* (Walsh, Klyubin

et al. 2002). Acute application of synthetic Aβ oligomers to hippocampal slices also inhibited LTP *in vitro* (Lambert, Barlow et al. 1998). Recent studies suggest that Aβ induces synaptic dysfunction through altering the trafficking and activity of AMPA receptor and NMDA receptor (Snyder, Nong et al. 2005; Hsieh, Boehm et al. 2006).

The majority of AD cases are late-onset in which patients are diagnosed after age 65. The only well-established genetic risk factor for late-onset AD is apolipoprotein E (ApoE). In human population, ApoE gene has three alleles: ε2, ε3, and ε4. ApoE3 is the most common variant. Compared to ApoE3, ApoE2 isoform has an amino acid substitution at position 158 (Arg → Cys), whereas ApoE4 differs from apoE3 by a change at amino acid 112 (Cys → Arg). ApoE-ε4 allele greatly predisposes its carriers to late-onset AD through unknown mechanisms (Corder, Saunders et al. 1993; Schmechel, Saunders et al. 1993).

ApoE is 299 amino acids long and a ligand for all members of the LDLR family. The amino-terminal region of ApoE contains the receptor-binding binding domain; the carboxyl-terminal domain of ApoE contains the lipid-binding site. The primary role for ApoE is to transport and deliver lipids throughout the circulation and between cells. Lipoprotein is a complex of apolipoproteins and lipids which transports lipids through the plasma. ApoE is a component of lipoproteins VLDL and chylomicron, both of which are enriched in triglyceride

and cholesterol. The ApoE-containing lipoprotein can be taken up by hepatic cells through ApoE receptor-mediated endocytosis. ApoE also stimulates the production and secretion of VLDL by the liver (Mensenkamp, Jong et al. 1999). Therefore ApoE plays a central role in lipid metabolism.

ApoE is the major apolipoprotein in the CNS and mainly produced by astrocytes (Boyles, Pitas et al. 1985). ApoE-containing lipoprotein transports cholesterol, the major component of myelin and neuronal and glial membranes (Dietschy and Turley 2001). *In vitro* evidences indicate that glia-derived cholesterol is crucial for the generation of new synapses (Pfrieger and Barres 1997; Mauch, Nagler et al. 2001). Consistently, reduced synaptic density was observed in the brains of ApoE-deficient mice (Masliah, Mallory et al. 1995).

Several mechanisms have been proposed to explain the neuropathological effect of ApoE4. Astrocyte-derived ApoE4 inhibited neurite extension of rat hippocampal neurons through a mechanism that required LRP1 (Holtzman, Pitas et al. 1995; Sun, Wu et al. 1998). ApoE4 increased Aβ deposition presumably through inhibiting Aβ clearance (Ma, Yee et al. 1994; Sanan, Weisgraber et al. 1994). ApoE4 was more susceptible to proteolysis than ApoE3 when synthesized by neurons which was likely due to the structural differences (Harris, Brecht et al. 2003). The N terminus part of ApoE4 resulted from the cleavage, which is also present in brains of AD patients, was toxic to cultured neurons (Huang, Liu et al. 2001). Transgenic mice expressing the N terminal product of ApoE4 displayed

neurodegenerative changes in the brain and NFT-like structures in neurons (Harris, Brecht et al. 2003).

Since AD initiates from the impairment of synaptic function, ApoE may also play a role in the synapse. The effect of ApoE in synapse has been highly suggested by numerous studies. However, the clear function of ApoE is obscured by the inconsistent results acquired from different research groups using different experimental conditions. ApoE-deficient mice had impaired synaptic plasticity in the CA1 region and working memory deficit which was evaluated by Morris water maze test (Gordon, Grauer et al. 1995; Valastro, Ghribi et al. 2001). However, when high-frequency stimulation protocol was used, the LTP in ApoE-deficient mice appeared to be normal (Anderson, Barnes et al. 1998). ApoE was also suggested to affect synaptic plasticity in an isoform-dependent manner. LTP of transgenic mice expressing human ApoE4 was reduced compared with wild-type mice and mice expressing human ApoE3 (Trommer, Shah et al. 2004). When measured under different condition, the LTP of ApoE4 expressing mice was comparable to wild-type control (Kitamura, Hamanaka et al. 2004).

So far, despite the genetic association between ApoE and AD is well established, understanding the pathological action of ApoE in the progression of AD remains a big challenge to neuroscientists. Understanding the function of ApoE related to synaptic activity will by all means provide a novel mechanism by which ApoE contributes to the development of AD.

CHAPTER TWO

Studying the Functional role of PI binding by Dab1

Abstract

Dab1 is a cytoplasmic adaptor protein essential for transmitting Reelin signaling pathway and the proper neuronal migration during embryonic development. An amino-terminal phosphotyrosine binding (PTB) domain of Dab1 interacts with NPxY motifs in the cytoplasmic tails of Reelin receptors Apoer2 and Vldlr. Previous structural study has revealed that the Dab1 PTB domain binds to both the NPxY motif in the receptor tails as well as the head group of phosphoinositide (PI) 4,5-P_2 in an energetically independent manner. Through expressing mutant Dab1 forms in primary neurons, we have demonstrated that PI binding of Dab1 PTB domain is required for proper membrane localization of Dab1 and for the transduction of Reelin signaling.

Introduction

The proper positioning of neurons in the developing mammalian brain is regulated in part by the signaling events initiated by a large extracellular protein Reelin. Binding of Reelin to its receptors Apoer2 and Vldlr on the neuronal

surface activates and phosphorylates adaptor protein Dab1, which binds to the cytoplasmic tails of the receptors.

Murine Dab1 is a 555-amino acid protein and mostly expressed in the brain. Dab1 has an amino-terminal PTB domain, a tyrosine-rich region and an acidic carboxyl terminus (Figure 2.1A) (Howell, Gertler et al. 1997). PTB domain of Dab1 associates with the NPxY motifs in the cytoplasmic tails of Apoer2 and Vldlr. Reelin-induced tyrosine phosphorylation of Dab1 takes place within the tyrosine-rich region. Dab1 phosphorylation is essential for the transduction of Reelin signaling, because mice in which 5 tyrosines (Tyr(185), Tyr(198), Tyr(200), Tyr(220), and Tyr(232)) in the tyrosine-rich region of Dab1 are mutated to phenylalanine exhibit identical phenotype to the Dab1 knockout mice (Howell, Herrick et al. 2000).

Previous structural study on the Dab1 PTB domain has revealed that this domain is able to simultaneously bind to the NPxY peptide motif and to the head group of PI 4,5-P_2 through separate binding sites and in an energetically independent manner (Figure 2.1B) (Stolt, Jeon et al. 2003; Yun, Keshvara et al. 2003). However, the significance of these binding events has not been elucidated. Binding of Dab1 PTB domain to the receptor tails most likely functions to recruit Dab1 to a complex with the other components of Reelin signaling. As Dab1 is preferentially recruited to the plasma membrane in primary neurons (Bock and

Herz 2003), PI binding by Dab1 may be responsible for the membrane localization of Dab1.

Dab1 mutants that have selective deficiencies in either NPxY or PI binding are powerful tools to study the distinct roles of the aforementioned binding events *in vivo*. The S114T/F158V mutant (Figure 2.1C) has deficiency in NPxY binding (K_D reduced by at least 150-200 fold) but retains normal affinity for PIs (K_D = 0.7 ± 0.1μM). The K45E mutant (Figure 2.1D) has deficiencies in PI binding (K_D reduced by at least 300 fold) but shows normal affinity for the NPxY peptide (Stolt, Vardar et al. 2004). In addition, the 5F mutant (Howell, Hawkes et al. 1997), in which tyrosines 185, 198, 200, 220, and 232 are mutated to phenylalanine, was used as a negative control because it cannot undergo tyrosine phosphorylation (Figure 2.1A). In order to study the function of these two binding sites in Dab1 PTB domain, we introduced these Dab1 mutants into primary neurons and examined the membrane localization and the ability to transduce Reelin signaling of these mutants.

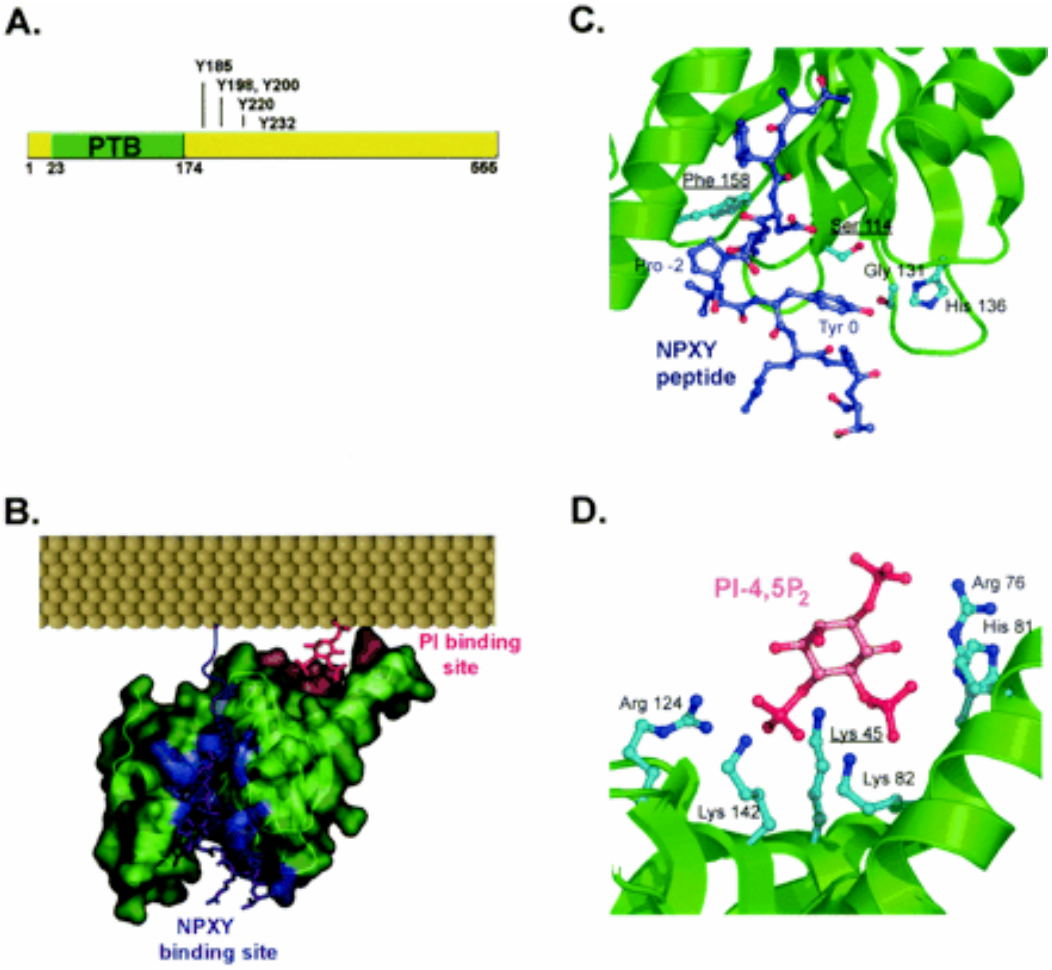

Figure 2.1 The Dab1 mutants. *A*, The schematic of murine Dab1. *B*, the structure of the Dab1 PTB domain complex, demonstrating the NPxY and PI binding sites. The Dab1 PTB domain is shown as a green molecular surface representation, whereas the ligands are shown in ball-and-stick representation. The surface residues of the PTB domain in contact with NPxY or PI are lavender and salmon respectively. *C*, residues involved in NPxY peptide binding. Residues mutated in this study are underlined. *D*, residues involved in PI 4,5-P_2 binding. The residue mutated in this study is underlined.

Results and Discussion

Full-length wild type Dab1 as well as the 5F, K45E, and S114T/F158V mutants containing a carboxyl-terminal 5-Myc tag were cloned into a lentiviral expression vector derived from LL3.7 (Rubinson, Dillon et al. 2003). These vectors were then incorporated into lentiviral particles for transduction of wild type primary cortical neurons.

We then used cell fractionation approach to examine the membrane localization of mutant Dab1 (Figure 2.2). Infected neurons were harvested, homogenized, and separated into cytosolic (S) and membrane containing (P) fractions. Wild type neurons transduced with vector alone served as negative control. Virally expressed Dab1 mutants were detected by an α-Myc antibody. Detection of Akt was used as a control for a cytoplasmic protein that is present predominantly in the cytosolic fraction, whereas LRP1 was used as a marker for membrane containing fraction. Wild type Dab1 (*lanes 3* and 4) and S114T/F158V mutant (*lanes 7* and *8*), which both retain PI binding ability, was found predominantly in the membrane containing fraction. By contrast, the majority of K45E mutant was present in the cytosolic fraction (*lanes 5* and 6). This result suggested that the interaction with phosphoinositides, but not with the NPxY motifs, is required for the membrane association of Dab1.

Next, we examined the ability of each mutant to transmit Reelin signaling, i.e. to undergo tyrosine phosphorylation upon Reelin binding to its receptors (Hiesberger, Trommsdorff et al. 1999). Wild type primary neurons were transduced with lentiviral particles expressing Dab1 mutants or empty virus. Three days after transduction, the neurons were treated in the presence (*R*) or absence (mock, *M*) of Reelin for 25 min at 37°C. Ectopically expressed Dab1 mutants were immunoprecipitated from cell lysates with an α-Myc antibody and analyzed by Western blotting with α-Myc and α-phosphotyrosine antibodies (Figure 2.3). Upon Reelin stimulation, wild type Dab1 is efficiently tyrosine phosphorylated (Figure 2.3, *A*, *upper panel*, *lanes 3* and *4*; *B*, *upper panel*, *lanes 1* and *2*). The 5F mutant, which does not contain tyrosine residues, could not be phosphorylated in response to Reelin as expected (Figure 2.3A, *lanes 5* and *6*). The S114T/F158V mutant (Figure2.3A, *lanes 7* and *8*) was not able to undergo tyrosine phosphorylation in response to Reelin either, suggesting that the interaction of the Dab1 PTB domain with the NPxY motifs is required for signal transduction. The K45E mutant was also resistant to Reelin-induced tyrosine phosphorylation (Figure 2.3B, *lanes 3* and *4*), indicating that PI-mediated membrane association of Dab1 is necessary for assembly of the Reelin signaling complex at the plasma membrane and signal transduction.

Taken together, the experiments presented in this chapter have identified two distinct roles of the Dab1 PTB domain, both of which are required for the

transmission of a Reelin signal by Dab1: (i) membrane recruitment of Dab1, which requires the PI binding site, and (ii) binding of Dab1 to the tails of Apoer2 and Vldlr, which is mediated by the interaction with the NPxY motif. Our data suggest that membrane recruitment occurs before receptor binding, because NPxY binding mutations have no effect on the membrane localization of Dab1. Thus, we propose that Dab1 first associates with the membrane through binding of PI 4,5-P_2, which facilitates the subsequent binding to the NPxY motif in the tails of Apoer2 and Vldlr by bringing the two binding partners into closer proximity. Simultaneous binding at both sites is required for tyrosine phosphorylation of Dab1 in response to Reelin.

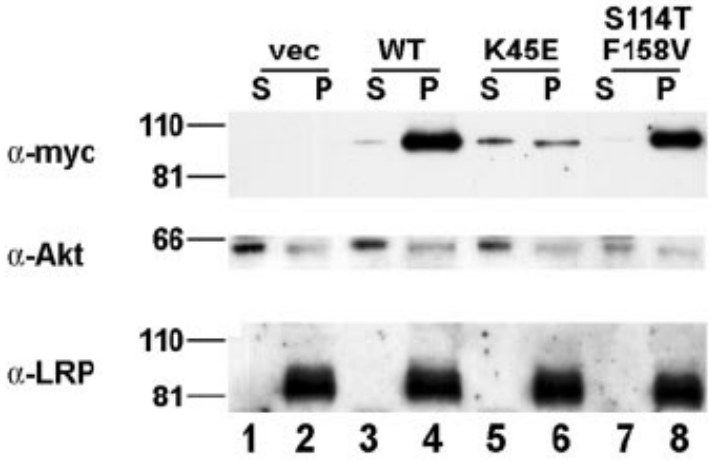

Figure 2.2. Fractionation of primary neurons expressing Dab1 mutants. Fractionation of wild type neuron lysates expressing empty vector (*vec*), wild type Dab1 (*WT*), K45E, or S114T/F158V mutant constructs. Fractions were analyzed by western blot for myc (*top panel*), Akt (*middle panel*), or LRP (*bottom panel*). *S*, soluble fraction; *P*, particulate fraction.

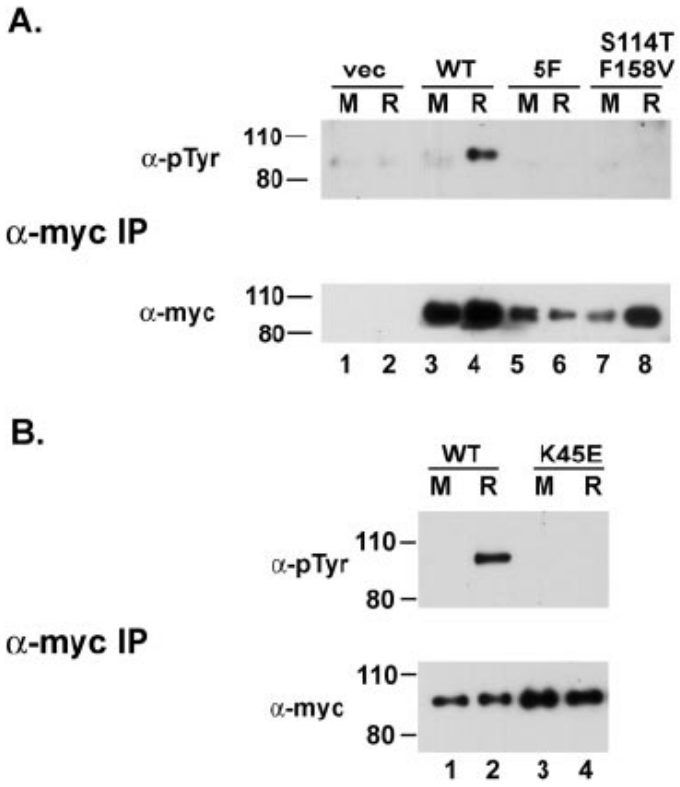

Figure 2.3. Tyrosine phosphorylation of Dab1 mutants upon Reelin stimulation. Primary neurons were transduced with lentiviral particles expressing different Myc-tagged Dab1 constructs. The neurons were exposed to mock or Reelin-conditioned media and then lysed. The virally expressed Dab1 was immunoprecipitated from the lysate using a polyclonal α-Myc antibody, and analyzed by western blot for phosphotyrosine (*top panel*) and Myc (*bottom panel*). *M*, mock-conditioned media; *R*, Reelin-conditioned media. *Vec*, empty vector; *WT*, wild-type Dab1.

Materials and Methods

Preparation of primary neurons

All animal experiments were conducted according to the procedures approved by the Institutional Animal Care and Use Committee (IACUC) at the University

of Texas Southwestern Medical Center. Forebrains were isolated from E18.5 embryos from timed pregnant Sprague-Dawley rats (Charles River Laboratories), or E16.5 embryos from timed pregnant mice. The meninges were carefully removed. Cortical lobes were treated by Hanks' Balanced Salt Solution (HBSS) (Invitrogen) which was supplemented with 1/10 volume of 10 x trypsin-EDTA (Sigma) at 37°C for 10 min. The trypsinization was stopped by adding equal volume of HBSS with 20% fetal calf serum (FCS). After washing with HBSS, the brain tissues were tritrated in HBSS containing 0.025% DNase I (Sigma), 0.4 mg/ml trypsin inhibitor (Roche), 3 mg/ml BSA (Sigma), and 12 mM $MgSO_4$. The cells were resuspended in Neuronbasal medium (Invitrogen) supplemented with 2% B27 (Invitrogen), 1 mM L-glutamine and 100 units/mL penicillin-streptomycin. Neurons were plated on poly-D-lysine (Sigma) coated 6-well plate (Corning Incorporated) at a density of 6×10^4 per cm^2 and were maintained at 37°C in a 5% CO_2 environment.

Preparation of Lentiviral Particles

293 FT cells were transfected with the pRSV, pRRE, and pVSV-G plasmids of a 3-vector lentiviral system (Naldini, Blomer et al. 1996; Dull, Zufferey et al. 1998), together with the lentiviral vector expressing myc-tagged wild type or mutant *Dab1*, or an empty vector control. 48 to 72 h after transfection the cell

media were collected and centrifuged at 800×g for 7 min at 4°C to remove cell debris. The supernatants were dialyzed against Dulbecco's modified Eagle's medium (DMEM)/F-12 (Invitrogen) using 100-kDa molecular mass cut-off dialysis membranes (Spectrum Labs) at 4°C over night. The viral supernatants were then frozen in liquid nitrogen and stored at -80°C.

Cellular Fractionation of Primary Neurons

On days 4-6 after culturing, the primary neurons were transduced with the lentiviral particles. 24 h after infection the viral supernatant was removed and replaced with conditioned Neurobasal media. 2 to 3 days after infection, neurons were harvested and homogenized in ice-cold hypotonic buffer A (20 mM Tricine, pH 7.8, 0.25 M sucrose, 1 mM EDTA, supplemented with protease inhibitor cocktails). Nuclei were removed by centrifugation at 900×g for 10min. Postnuclear supernatants were separated into soluble and particulate fractions by ultracentrifugation at 200,000×g for 1.5 h. Particulate fractions were re-solubilized in Tris buffer, pH 7.5 (50 mM, 0.15 M NaCl, with protease inhibitor cocktails) containing 1% Triton X-100. The protein concentrations of the particulate and soluble fractions were estimated using the Bio-Rad detergent-compatible assay. Equal amounts of protein from each fraction were then analyzed by Western blot with a monoclonal α-Myc antibody (9E10), a

polyclonal α-Akt antibody (Cell Signaling Technology), and a polyclonal α-LRP1 antibody (May, Rohlmann et al. 2004).

Reelin preparation

Stably transfected HEK-293 cells expressing recombinant mouse full-length Reelin or HEK-293 control cells were seeded in 1L tissue culture roller bottles in DMEM (low glucose, Cellgro) containing 10% FCS and 100 units/mL penicillin-streptomycin. Cells were maintained at 37°C in a 5% CO_2 environment. Once grown to confluence, cells continued growing in DMEM (low glucose, Cellgro) containing 0.1% bovine serum albumin (BSA, Sigma) for 48 hr. Then the Reelin-containing or mock media were collected and concentrated 50-fold with centrifugal filters with a 100-kDa cut-off membrane (Millipore).

Immunoprecipitation of Dab1

On day 5-7 after culturing, the primary neurons were transduced with the lentiviral particles as described above. 3 days after infection, the neurons were stimulated with concentrated Reelin-conditioned or mock-conditioned media for 25 min at 37°C and lysed in cold lysis buffer (150 mM NaCl, 20 mM Tris [pH 7.4], 1 mM $CaCl_2$, 1 mM $MgCl_2$, 1% Triton X-100, protease and phosphatase inhibitors). The cleared lysates were incubated with 5 μg polyclonal rabbit α-

Myc antibody (Bethyl Labs) at 4°C over night. This mixture was subsequently incubated with Protein A agarose beads (Sigma) for 2 h at 4°C. The beads were washed 3 times and then resuspended in SDS-PAGE loading buffer. The supernatants were analyzed by Western blot using a monoclonal α-Myc antibody (9E10) as well as a monoclonal α-phosphotyrosine antibody (4G10, Upstate Biotechnology).

CHAPTER THREE

Reelin Signaling Modulates NMDA Receptor Activity in Primary Neurons

Abstract

Reelin is a secreted protein and activates a signaling pathway that involves its receptors, Vldlr and Apoer2, the cytoplasmic adaptor protein Dab1 and Src family tyrosine kinases (SFKs). This pathway is essential for proper neuronal migration during embryonic development. Reelin also markedly enhances long-term potentiation (LTP) in the adult murine hippocampus, suggesting that this signaling pathway can modulate synaptic activity, learning and memory. In the chapter, we show that Reelin can potentiate the tyrosine phosphorylation and the Ca^{2+} conductance of NMDA-type glutamate receptor through a mechanism that requires SFKs and Dab1. Reelin enhances the calcium influx through NMDA receptors in wild type cortical neurons, but not in Dab1 deficient neurons, or in the presence of antagonist of Reelin receptors, or in the presence of inhibitors of SFKs. We also show that Reelin-induced augmentation of Ca^{2+} entry through NMDA receptor increases the phosphorylation of the transcription factor cAMP-response element binding protein (CREB) on an activation site. Thus, Reelin may physiologically modulate the function of synapses, learning and memory by regulating NMDA receptor activity.

Introduction

Reelin is a large secreted signaling protein with critical roles in the developing nervous system. Reelin binding to its receptors, Vldlr and Apoer2, on migrating neurons activates Src tyrosine kinase (Bock and Herz 2003) and therefore induces tyrosine phosphorylation of Dab1, an adaptor protein that interacts with the cytoplasmic tails of both receptors (D'Arcangelo, Homayouni et al. 1999; Hiesberger, Trommsdorff et al. 1999). Successful transmission of Reelin signaling is essential for the positioning of neurons and the lamination of the cortex and the cerebellum (D'Arcangelo, Miao et al. 1995; Howell, Hawkes et al. 1997; Trommsdorff, Gotthardt et al. 1999).

Besides the function during development, Reelin signaling can also modulate synaptic plasticity, and learning and memory in the adult brain (Weeber, Beffert et al. 2002). Reelin enhances long-term potentiation (LTP) in mouse hippocampus, which is abolished if either Vldlr or Apoer2 is deficient. These observations raise the possibility of a functional cross-talk between the Reelin signaling complex and synaptic ion channels. In the CNS, synaptic strength and activity-dependent synaptic plasticity of glutamatergic synapse depend primarily on the function of NMDA receptor (Bliss and Collingridge 1993). By controlling Ca^{2+} entry in the neurons, NMDA receptor has been shown to regulate both synapse formation during development as well as synaptic plasticity in the adult

brain (Ghosh and Greenberg 1995). NMDA receptor is also required for the LTP in the CA1 region of the hippocampus (Malenka 2003). NMDA receptor activity can be regulated by phosphorylation and dephosphorylation on tyrosine residues in the cytoplasmic domains of the NR2A or NR2B subunits, and phosphorylation increases ion conductance.(Salter and Kalia 2004).

Taken together, these findings raise a possible role of Reelin in the regulation of the NMDA receptor and hence synaptic activity. To test this hypothesis, we have quantitatively determined glutamate-stimulated and NMDA receptor-dependent Ca^{2+} influx in primary cortical neurons in response to Reelin. We find that Reelin is a potent enhancer of glutamate-stimulated Ca^{2+} influx through NMDA receptor. This finding provides the first direct evidence for a physiological role of Reelin signaling in the regulation of NMDA receptor function and synaptic strength.

Results and Discussion

Reelin enhances glutamate-stimulated Ca^{2+} influx in cortical neurons

We first investigated whether Reelin could modulate glutamate stimulated Ca^{2+} influx in wild type primary cortical neurons after 12 or 13 days *in vitro* (DIV). We incubated cortical neurons with 5 μM fura-2-AM, a fluorescent

calcium indicator. The ratio of fura-2 signals at 340 nm and 380 nm excitation wavelengths was used to quantitatively determine the concentration of intracellular Ca^{2+} ($[Ca^{2+}]_i$). $[Ca^{2+}]_i$ increased dramatically after glutamate (40 μM) application, which shows that glutamate receptors were expressed and that cortical neurons responded normally under our culture conditions (data not shown). Glutamate evoked very little $[Ca^{2+}]_i$ increase when neurons were perfused with 5 μM nimodipine (an inhibitor of L-type Ca^{2+} channels), 40 μM CNQX (an inhibitor of AMPA-type glutamate channels) and 1 μM tetrodotoxin, which blocks basal neuronal activity (Figure 3.1, first row; Figure 3.2A, 3.2B). The NMDA receptor cannot overcome voltage gating under these conditions. To test the effect of Reelin, cortical neurons were treated with Reelin and then assessed for $[Ca^{2+}]_i$ changes in response to glutamate stimulation under the same perfusion conditions described above. Reelin alone can't stimulate $[Ca^{2+}]_i$ increase as observed from baseline level, however, glutamate stimulated a large increase of $[Ca^{2+}]_i$ in Reelin treated neurons (Figure 3.1, second row; Figure 3.2D, 3.2E).

To better evaluate the effect of Reelin, we plotted the changes of $[Ca^{2+}]_i$ in response to glutamate as a histogram depicting the distribution of the magnitude of the response of the analyzed cell population (Figure 3.2). A cut-off value was defined as described in Experimental Procedures. By this definition, 18% of the neurons responded to glutamate in the absence of Reelin addition (Figure 3.2C).

By contrast, after Reelin treatment, 75% of the neurons responded to glutamate (Figure 3.2F).

Reelin-induced enhancement of glutamate-stimulated Ca^{2+} influx requires NMDA receptors

To exclude the contribution of intracellular Ca^{2+} release to the observed effect of Reelin, we performed a control experiment in which we removed the Ca^{2+} ions from the perfusion buffer. Only 2% of the neurons treated with Reelin responded to glutamate in the absence of extracellular Ca^{2+} (Figure 3.2G, 3.2H, 3.2I) indicating that Reelin stimulated Ca^{2+} influx from the extracellular space, as opposed to release from intracellular storage compartments. To further investigate whether this effect of Reelin on glutamate-stimulated Ca^{2+} influx requires NMDA receptors, we pretreated cortical neurons with the NMDA receptor antagonist 2-amino-5-phosphonovalerate (D-APV) prior to Reelin application. D-APV decreased the percentage of responding cells to 5.6% (Fig 3.2J, 3.2K, 3.2L), indicating that NMDA receptors are required for the observed Reelin-mediated increase of Ca^{2+} influx.

Reelin-mediated enhancement of glutamate-stimulated Ca^{2+} influx is receptor dependent

Reelin binding to the LDL receptor family members Apoer2 and Vldlr is required for the transmission of Reelin signal and the activation of kinases in the neuronal cytoplasm. To investigate whether Reelin-mediated modulation of NMDA receptor activity requires binding of this ligand to Apoer2 and Vldlr, we incubated cortical neurons with recombinant GST-RAP fusion protein prior to Reelin treatment. Receptor associated protein (RAP) is a universal competitor for ligand binding to LDL receptor family members and blocks Reelin binding to Apoer2 and Vldlr (Strickland, Ashcom et al. 1990; Herz, Goldstein et al. 1991). In the presence of GST-RAP only 19% of Reelin-treated neurons responded to glutamate, while 64% of the neurons responded to Reelin and glutamate when GST control protein was used (Figure 3.3D-I). Only 6% of mock treated neurons responded to glutamate (Figure 3.3A-C). These findings indicate that Reelin binding to LDL receptor family members, and thus activation of the signaling pathway, is required to enhance glutamate-stimulated Ca^{2+} currents.

Reelin-induced enhancement of glutamate-stimulated Ca^{2+} influx requires Dab1

Dab1 is a cytoplasmic adaptor protein that interacts with Apoer2 and Vldlr. Binding of Reelin to Apoer2 or Vldlr leads to tyrosine phosphorylation of Dab1 by SFKs, resulting in further feed-back of tyrosine kinase activation (Bock and Herz 2003). To determine the role of Dab1 in the Reelin-mediated modulation of

NMDA receptor activity, we compared the response of neurons from wild type and Dab1-deficient mouse embryos to Reelin (Figure 3.4). After glutamate application alone, the relative response of Dab1+/+ and Dab1-/- neurons was low and comparable (7.7% and 0%, respectively, Figure 3.4A-C and G-I). However, after Reelin treatment, 62.5% of the Dab1+/+ neurons (Figure 3.4D-F) responded to glutamate while only 4.8% of the Dab1-/- neurons (Figure 3.4J-L) showed any increase in intracellular Ca^{2+} levels.

Reelin-induced enhancement of glutamate-stimulated Ca^{2+} influx requires Src family tyrosine kinases

Reelin binding to Apoer2 and Vldlr activates Src family tyrosine kinases (SFKs) (Bock and Herz 2003) and tyrosine phosphorylation is known to modulate NMDA receptor activity (Yu, Askalan et al. 1997). To investigate the role of SFKs in the Reelin-induced enhancement of glutamate-stimulated Ca^{2+} influx, we employed a commonly used SFK inhibitor, PP2, and its inactive structural analog, PP3, in our assay. Pretreatment of neurons with PP2 almost completely abolished the Reelin response, with only 10.8% of neurons responding (Figure 3.5D-F), while 67.7% of the neurons responded to Reelin glutamate in presence of PP3 (Figure 3.5J-L). PP2 or PP3 alone did not affect the basal response rate with only 17.4% of the neurons treated with PP2 and 10.5% of the neurons treated with PP3 responding to glutamate.

Reelin increases tyrosine phosphorylation of NMDA receptors and NMDA currents

Src family kinases (SFK) can modulate NMDA receptor activity by altering the tyrosine phosphorylation status of NR2 subunits (Yu, Askalan et al. 1997). Since Reelin binding to Apoer2 and/or Vldlr could activate SFK in a Dab1-dependent manner (Bock and Herz 2003), we thus tested whether Reelin could modulate the tyrosine phosphorylation of NMDA receptor, which is likely the biochemical evidence for Reelin-mediated upregulation of NMDA activity. Since NR2B was the predominant NR2 subunit expressed in our cultured neurons, our study was focused on NR2B.

Myc-NR2B and c-Src were expressed in HEK-293 cells in the absence or presence of Dab1 (Figure 3.6A). NR2B then was immunoprecipitated and the tyrosine phosphorylation status of NR2B was determined by 4G10, an anti-phosphotyrosine antibody. The antibody specifically against the phosphorylated SFKs at Y416 was used to monitor the activity of c-Src, since phosphorylation of this residue is critical for Src activation (Brown and Cooper 1996). The tyrosine phosphorylation of NR2B was increased slightly by c-Src expression (lane 4), but increased dramatically when c-Src and Dab1 were coexpressed and mutually activated (lane 5). The Dab1-5F mutant (Howell, Lanier et al. 1999), in which tyrosines 185, 198, 200, 220, and 232 are mutated to phenylalanine, cannot undergo tyrosine phosphorylation and failed to activate c-Src (third panel of lane

6). As a result, c-Src didn't induce detectable increase in tyrosine phosphorylation of NR2B when coexpressed with Dab1-5F. This suggested that Dab1 could activate c-Src and subsequently increase the tyrosine phosphorylation of NR2B, which requires the tyrosine phosphorylation of Dab1.

We next examined the tyrosine phosphorylation of endogenous NR2B in cortical neuron cultures. We treated the neurons with Reelin-conditioned or control media at 4°C to avoid the rapid internalization of NR2B which could make the biochemical changes on NR2B undetectable. Since activities of most biological enzymes are largely lower at 4°C, we prolonged the treatment to 2 and 4 hours. Reelin treatment increased the tyrosine phosphorylation of NR2B (Figure 3.6B), which strongly implied that Reelin could alter the NMDA receptor channel property. To address this, a whole-cell patch clamp was performed on mouse hippocampal slices where synaptically evoked NMDA currents were recorded with holding potentials from –70 to 70 mV. 10 minutes Reelin treatment significantly increased the NMDA currents from –50 mV and throughout the holding potentials (Figure 3.7). This suggested that Reelin could increase the open probability of NMDA receptors.

Reelin increases glutamate-induced CREB Ser^{133} phosphorylation

cAMP-response element binding protein (CREB) is a transcription factor that is activated by increased intracellular calcium concentration. It turns on gene

transcriptions essential for neuronal survival and development, and synaptic plasticity (Shaywitz and Greenberg 1999). Phosphorylation of CREB at Ser133 is required for CREB-mediated gene transcription. To test whether Reelin-mediated modulation of the NMDA receptor can activate CREB, we determined the effect of Reelin on glutamate-stimulated CREB Ser133 phosphorylation in cortical neurons (Figure 3.8A). Cellular depolarization with KCl was used as a positive control to elicit Reelin and NMDA receptor independent stimulation of CREB phosphorylation (lane 6). Activation of the Reelin signaling pathway under the indicated conditions was monitored by determining tyrosine phosphorylation of Dab1 (Figure 3.8A, bottom panel). In the absence of Reelin and glutamate (lane 1) CREB phosphorylation was virtually undetectable. In the presence of Reelin alone, CREB phosphorylation increased slightly probably through Reelin activated kinases (lane 2). Addition of glutamate alone, without Reelin pretreatment, induced CREB phosphorylation, consistent with the small number of neurons that responded to glutamate alone in the Fura2 experiments. However, after pretreatment with Reelin, glutamate induced strong CREB Ser133 phosphorylation (lane 4), which was reduced to baseline levels (i.e. glutamate alone) by the NMDA receptor inhibitor D-APV (lane 5). Thus, all the observed Reelin-mediated increase of glutamate-induced CREB Ser133 phosphorylation was mediated by the effect of Reelin on the NMDA receptor.

To further confirm that Reelin can enhance glutamate-stimulated CREB Ser133 phosphorylation and nuclear localization, immunofluorescent staining was performed on cultured cortical neurons (Figure 3.8B). Microtubule-associated protein 2 (MAP2) was used to identify the neuronal cell population. Consistent with the results shown in Figure 3.8A, Reelin pretreatment dramatically increased the amounts of phosphorylated CREB in the nuclei of neurons upon glutamate stimulation, whereas glutamate or Reelin alone had little effect.

Discussion

The role of Reelin signaling pathway in the regulation of neuronal migration during development has been studied extensively (Tissir and Goffinet 2003). However, its function in mature synapse is unknown. In the current study, we have investigated the effect of Reelin signaling on the function of NMDA receptors by measuring NMDA receptor-dependent calcium influx in primary cortical neurons. We show that Reelin can potently enhance NMDA receptor activity upon glutamate stimulation in wild type cortical neurons (Figure 3.2) but not in Dab1-deficient neurons (Figure 3.4), which are unable to respond to Reelin. Inhibition of either SFK activity (Figure 3.5) or of Reelin binding to its receptors Apoer2 and Vldlr by RAP (Figure e.3) abolished this modulatory effect of Reelin. Reelin could increase NMDA receptor tyrosine phosphorylation and potentiate the NMDA receptor-mediated currents (Figure 3.6 and 3.7). Reelin-induced

increase of Ca^{2+} entry through NMDA receptors increased the phosphorylation of the transcription factor CREB (Figure 3.8). Taken together, we propose a model in which Reelin binding to its receptors results in the activation of SFKs (Figure 3.9). These kinases in turn enhance NMDA receptor activity through phosphorylation of tyrosine residues in the cytoplasmic domains of NR2 subunits, and alter the gating of the channel. The NMDA receptor is crucial for regulating synaptic plasticity, and thus for learning and memory, by controlling the flow of calcium ions during synaptic signal transmission. The present findings raise the possibility that Reelin might serve a function as a novel physiological signaling molecule that can selectively modulate synaptic plasticity and activity-dependent gene transcription by gating NMDA receptor-mediated calcium currents in mature synapses.

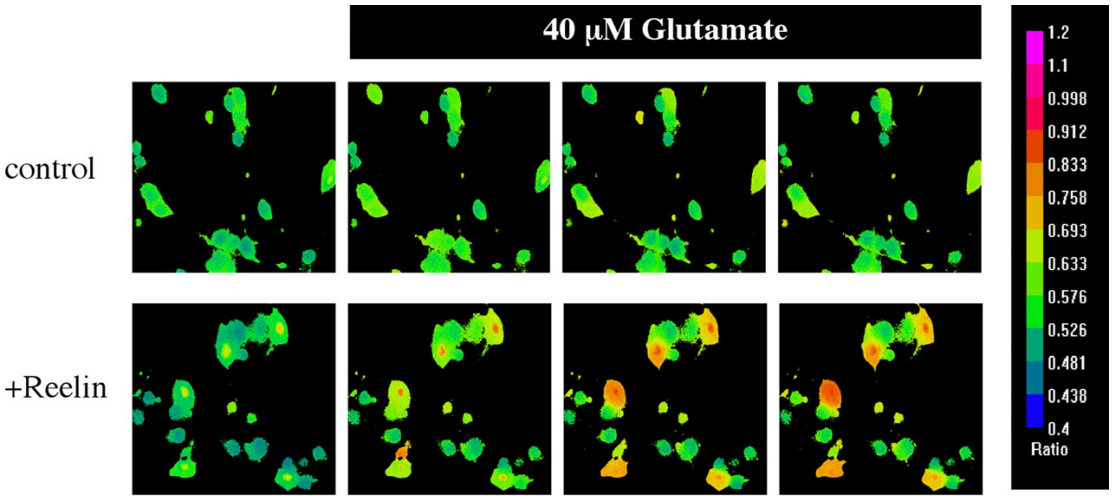

Figure 3.1. Representative images of Reelin-induced enhancement of Ca^{2+} influx in cortical neurons. Representative images representing fura-2-AM 340/380 ratios of Ca^{2+} transients induced by 40 μM glutamate in cortical neurons are shown. A pseudocolored calibration scale for 340/380 ratios is shown on the right. All recordings were carried out in ACSF supplemented with TTX, nimodipine and CNQX. Wild type neurons were recorded without (first row), and with Reelin treatment (second row). Fura-2-AM 340/380 ratio images are shown 30 seconds before (first column), and 30 seconds (second column), 1.5 minutes (third column), 3 minutes (fourth column) after application of 40 μM glutamate.

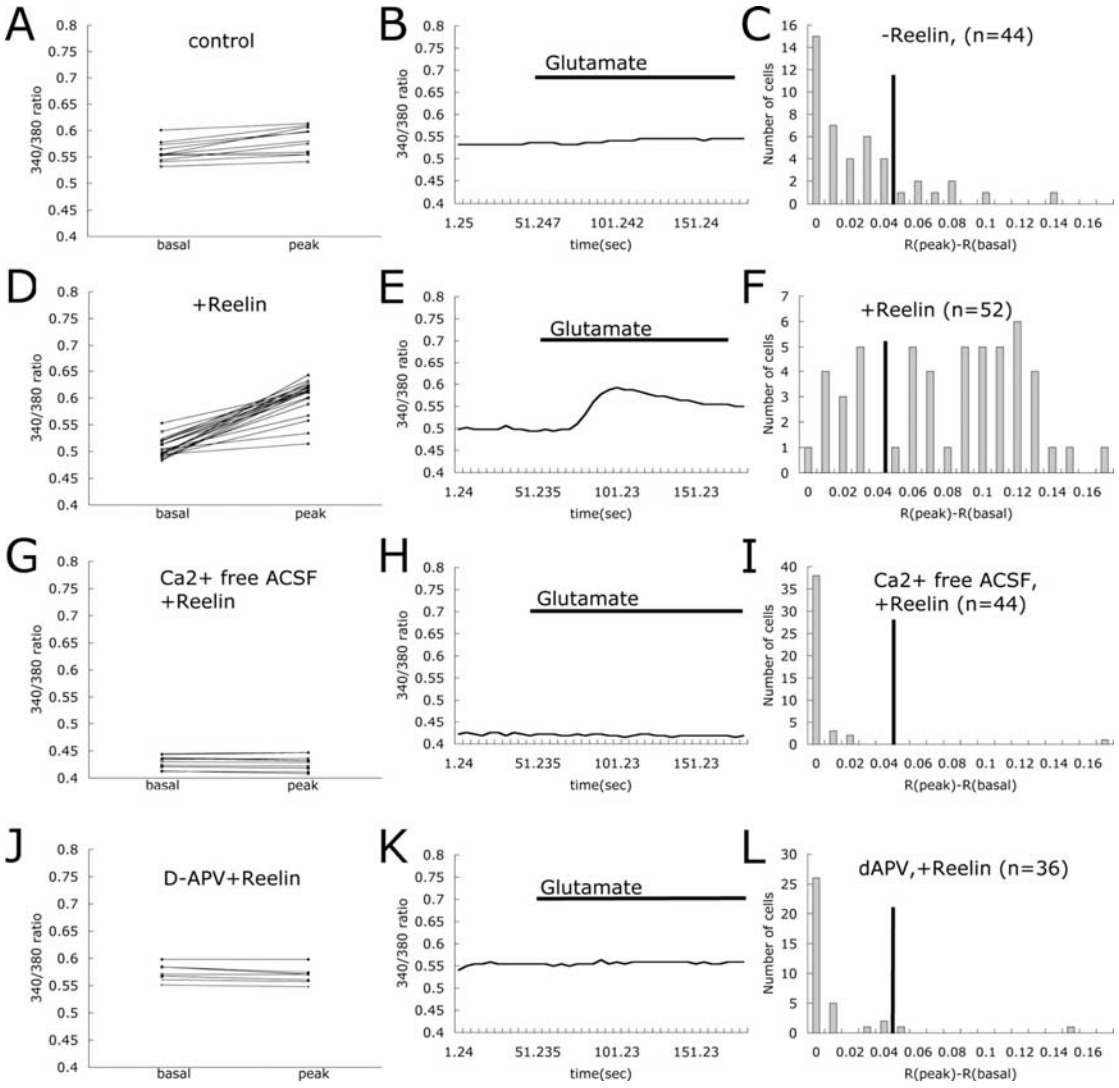

Figure 3.2. Reelin enhances glutamate stimulated Ca^{2+} influx through NMDA receptor in wild type cortical neurons. At 12-13 DIV, the cultured neurons were stimulated with glutamate in the presence of TTX, nimodipine and CNQX. *A*, basal and peak 340/380 ratios are shown for individual cortical neurons. Basal ratios were determined as the average of the ratio values 35 to 15 seconds prior to glutamate application. Peak values were determined from maximal signals observed 25 to 60 seconds after glutamate application. Trace of 340/380 ratio for the representative cell is shown in *B*. Presence of glutamate in the buffer is indicated by the horizontal bar. Changes of 340/380 ratios at peak and basal were calculated for each cells as R(peak)-R(basal). Cells from

representative 3 or 4 experiments were categorized by their R(peak)-R(basal) values and responding distribution of the cells was plotted in *C* (*n*=number of cells). Basal and peak 340/380 ratio, trace of representative 340/380 ratio and distribution of Reelin responding cells are shown in *D*, *E* and F respectively. Basal and peak 340/380 ratios are shown for individual Reelin treated neurons perfused with Ca^{2+} free ACSF (*G*) and D-APV (*J*). Traces of 340/380 ratios for representative cells are shown in *H* and *K*. Responding distributions for each different treatment are shown in *I* and *L* (*n*=number of cells).

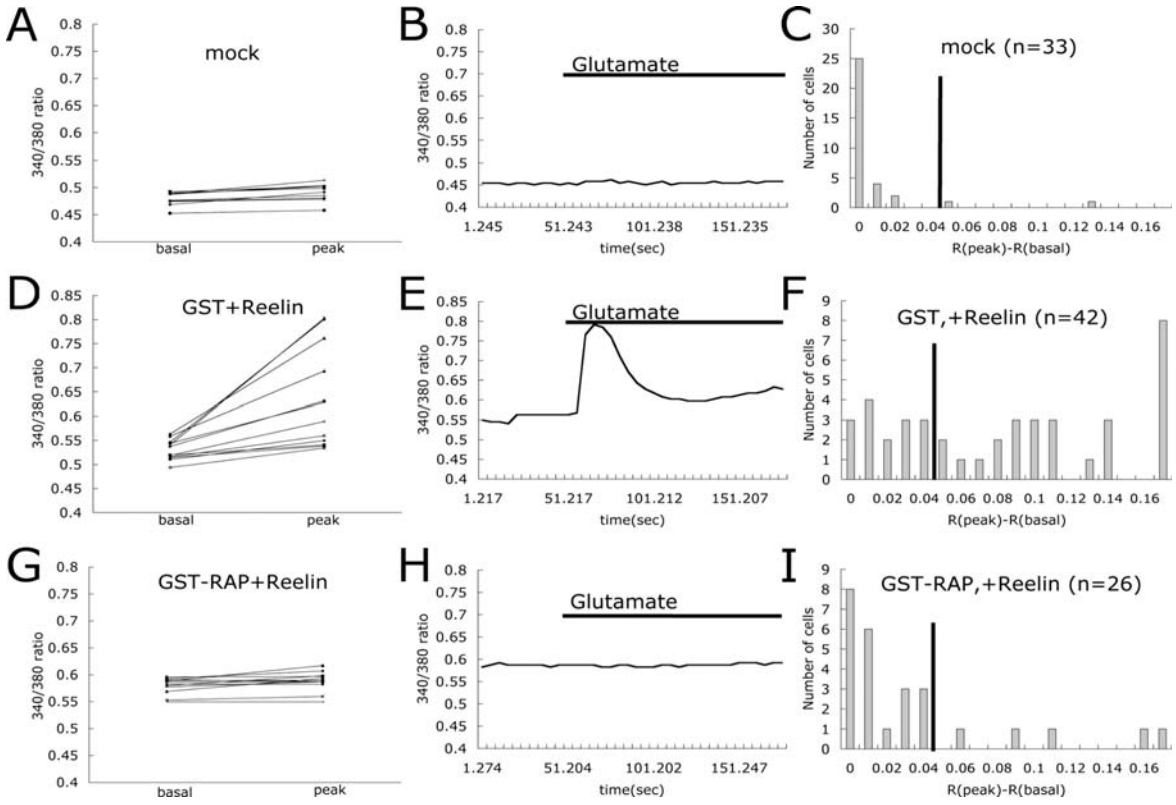

Figure 3.3. RAP, a ligand for LDLR family members, blocks Reelin-mediated enhancement of glutamate stimulated Ca^{2+} influx. Basal and peak 340/380 ratios are shown for individual cortical neurons treated with mock media (A), GST and Reelin (*D*), GST-RAP and Reelin (*G*). Traces of 340/380 ratios for representative cells are shown in (*B*), (*E*) and (*H*). Presence of glutamate in the buffer is indicated by the horizontal bar. Responding distributions for each different treatment are shown in (*C*), (*F*) and (*I*) (*n*=number of cells).

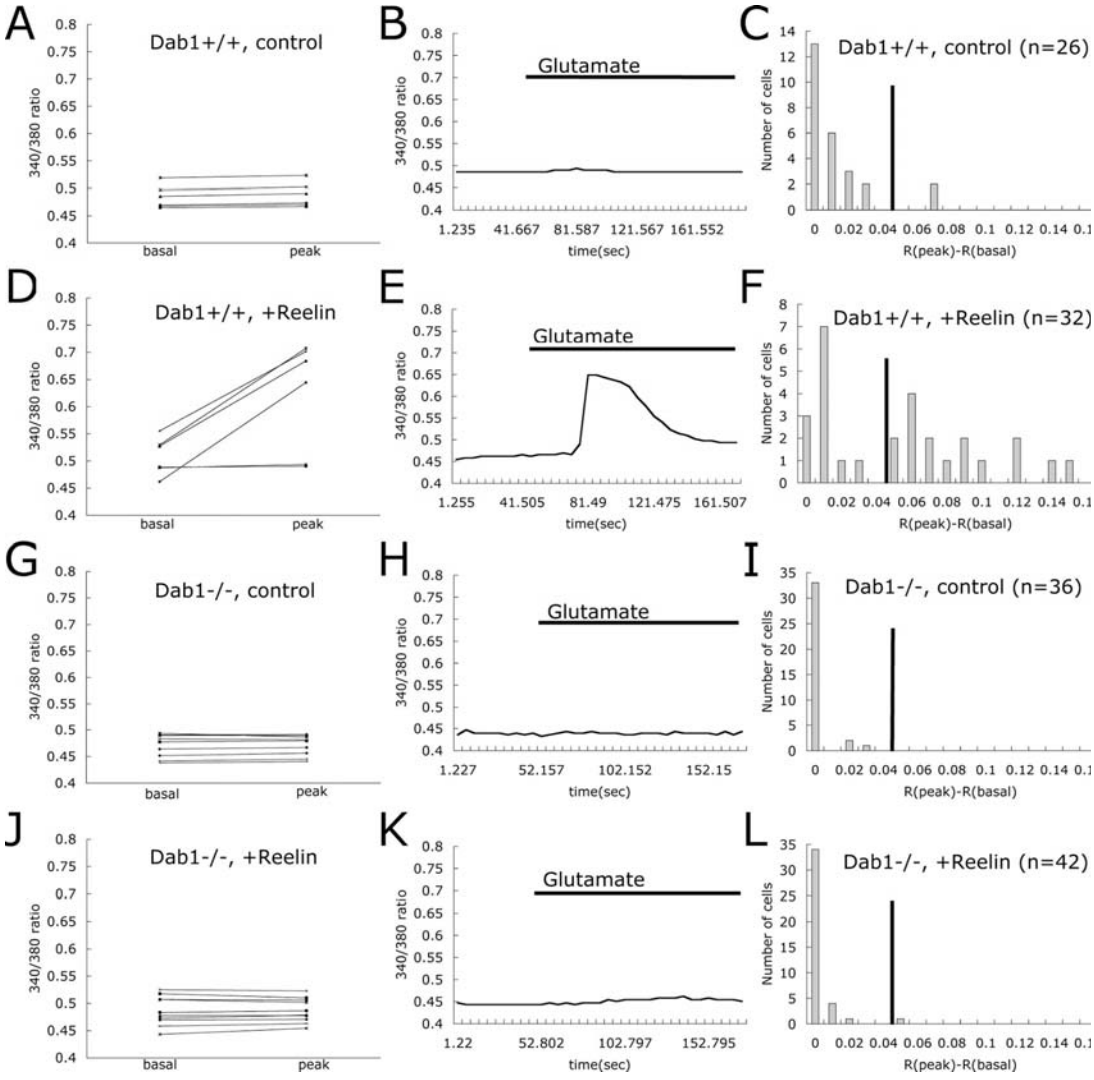

Figure 3.4. Dab1 is required for Reelin-induced enhancement of Ca^{2+} influx. Basal and peak 340/380 ratios are shown for individual Dab1 +/+ cortical neurons without treatment (*A*), Dab1 +/+ neurons treated with Reelin (*D*), Dab1 -/- neurons without treatment (*G*), Dab1 -/- neurons treated with Reelin (*J*). Traces of 340/380 ratio for representative cells are shown in (*B*), (*E*), (*H*) and (*K*). Presence of glutamate in the buffer is indicated by the horizontal bar. Responding distributions for each different treatment are shown in (*C*), (*F*), (*I*) and (*L*) (*n*=number of cells).

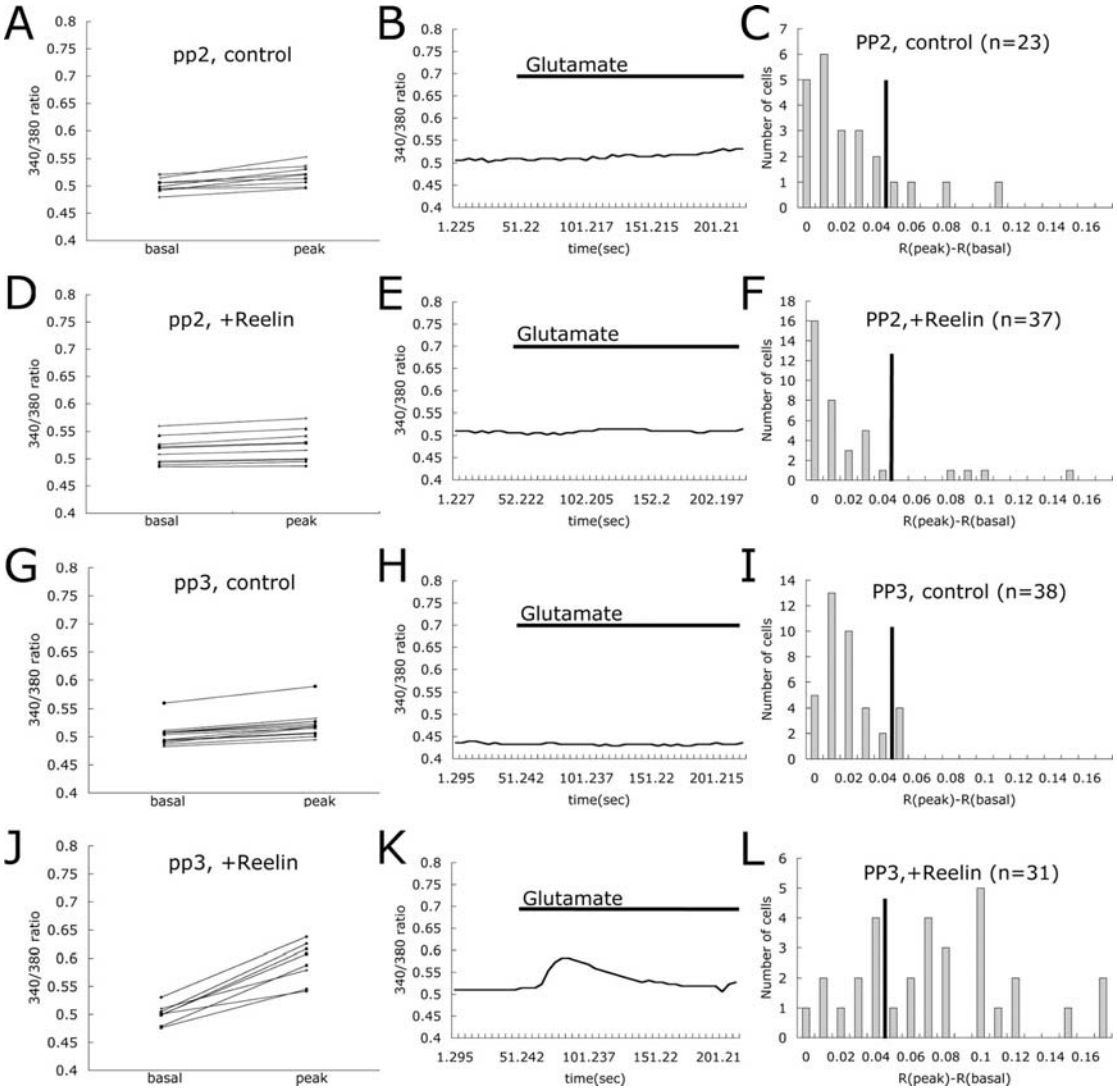

Figure 3.5. Src family tyrosine kinases are required for Reelin-induced enhancement of Ca^{2+} influx. Basal and peak 340/380 ratios are shown for individual cortical neurons treated with PP2 (*A*), PP2 and Reelin (*D*), PP3 (*G*), PP3 and Reelin (*J*). Traces of 340/380 ratio for representative cells are shown in (*B*), (*E*), (*H*) and (*K*). Presence of glutamate in the buffer is indicated by the horizontal bar. Responding distributions for each different treatment are shown in (*C*), (*F*), (*I*) and (*L*) (*n*=number of cells).

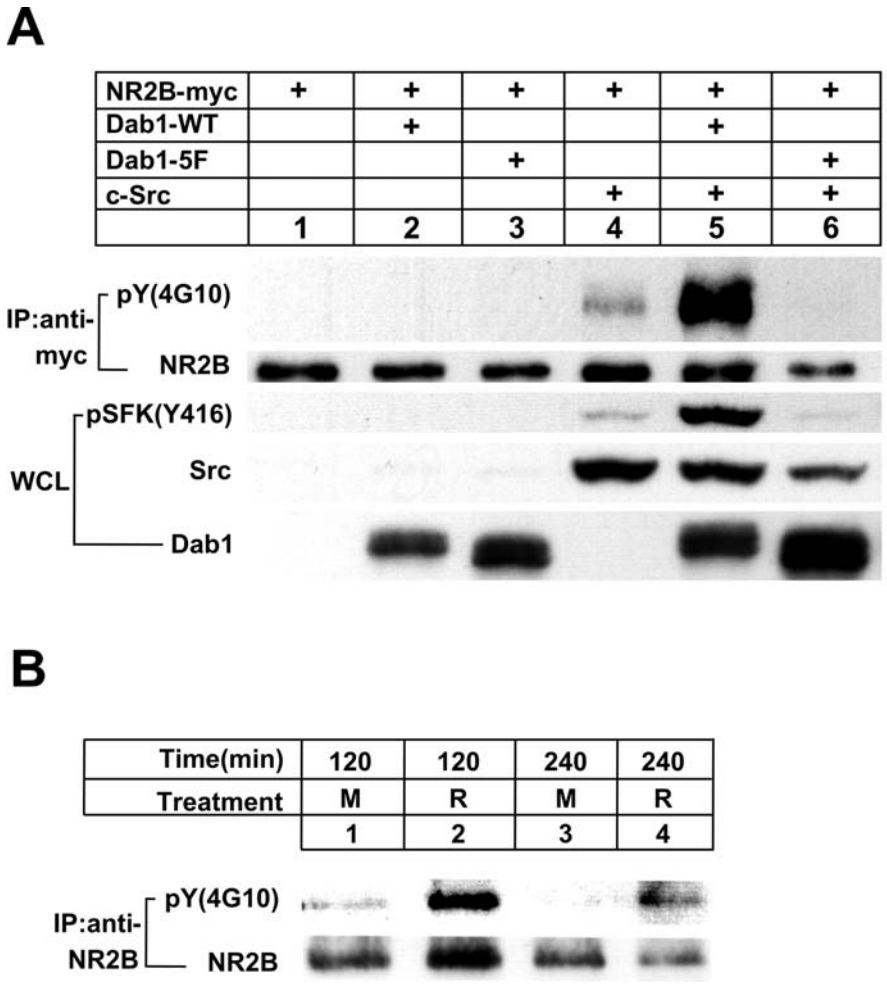

Figure 3.6. Reelin-Dab1 signal increases the tyrosine phosphorylation of NR 2B. *A*, HEK-293 cells were transfected with indicated expression vectors and cell lysates were analyzed by Western blotting for levels of phospho-SFK at Y416 (third panel), total Src (fourth panel), and total Dab1 (fifth panel). Myc-NR2B was immunoprecipitated from the lysates and analyzed for the level of tyrosine phosphorylation (pY, first panel). The level of NR2B (second panel) was used as the control to indicate the amount of immunoprecipitated myc-NR2B. *B*, Cortical neurons were treated in the absence (M) or presence (R) of Reelin at 4°C for indicated time. Cells were lysed and NR2B was immunoprecipitated from the lysates and analyzed for the level of tyrosine phosphorylation (pY, upper panel). The level of NR2B (lower panel) was used as the control to indicate the amount of precipitated NR2B.

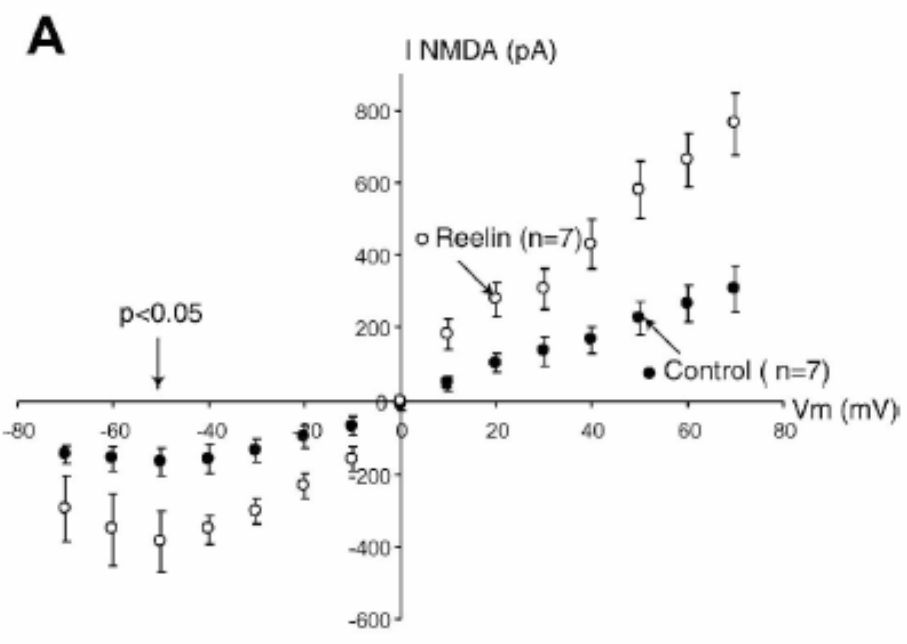
A
I NMDA (pA)
800
600
400
200
0
-200
-400
-600
Reelin (n=7)
Control (n=7)
p<0.05
-80
-60
-40
-20
0
20
40
60
80
Vm (mV)

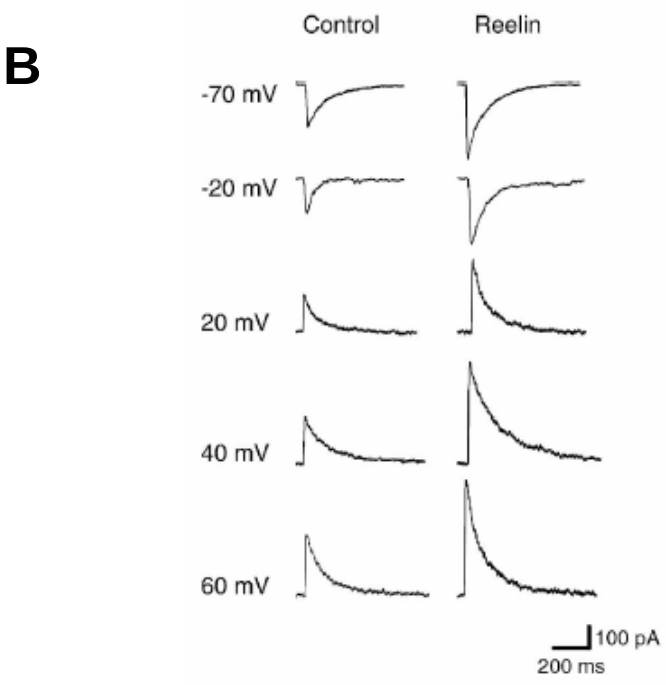
B
Control
Reelin
-70 mV
-20 mV
20 mV
40 mV
60 mV
100 pA
200 ms

Figure 3.7. Reelin potentiates synaptically evoked NMDA currents. *A*, responses were recorded using whole-cell voltage clamp at potentials varying between -70 and +70 mV. The graph illustrates the I-V relationship of the NMDA current recorded in the presence of $GABA_A$ and AMPA receptor antagonists in the presence of either control or Reelin-conditioned media. Values were obtained from 7 different CA1 pyramidal neurons. *I-V* curves were recorded 10 min after Reelin application. *B*, representative responses recorded at holding potentials between -70 and +70 mV (steps of 10 mV) after application of either control or Reelin-conditioned media. Reelin treatment significantly increased the amplitudes of NMDA currents at holding potentials greater than –50 mV.

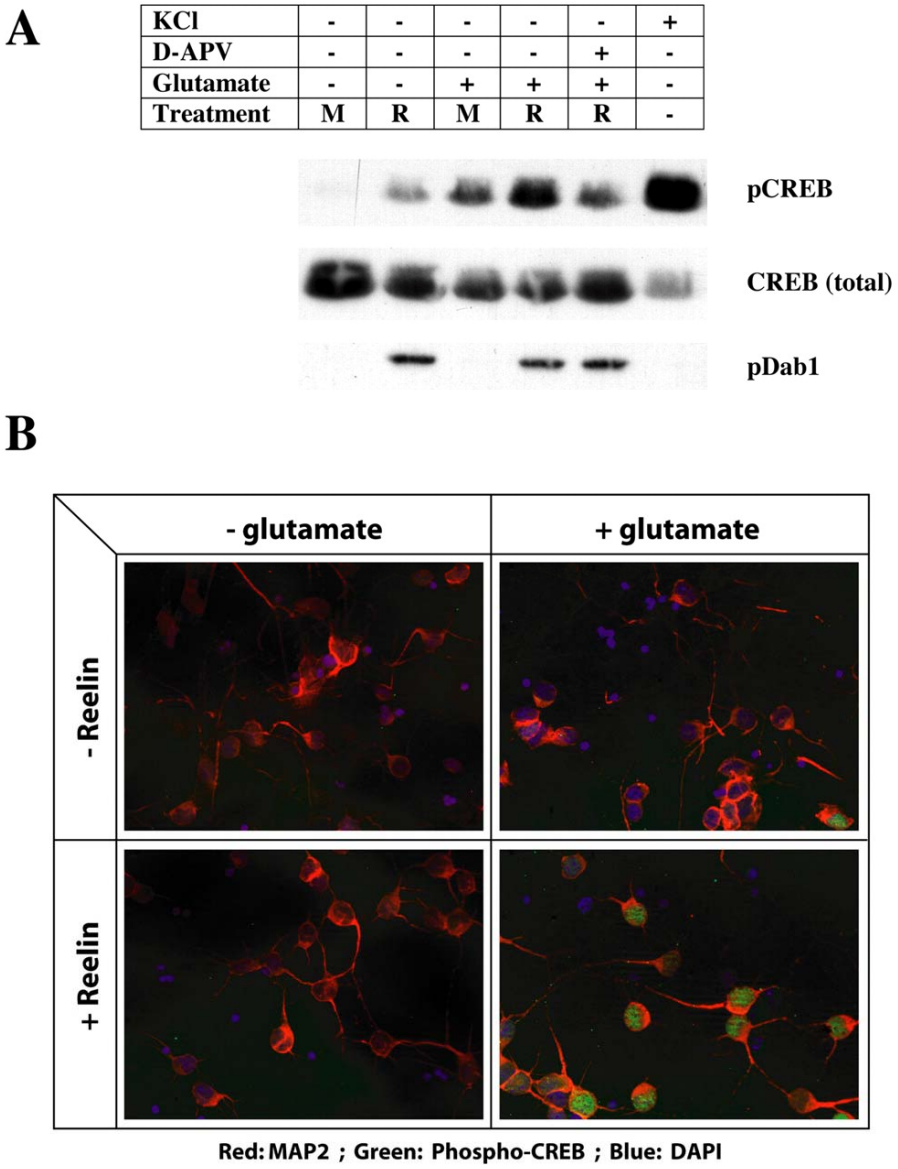

Figure 3.8. Reelin increases glutamate-induced CREB Ser^{133} phosphorylation. *A*, primary cortical neurons at 7 DIV were treated in the absence (M) or presence (R) of Reelin in ACSF supplemented with TTX, nimodipine and CNQX. D-APV (100µM) was applied to block NMDA receptors. Cells were stimulated with 10µM glutamate for 8 min, and lysates were analyzed by Western blot for levels of CREB phosphorylated at Ser133 (pCREB, top panel), total CREB (middle panel), and tyrosine phosphorylated Dab1 (pDab1,

bottom panel). The latter serves as an indicator of activation of the Reelin signaling pathway. 55mM KCl was applied in the absence of channel inhibitors as positive control to depolarize neurons and induce calcium entry through voltage-gated channel. *B*, mixed neuronal cultures were treated as described in *A* and analyzed by immunocytochemistry for the presence of Ser133 phosphorylated CREB in the nucleus (green). The neuronal cell population was identified with a monoclonal α-MAP2 antibody (red). Nuclei were visualized using DAPI (blue).

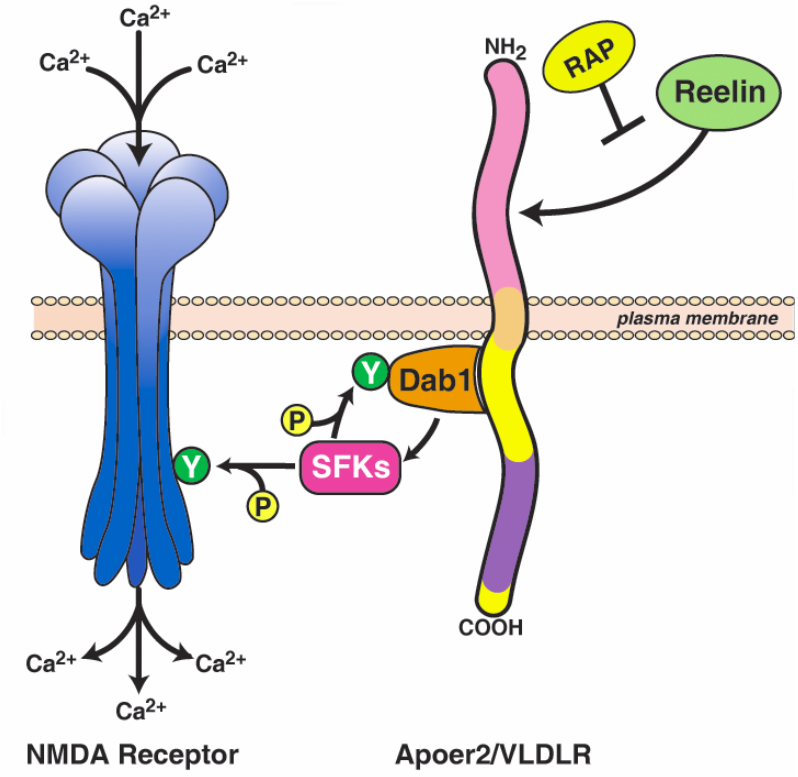

Figure 3.9 Model of Reelin-induced modulation of NMDA receptor function. Reelin binding to Apoer2 and/or Vldlr activates Src family tyrosine kinases (SFK) in the presence of Dab1. Dab1 is phosphorylated on tyrosine residues by activated SFK and further activates SFK, which may induce phosphorylation on NMDA receptor subunits or other components of the NMDA receptor complex. This results in increased Ca^{2+} conductance by NMDA receptors. Increased Ca^{2+} influx promotes the phosphorylation and thus activation of the transcription factor CREB and enhances the activity-dependent gene

transcription. RAP is a competitive inhibitor of ligand binding to all LDL receptor family members and blocks the interaction of Reelin with Apoer2 and Vldlr.

Materials and Methods

Calcium imaging

Primary neuron culture was prepared as described in Chapter 2. Neurons were plated on poly-D-lysine (Sigma) coated 12 mm round coverslips (Carolina biological supply company) at a density of 5×10^4 per cm^2 and were maintained at 37°C in a 5% CO_2 environment. At 12-13 DIV, the cortical neurons were loaded with 5 μM Fura2-AM (Molecular Probes) for 30 min at 37°C in artificial cerebrospinal fluid (ACSF) (140 mM NaCl, 5 mM KCl, 2.5 mM $CaCl_2$, 1.6 mM $MgCl_2$, 10 mM HEPES [pH 7.3], 24 mM D-glucose) supplemented with 1 μM tetrodotoxin (Sigma), 5 μM nimodipine (Sigma) and 40 μM CNQX (6-cyano-7-nitroquinoxaline-2,3-dione, Sigma). Calcium free ACSF was prepared by omitting $CaCl_2$ from ACSF and supplementing with 100 μM EGTA. The coverslips were then mounted onto a recording/perfusion chamber (RC-26G, Warner Instrument), positioned on the movable stage of an Olympus IX-70 inverted microscope, and perfused with supplemented ACSF by gravity flow. Images at 340 and 380 nm excitation wavelengths were acquired every 5 seconds

and shown as 340/380 image ratios as described (Tang, Tu et al. 2003). Neurons were stimulated with 40 μM glutamate (Sigma) after baseline measurements.

Data processing

Responses R(basal) and R(peak) indicate the fura-2 340/380 ratio values before and after glutamate application, respectively. [R(peak)- R(basal) = ΔR] indicates the change in the fura-2 340/380 ratios induced by glutamate in a certain cell. In the responding distribution chart, we defined the 0 value of ΔR as a response $0<\Delta R<0.01$, 0.01 as $0.01<\Delta R<0.02$, and so on. $\Delta R=0.17$ was defined as an upper cut-off value beyond which all cells were classified as ($\Delta R>0.17$). The basal ratios R(basal) were determined as the average of the ratio values 35 to 15 seconds prior to glutamate application. The peak values were determined from maximal signals observed 25 to 60 seconds after glutamate application. For each coverslip, we calculated the mean value and standard deviation (SD) of R(basal). Cells with R(basal) values > or < mean±SD were excluded. Cells were thus categorized into 18 groups (from 0 to 0.17) by their ΔR values. The total number of cells in each group was plotted as frequency histograms. To identify responding and non-responding cell populations we defined a threshold value in the valley between the peaks of the resulting bimodal distribution. This value was

set to ΔR=0.05, and cells with ΔR values equal or greater to 0.05 were defined as responders. A summary of the data is shown in Table 1.

Treatment	Percentage of responsive cells	*n* (number of coverslips)
Group 1		
Control	29.7 ± 1.6	5
Reelin	57.5 ± 4.4**	5
Reelin plus Ca^{2+}-free ACSF	2.50 ± 2.5	4
Reelin plus D-APV	5.50 ± 3.2	4
Group 2		
Mock control	10.4 ± 7.4	5
GST plus Reelin	44.6 ± 11.2*	5
GST–RAP plus Reelin	15.3 ± 1.7	4
Group 3		
Dab1+/+, control	24.6 ± 8.8	4
Dab1+/+, Reelin	47.9 ± 6.6**	7
Dab1−/−, control	14.4 ± 4.5	10
Dab1−/−, Reelin	11.7 ± 3.4	9
Group 4		
PP2, control	5.57 ± 3.8	7
PP2, Reelin	10.6 ± 3.3	5
PP3, control	27.4 ± 8.8	7
PP3, Reelin	48.1 ± 18.3*	5

Table 3.1. Activation of the Reelin signaling pathway enhances the response of cortical neurons to glutamate. At 12-13 DIV, the cultured cortical neurons were subjected to different treatments and stimulated with glutamate in the presence of TTX, nimodipine and CNQX. Percentage of responsive cells of each individual coverslip was calculated as described in 'Results'. Data are presented in the form of mean±SE (standard error). [$^{*}P<0.05$ and $^{**}P<0.01$ versus the first control in each group, one-way ANOVA test]

Reelin stimulation and inhibitors

Reelin- and mock- conditioned media were collected and concentrated as described in Chapter 2. Concentrated Reelin samples were purified by ion exchange on HiTrap Q HP (Amersham) and then by gel filtration on Sephacryl S300 (Amersham). Concentrated mock samples were subjected to the same purification procedure and the according fractions were collected. Reelin was applied to neuron culture at about 2.4-3 μg/ml for 25-30 minutes. The mock fractions were applied to neurons in exactly the same relative concentrations as Reelin samples. The GST receptor associated protein (RAP) fusion protein and GST protein were prepared as described (Herz, Goldstein et al. 1991). GST-RAP and GST were applied at 50 μg/ml for 50-60 min prior to and during Reelin stimulation. D-APV (2-amino-5-phosphonovalerate; Sigma) was applied at 10 μM to block NMDA receptors. PP2 (Calbiochem) and PP3 (Calbiochem) were applied at 10 μM for 60 min prior to and during Reelin stimulation or prior to acquiring images.

293 transfection and immunoprecipitation

HEK-293 cells (CRL-1573, ATCC) were cultured in DMEM (Cellgro) supplemented with 10% FCS and penicillin-streptomycin in 6-well culture plates. HEK-293 cells were transfected by FuGene 6 (Roche) with 1 μg pCMV-myc-NR2B, 1 μg pEF1α-mDab1 or 1 μg pEF1α-mDab1-5F and 0.5 μg pCMV-cSrc.

Dab1-5F bears mutations Y185F, Y198F, Y200F, Y220F, and Y232F. After 36-48 h, cells in each well were harvested by 200 μl lysis buffer as described in Chapter 2. The cell lysates were analyzed by Western blot using a polyclonal α-p-SFK antibody (Y416, Cell Signaling), a monoclonal α-Src antibody (GD11, Upstate Biotechnology) and a polyclonal α-Dab1 antibody (Trommsdorff, Gotthardt et al. 1999). Myc-NR2B was immunoprecipitated as described in Chapter 2. Elution from the beads was analyzed by Western blot using a monoclonal α-phosphotyrosine antibody (4G10, Upstate Biotechnology) and a polyclonal α-NR2B antibody (Santa Cruz Biotechnology).

Immunoprecipitation of neuronal NR2B

Primary neurons were treated with concentrated mock or Reelin-conditioned media for indicated time at 4°C and then lysed by RIPA buffer (PBS [pH 7.4], 2 mM EGTA, 5 mM EDTA, 1% Triton X-100, 0.5% SDS, 0.25% sodium deoxycholate, and protease and phosphatase inhibitor cocktails [Sigma]). Lysates were precleared by goat non-immune serum (Sigma) and incubated with 4 μg polyclonal α-NR2B antibody (Santa Cruz Biotechnology) at 4°C overnight. Immune complexes were precipitated by 40 μl protein G-sepharose slurry (Sigma). The elution from the beads was analyzed by Western blot using an α-

phosphotyrosine antibody (4G10, Upstate Biotechnology) and a polyclonal α-NR2B antibody (Upstate Biotechnology).

Hippocampal slice preparation

Transverse hippocampal brain slices (400 μm) were prepared from 12 to 21-day-old deeply anesthetized mice and incubated in oxygenated ACSF (123 mM NaCl, 5 mM KCl, 12 mM NaH_2PO_4, 26 mM $NaHCO_3$, 2 mM $CaCl_2$, 1 mM $MgCl_2$, 10 mM D-glucose) at 34°C for 30 min and thereafter at room temperature (24-27°C) for no less than 45 min. After cutting between CA1 and CA3 regions, individual slices were transferred to the recording chamber mounted on a Nikon (Tokyo, Japan) E600FN microscope. Slices were submerged and perfused with ACSF, which was continuously exchanged by through a gravity-driven perfusion system. Neurons were visualized using a water-immersion objective and Nomarski differential interference contrast optics. Images were detected with an infrared-sensitive video camera.

Whole-cell voltage-clamp recordings on CA1 pyramidal neurons

Patch electrodes (3-6 MΩ) were filled with the following (in mM): 110 K-gluconate, 20 KCl, 10 NaCl, 10 HEPES, 0.6 EGTA, 4 Mg-ATP, 0.3 GTP, and 10 *N*-ethyl bromide quaternary salt, pH 7.2. Series resistance (R_s) ranged from 5 to 15 MΩ. Experiments in which R_s varied ≥20% within a recording session were

discarded. Recordings were obtained with an Axopatch-200B patch-clamp amplifier (Molecular Devices) digitized and 10 kHz through Digidata 1322A (Molecular Devices). EPSCs were evoked by stimulation (duration, 200 μs; amplitude, 10-100 μA) of Schaeffer collateral commissural afferents using concentric bipolar electrodes through a stimulus isolation unit (A365, World Precision Instruments) driven by a stimulator (Grass S88, Grass Instruments). I-V curves for NMDA currents were plotted in the presence of Reelin (estimated at about 5 nM) or control media. To isolate NMDA currents, the AMPA receptor antagonist CNQX (10 μM, Sigma) and the GABA receptor antagonist picrotoxin (50 μM, Sigma) were added. Statistical differences were established using the two-tailed student's t test. All data are expressed as mean ± SEM.

Phospho-CREB immunoblot

After treatment with concentrated mock or Reelin-conditioned media for 20 min at 37°C, neurons were lysed in SDS-PAGE sample buffer. Lysates were separated by SDS-PAGE. The gel was transferred to PVDF membrane and the membrane was immunoblotted with a polyclonal -phospho-CREB (Ser133) antibody (Cell Signaling), a polyclonal α-CREB antibody (Cell Signaling) and a monoclonal α-phosphotyrosine antibody (4G10, Upstate Biotechnology).

Immunofluorescent imaging

After treatment, primary neurons were fixed by 4% paraformaldehyde for 10 min at room temperature. After rinsing in PBS, fixed cells were incubated in blocking buffer (PBS with 1% BSA and 5% normal goat serum) for 1 hour. Neurons were then incubated overnight with primary antibodies diluted in blocking solution at 4°C. An α-phospho-CREB (Ser133) antibody (Cell Signaling) and a monoclonal α-MAP2 antibody (Sigma) were used at final concentrations of 1:100 and 1:500, respectively. After washing with PBS containing 0.1% BSA, cells were incubated with the appropriate secondary antibodies (Molecular Probes) for 1 hour at room temperature and mounted on microscope slides with DAPI-containing mounting medium (VECTASHIELD, Vector Laboratories, VT). Fluorescent images were acquired using a Zeiss Axioplan 2 imaging microscope and AixoVision software.

CHAPTER FOUR

Role of the Intracellular Domain of Apoer2 in NMDA Receptor Regulation

Abstract

Apoer2 and Vldlr transmit signaling from their ligand Reelin to cytoplasmic adaptor protein Dab1 and Src family kinases (SFKs) on the surface of neurons. The activation of this pathway is essential for proper neuronal migration during embryonic development. We recently have found that this Reelin induced signaling can physiologically modulate the tyrosine phosphorylation and the activity of NMDA-type of glutamate receptor in primary cortical neurons. In this chapter, we show that Apoer2 is required for Reelin to potentiate the tyrosine phosphorylation of as well as the calcium influx through NMDA receptor whereas Vldlr is dispensable. Reelin-mediated regulation of NMDA receptor function requires the binding of Dab1 to a conserved NPxY motif in Apoer2 as well as the presence of amino acids that are encoded by an alternatively spliced exon 19 in the cytoplasmic domain of Apoer2. These findings reveal the signaling mechanism by which the receptors for Reelin regulate NMDA receptor activity.

Introduction

Apoer2 and Vldlr, members of LDL receptor gene family, are receptors for Reelin, a large secreted protein produced by Cajal-Retzius neurons at the surface of the developing neocortex (D'Arcangelo, Homayouni et al. 1999; Hiesberger, Trommsdorff et al. 1999). The association of Reelin to Apoer2 and Vldlr activates non-receptor tyrosine kinases of the Src family (SFKs) and induces tyrosine phosphorylation of Dab1, an adaptor protein that binds to the NPxY motifs in the intracellular domains of Vldlr and Apoer2 (Trommsdorff, Borg et al. 1998; Howell, Herrick et al. 1999; Bock and Herz 2003). This Reelin signaling is essential for the proper neuronal migration and layering of neocortex during embryonic development (D'Arcangelo, Miao et al. 1995; Howell, Hawkes et al. 1997; Trommsdorff, Gotthardt et al. 1999). In this process, Apoer2 and Vldlr function in a partly redundant manner. Either Apoer2 or Vldlr is able to tyrosine phosphorylate Dab1 in response to Reelin (Beffert, Morfini et al. 2002). The brains of mice that are deficient in only one of the receptors only display mild neuroanatomical abnormalities (Trommsdorff, Gotthardt et al. 1999).

After the fetal neuronal migration period, Reelin-expressing Cajal-Retzius neurons are largely replaced by Reelin-expressing GABA-ergic interneurons that are dispersed throughout the neocortex and hippocampus. The Reelin receptors Apoer2 and Vldlr, and the adaptor protein Dab1 remain expressed in the adult brain. Our lab has shown that Reelin signaling can potently modulate long-term

potentiation (LTP) and learning in the adult mice (Weeber, Beffert et al. 2002). In this process, Apoer2 and Vldlr function in a non-redundant fashion. Neither in the Vldlr-deficient mice nor in the Apoer2-deficient mice did Reelin produce any enhancement of LTP induction, suggesting that both Apoer2 and Vldlr are required for Reelin to regulate synaptic plasticity *in vivo*.

The intracellular domain (ICD) of Apoer2 interacts with several cytoplasmic adaptor and scaffolding proteins, including Dab1 (Trommsdorff, Gotthardt et al. 1999), PSD-95 (Gotthardt, Trommsdorff et al. 2000), and JIP1 and 2 (Trommsdorff, Gotthardt et al. 1999; Gotthardt, Trommsdorff et al. 2000). Dab1 binds through its PTB domain to a conserved NPxY motif in the ICD of Apoer2 (Stolt, Jeon et al. 2003; Yun, Keshvara et al. 2003). PSD-95 and JIP1/2 interact with the amino acid sequences encoded by the alternatively spliced exon19 in the Apoer2 ICD (Trommsdorff, Gotthardt et al. 1999; Stockinger, Brandes et al. 2000). Beffert et al, using knockin approach, generated four strains of mice with mutations in the Apoer2 ICD (Figure 4.1). Two of these mice express Apoer2 that either constitutively express the alternatively spliced exon19 (*ex19*) or lack it completely (*Δex19*) (Beffert, Weeber et al. 2005). The third strain expresses receptor that is truncated four amino acids after the NPxY motif (*Stop*). The fourth strain expresses full length Apoer2 tail with amino acid replacements in the Dab1 binding motif that prevent Dab1 interaction (*EIG*) (Beffert, Durudas et al. 2006). Reelin could not enhance LTP in hippocampal slices from *Apoer2* (*EIG)*,

Apoer2 (*Δex19)*, or *Apoer2* (*Stop)*, suggesting that both Dab1 binding and exon 19 are required for Reelin and Apoer2-dependent regulation of synaptic plasticity.

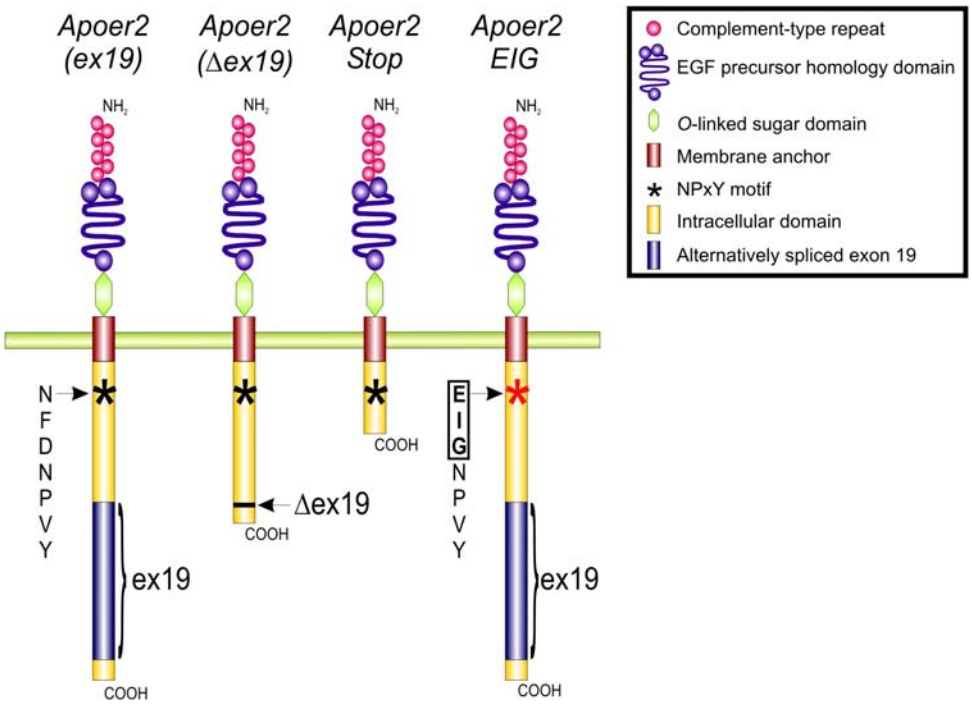

Figure 4.1 Schematic illustration of the four receptor mutants. *Apoer2* (*ex19)* and *Apoer2* (*Δex19)* represent wild type splice variants of exon 19. *Apoer2* (*Stop)* terminates the ICD at residue 904 (full length receptor, 996 amino acids) in exon 18, between the NPxY motif and exon 19. *Apoer2* (*EIG)* is identical to *Apoer2* (*ex19)* except for the amino acid changes N893E, F894I and D895G immediately preceding the NPxY motif. (Not drawn to scale).

In chapter 3, we have shown that Reelin regulates the activity of and the Ca^{2+} influx through NMDA receptor in primary neurons. This is the first direct evidence for a physiological role of Reelin signaling in the regulation of glutamatergic synaptic activity. We have also demonstrated that this function of

Reelin requires Dab1 and SFKs and the binding of Reelin to its lipoprotein receptors. However, the specific roles of Apoer2 and Vldlr in the process are not clear. In this chapter, we have characterized the role of Apoer2 and Vldlr in NMDA receptor regulation, and identified the cytoplasmic domains of Apoer2 that are required for NMDA receptor regulation.

Results and Discussion

Apoer2 and Vldlr function in a partly redundant manner in regulating neuronal migration during development (Trommsdorff, Gotthardt et al. 1999). However, Apoer2 and Vldlr function in a non-redundant fashion when enhancing LTP in response to Reelin (Weeber, Beffert et al. 2002). In order to identify the precise role of Apoer2 and Vldlr in NMDA receptor regulation, we prepared primary neurons from Apoer2-deficient (*Apoer2-/-*) or Vldlr-deficient (*Vldlr-/-*) mouse embryos (Trommsdorff, Gotthardt et al. 1999) and measured the calcium influx in response to Reelin and glutamate as described in Chapter 3. Under our experimental condition, glutamate alone could not elicit Ca^{2+} influx. After Reelin treatment, glutamate evoked strong Ca^{2+} influx in wild type neurons as described in Chapter 3. Neither Apoer2- or Vldlr-deficient neurons responded to glutamate as expected. After Reelin treatment, glutamate stimulated significantly large Ca^{2+} influx in Vldlr-deficient neurons (Figure 4.2B). However, after Reelin treatment, glutamate-stimulated Ca^{2+} influx in Apoer2-deficient neurons was only

comparable to that in cells in control group (Figure 4.2A). Next, we went on to determine whether Reelin could stimulate tyrosine phosphorylation of NMDA receptor in the absence of Apoer2 or Vldlr. Reelin could not induce tyrosine phosphorylation of NR2A or NR2B subunits in Apoer2-deficient neurons (Figure 4.3A); whereas in Vldlr-deficient neurons Reelin stimulated tyrosine phosphorylation of NR2A and NR2B to the similar level as observed in wild type neurons (Figure 4.3B). These data suggest that Apoer2 is required for Reelin to potentiate the tyrosine phosphorylation of as well as the calcium influx through NMDA receptor, whereas Vldlr is dispensable.

Primary cortical neurons were prepared from knockin mice strains that express Apoer2 mutants *Apoer2* (*ex19*), *Apoer2* (*Δex19*), *Apoer2* (*EIG*), or *Apoer2* (*Stop*) respectively. As described above, glutamate-stimulated calcium influx and tyrosine phosphorylation of NR2 subunits were determined in these neurons treated with control or Reelin-conditioned media. In neurons expressing *Apoer2* (*Stop*), Reelin could not stimulate Ca^{2+} influx (Figure 4.4) or tyrosine phosphorylation of NR2 subunits (Figure 4.5), suggesting that the C-terminus of Apoer2 is required for NMDA receptor regulation. Neurons expressing *Apoer2* (*ex19*) responded to Reelin similarly to wild type neurons in both Ca^{2+} imaging and NR2 phosphorylation assays. However, in neurons expressing *Apoer2* (*Δex19*), we did not observe any Ca^{2+} influx or tyrosine phosphorylation of NR2 in response to Reelin treatment (Figure 4.6). This indicates that ex19 of Apoer2 is

required for Reelin-mediated NMDA receptor regulation. Last, Reelin could neither stimulate Ca^{2+} influx through NMDA receptor nor tyrosine phosphorylate NR2 subunits in neurons expressing *Apoer2* (*EIG*) (Figure 4.7), suggesting that the interaction of Apoer2 ICD with Dab1 is required for Reelin to regulate NMDA receptor activity.

In summary, Apoer2 is the major receptor for Reelin to regulate NMDA receptor activity, whereas Vldlr only plays a minor role. Two functional domains in Apoer2 ICD are required in this process: Dab1 binding motif as well as the amino acids encoded by exon 19. An intact Dab1 binding motif is necessary for the relay of kinase signaling stimulated by Reelin (Beffert, Durudas et al. 2006). Ex19-encoded sequence preferentially binds PSD-95, an abundant scaffolding protein in the post-synaptic density that physically couples Apoer2 with NMDA receptor complex (Beffert, Weeber et al. 2005). The results in this chapter indicate that both events are essential for the regulation of NMDA receptor activity by Reelin and Apoer2.

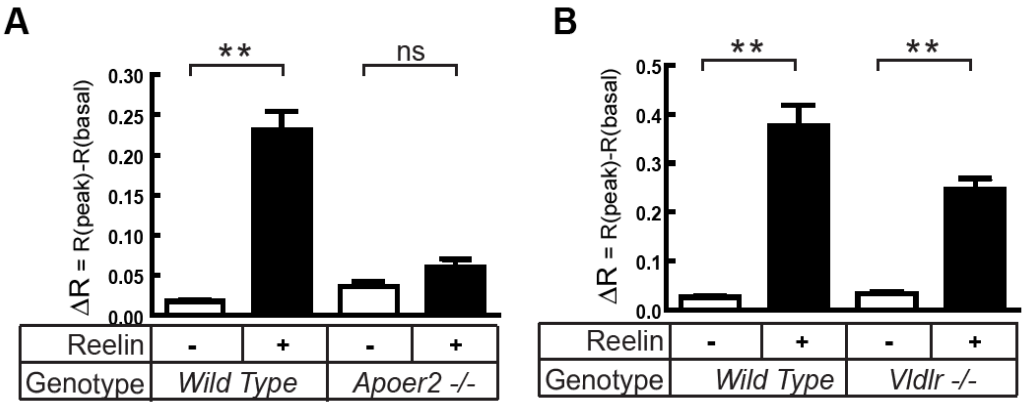

Figure 4.2 Apoer2, but not Vldlr, is required for Reelin-induced enhancement of Ca^{2+} influx through NMDA receptor. The primary neurons from wild type, Apoer2-deficient (*A*) or Vldlr-deficient (*B*) mouse embryos were stimulated with 20 μM glutamate in the presence of TTX, nimodipine and CNQX at 12-13 DIV. ΔR values, indicating the maximal changes in fura-2 340/380 ratio induced by glutamate, are summarized. ** or 'ns' on the brackets indicates significant difference ($p<0.001$) or not significant respectively. Error bars indicate SEM.

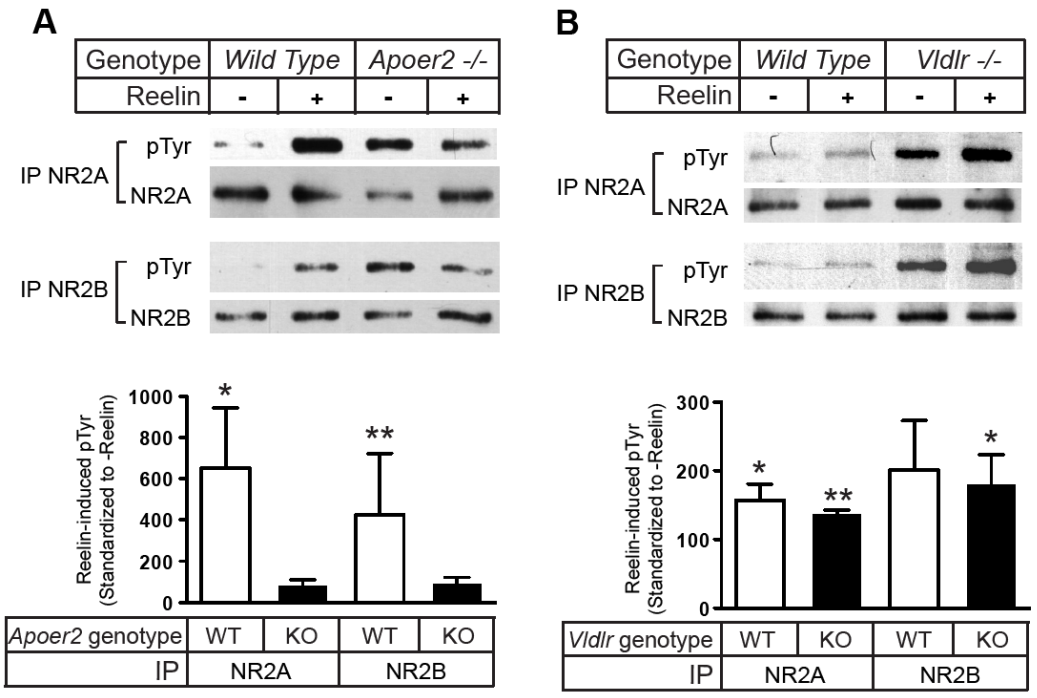

Figure 4.3 Reelin-stimulated tyrosine phosphorylation of NR2A and NR2B requires Apoer2. Primary neurons obtained from wild type, Apoer2-/- (*A*), or Vldlr-/- (*B*) mouse embryos were treated with control or Reelin-conditioned media. NR2A and NR2B were immunoprecipitated from the homogenized cell lysates and analyzed for tyrosine phosphorylation (pTyr). Total amounts of immunoprecipitated NR2A and NR2B are also shown (NR2A, NR2B). Quantification analysis from 4 independent experiments is summarized in the form of column graph shown below the blots. Phospho-tyrosine levels of NR2A and NR2B were firstly normalized to total NR2A and NR2B respectively. Reelin-induced tyrosine phosphorylation levels were then standardized to control (-Reelin) as presented in the graphs. * above individual column indicates significant difference (*$p<0.1$, **$p<0.05$) compared to control (-Reelin). Reelin treatment significantly increased tyrosine phosphorylation of both NR2A and NR2B in both wild type and *Vldlr-/-* neurons, but did not significantly change the tyrosine phosphorylation of either NR2A or NR2B in *Apoer2 -/-* neurons. Error bars indicate SEM.

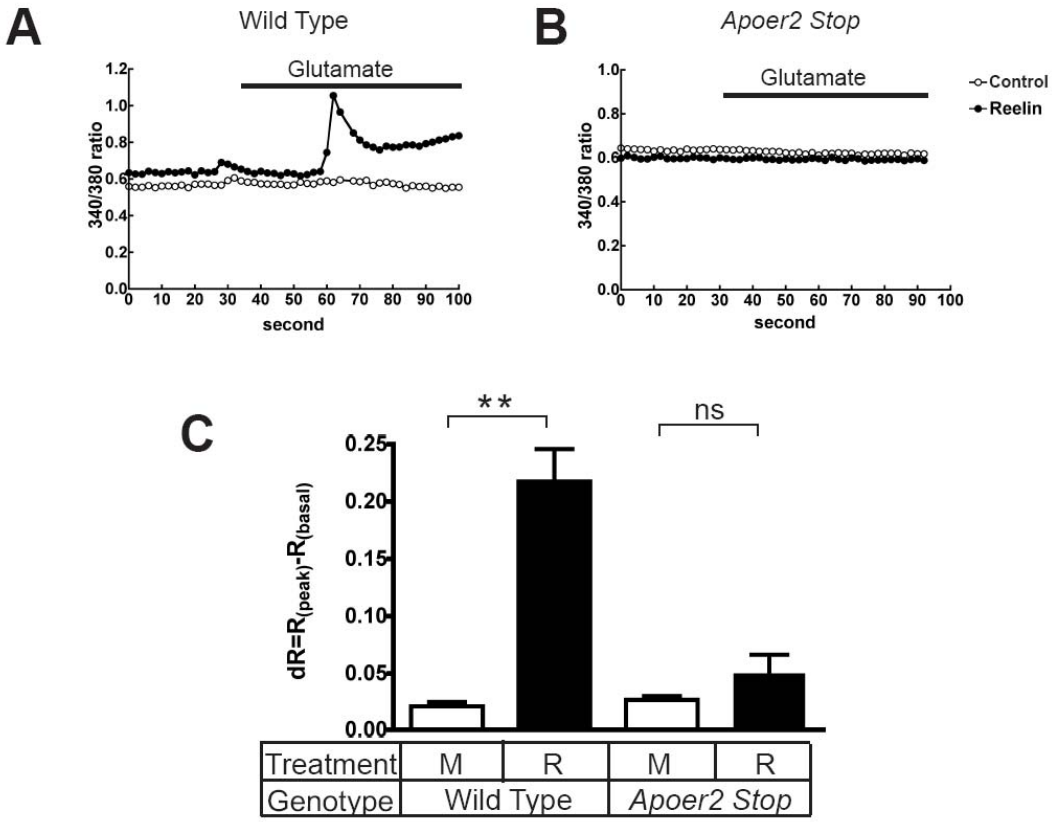

Figure 4.4 C-terminus of Apoer2 is required for Reelin to enhance NMDA receptor-mediated Ca^{2+} influx. The cortical neurons were stimulated with glutamate in the presence of TTX, nimodipine and CNQX at 12-13 DIV. *A*, the $[Ca^{2+}]_i$ of wild type neurons pretreated with control (open circle) or Reelin (black circle) are represented as the traces of 340/380 ratio of fura-2. The presence of glutamate in the perfusion buffer is indicated by the horizontal bar. Traces of 340/380 ratios from *Apoer2 Stop* neurons pretreated with control (open circle) or Reelin (black circle) are shown in (*B*). Maximum changes in 340/380 ratio induced by glutamate (ΔR) are summarized in (*C*). ΔR values of Reelin-treated wild type neurons (n=38) is significantly higher than those of control-treated wild type neurons (n=32). (** $p<0.001$) There is no significant (ns) difference in ΔR values between control-treated (n= 49) and Reelin-treated (n=50) *Apoer2 Stop* neurons. Error bars indicate SEM.

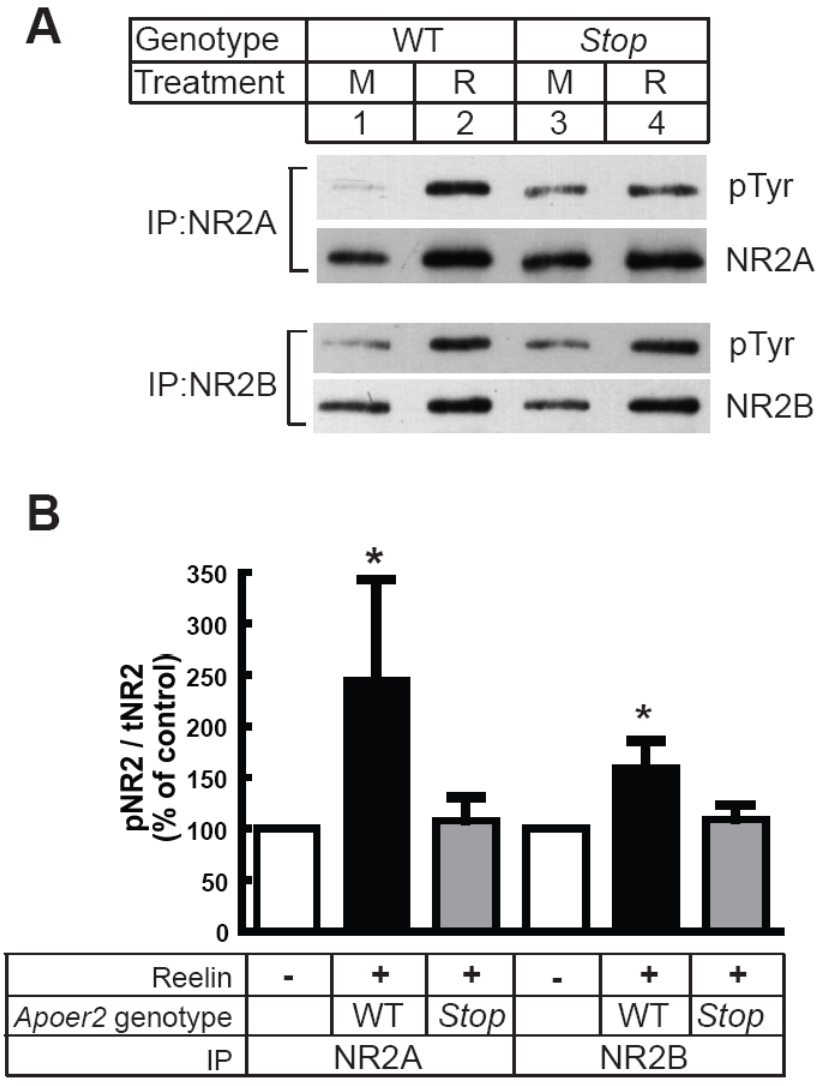

Figure 4.5 C-terminus of Apoer2 is required for Reelin-stimulated NMDA receptor phosphorylation. *A*, acute hippocampal slices obtained from wild type and *Apoer2 Stop* mice were treated by control (*M*) or Reelin (*R*) containing media. NR2A and NR2B were immunoprecipitated from the homogenized lysates of the slices and analyzed for tyrosine phosphorylation (pTyr). Total amounts of immunoprecipitated NR2A and NR2B are also shown (NR2A, NR2B). *B*, Quantification analysis from 4 independent experiments is summarized. Tyrosine-phosphorylated NR2A and NR2B levels were normalized to total NR2A and NR2B respectively. Reelin treatment (+Reelin) significantly increased tyrosine phosphorylation of both NR2A and NR2B in wild type slices

(* $p<0.1$ compared to control (-Reelin)). Reelin treatment did not significantly change the tyrosine phosphorylation of either NR2A or NR2B in *Apoer2 Stop* slices. Error bars indicate SEM.

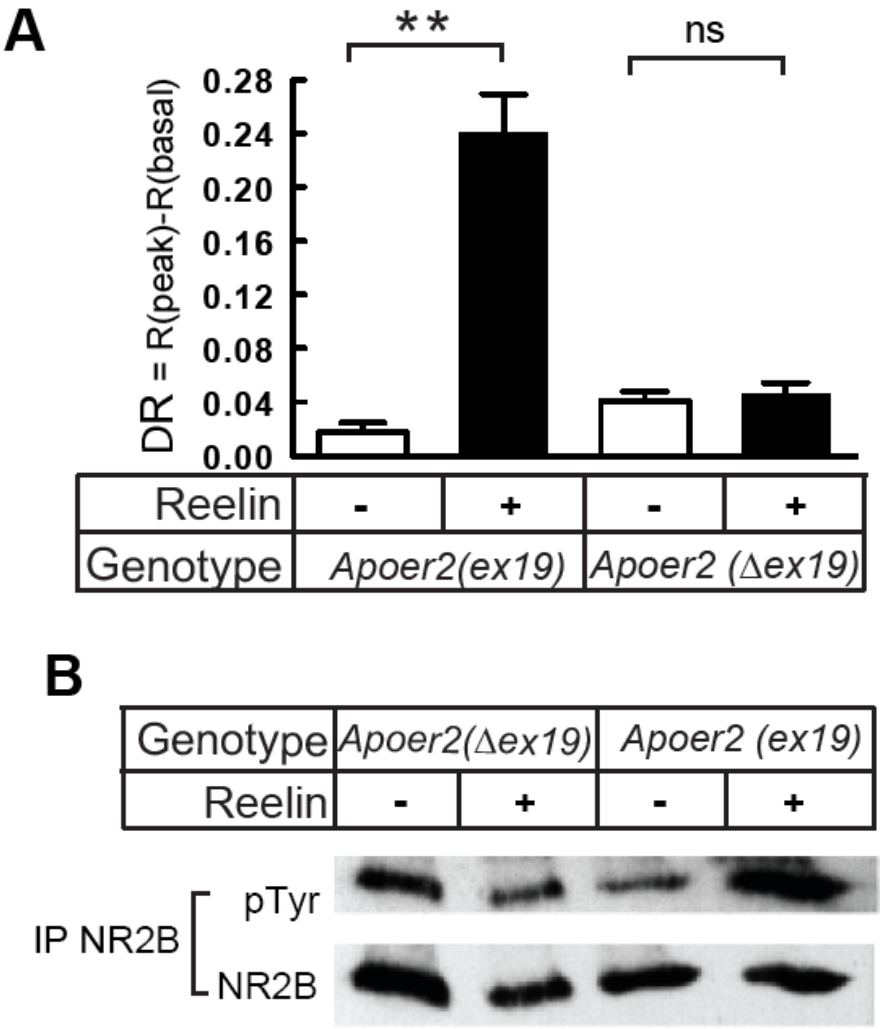

Figure 4.6 Ex19 of Apoer2 is required for Reelin-induced regulation of NMDA receptor activity. *A,* the primary neurons from *Apoer2(ex19)* or *Apoer2(Δex19)* mouse embryos were stimulated with glutamate in the presence of TTX, nimodipine and CNQX at 12-13 DIV. ΔR values, indicating the maximal changes in fura-2 340/380 ratio induced by glutamate, are summarized. ** or 'ns' on the brackets indicates significant difference ($p<0.001$) or not significant respectively. Error bars indicate SEM. *B*, primary neurons obtained from *Apoer2(ex19)* or *Apoer2(Δex19)* mouse embryos were treated by control or Reelin-conditioned media. NR2B were immunoprecipitated from the homogenized cell lysates and analyzed for tyrosine phosphorylation (top panel). Total amounts of immunoprecipitated NR2B are also shown (bottom panel).

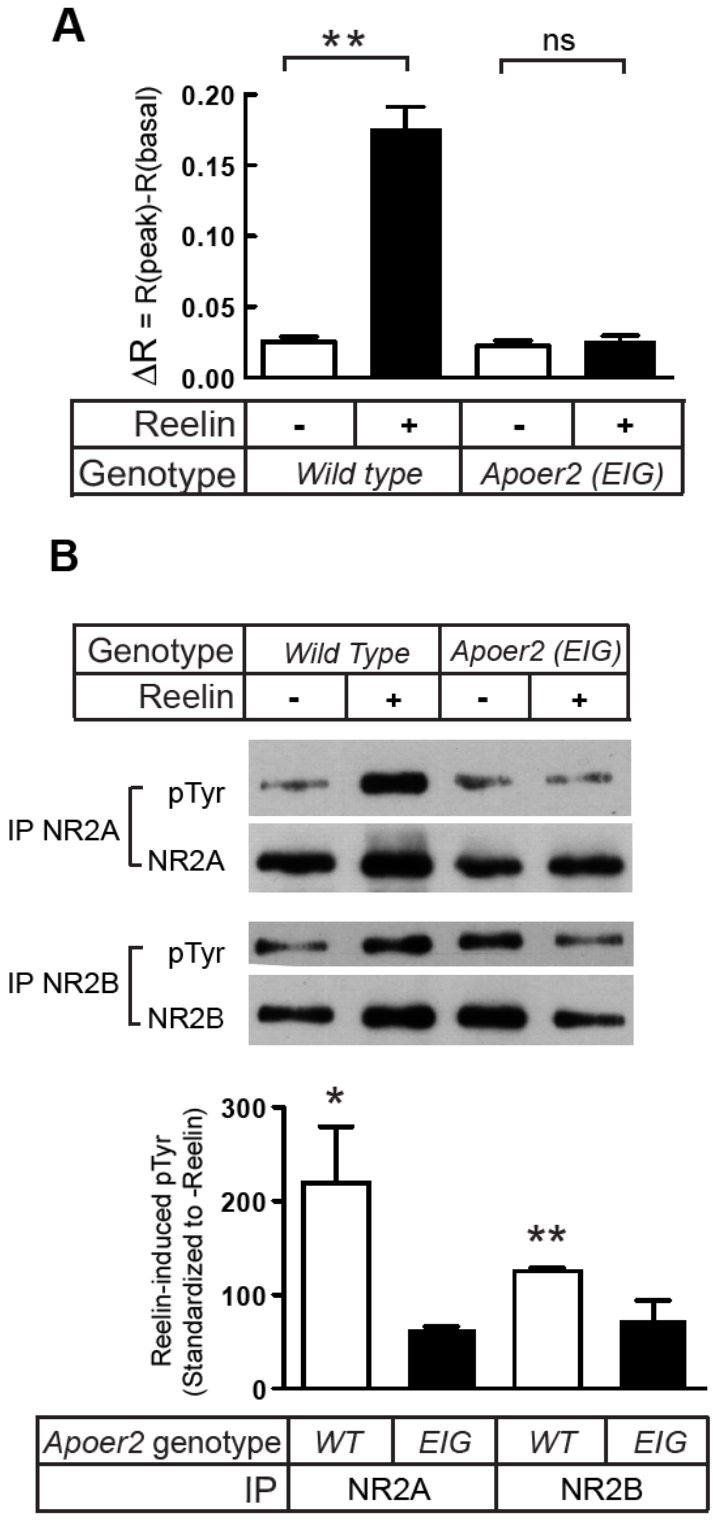
A
**
ns
ΔR = R(peak)-R(basal)
0.20
0.15
0.10
0.05
0.00
Reelin - + - +
Genotype Wild type Apoer2 (EIG)
B
Genotype Wild Type Apoer2 (EIG)
Reelin - + - +
IP NR2A
pTyr
NR2A
IP NR2B
pTyr
NR2B
Reelin-induced pTyr
(Standardized to -Reelin)
300
200
100
0
*
**
Apoer2 genotype WT EIG WT EIG
IP NR2A NR2B

Figure 4.7 Direct interaction of Apoer2 and Dab1 is necessary for Reelin-induced regulation of NMDA receptor activity. *A*, the primary neurons from wild type and *Apoer2(EIG)* mouse embryos were stimulated with glutamate in the presence of TTX, nimodipine and CNQX. ΔR values, indicating the maximal changes in fura-2 340/380 ratio induced by glutamate, are summarized. ** or 'ns' on the brackets indicates significant difference ($p<0.001$) or not significant respectively. Error bars indicate SEM. *B*, primary neurons obtained from wild type and *Apoer2(EIG)* mouse embryos were treated by control or Reelin-conditioned media. NR2A and NR2B were immunoprecipitated from the homogenized cell lysates and analyzed for tyrosine phosphorylation (pTyr). Total amounts of immunoprecipitated NR2A and NR2B are also shown (NR2A, NR2B). Quantification analysis from 4 independent experiments is summarized in the form of column graph shown below the blots. Phospho-tyrosine levels of NR2A and NR2B were firstly normalized to total NR2A and NR2B respectively. Reelin-induced tyrosine phosphorylation levels were then standardized to control (-Reelin) as presented in the graph. * above individual columns indicates significant difference (*$p<0.1$, **$p<0.001$) compared to control (-Reelin). Reelin treatment significantly increased tyrosine phosphorylation of both NR2A and NR2B in wild type neurons, but did not significantly change tyrosine phosphorylation of either NR2A or NR2B in *Apoer2(EIG)* neurons. Error bars indicate SEM.

Materials and Methods

Calcium imaging.

Primary cortical neurons were prepared from embryonic day16 (E16) embryos from timed pregnant mice as described in Chapter 3. At 12-13 days *in vitro* (DIV), neurons were treated with control or Reelin-conditioned medium and 2 μM fura-2 AM (Molecular Probes) for 30 min at 37°C in artificial cerebrospinal fluid [ACSF; containing (in mM): 140 NaCl, 5 KCl, 2.5 $CaCl_2$, 1.6 $MgCl_2$, 10 HEPES, and 24 D-glucose, pH 7.3] supplemented with 1 μM tetrodotoxin

(Sigma), 5 μM nimodipine (Sigma), and 40 μM 6-cyano-7-nitroquinoxaline-2,3-dione (CNQX; Sigma). Live cell images were acquired every 2 sec and shown as 340/380 ratios as described in Chapter 3. 20 μM glutamate (Sigma) was applied to stimulate neurons after baseline measurement. Basal 340/380 ratios [R(basal)] were determined as the average of the ratio values 15-5 s before glutamate application. Peak 340/380 ratios [R(peak)] were determined as the maximal ratio values 20-60 s after glutamate application. ΔR [ΔR = R(peak) - R(basal)] was defined to indicate the maximal change in 340/380 ratio induced by glutamate.

NMDA receptor phosphorylation.

Transverse hippocampal slices (400 μm) were prepared from 3-week-old mice as described in Chapter 3. Hippocampal slices were incubated in oxygenated ACSF supplemented with control or Reelin-containing medium for 20 min at room temperature. Slices were then homogenized in 900 μl immunoprecipitation buffer (IP buffer; containing 150 mM NaCl, 50 mM Tris-HCl, pH7.4, 1 mM EDTA, and 1% Nonidet P 40) supplemented with protease and phosphotase inhibitor cocktails (Sigma). NR2A and NR2B were immunoprecipitated from the lysate and the phosphorylation was detected by Western blot analysis as described in Chapter 3.

CHAPTER FIVE

Opposing Effects of Reelin and β-Amyloid on NMDA Receptor Phosphorylation and Trafficking

Abstract

Abnormal deposit of amyloid- β (Aβ) plaque and elevation of Aβ peptide are the characteristic hallmarks of Alzheimer's disease (AD), a neurodegenerative disease that is featured by progressive synapse loss and neuronal death. Aβ inhibits glutamatergic synaptic transmission and synaptic plasticity in part by altering the endocytosis and trafficking of AMPA and NMDA receptors. Apolipoprotein E (ApoE) is the major genetic risk factor for late-onset AD through unknown mechanisms. ApoE receptor, Apoer2, mediates the signaling events from its endogenous ligand Reelin, which potently enhances glutamatergic synaptic transmission and synaptic plasticity. Here we show that ApoE receptor and Reelin can block NMDA receptor internalization induced by low, physiological levels of Aβ. Therefore, ApoE receptor and Reelin can reverse Aβ-induced suppression of NMDA receptor surface expression. In addition, Reelin-induced tyrosine phosphorylation of NR2 subunit is inhibited by Aβ. We propose that ApoE receptors and Aβ, as opposing regulators of synaptic strength,

modulate glutamatergic synaptic transmission and the stability of synaptic network.

Introduction

Alzheimer's disease (AD) is a genetically complex neurodegenerative disease that afflicts 10 percent elderly population. Less than 10 percent of all AD cases are of the early-onset familial form, in which patients inherit mutations in the amyloid precursor protein (APP) or compartments in the APP processing protease, γ-secretase (Presenilins 1 or 2). These mutations are directly responsible for the preferential generation of the amyloidogenic and neurotoxic $A\beta_{1-42}$ form of the amyloid-β peptide from APP (Selkoe 2000; De Strooper 2007). On the contrary, in late-onset AD cases (over age 65), which is the major form of AD, the genes that are mutated in early-onset AD are normal, yet that pathologic presentation of the disease is the same. The underlying mechanisms that lead to abnormal Aβ processing, synapse loss and neuronal death in AD are largely unclear. In addition, the physiological role of Aβ peptide remains unknown.

The potential physiological role of Aβ is suggested by the observation that Aβ significantly impairs synaptic function and long-term potentiation (LTP), which is a form of synaptic plasticity underlying the formation of memories and the maintenance of synaptic stability. Recent studies have shown that synaptic

activity increases APP processing (Kamenetz, Tomita et al. 2003; Cirrito, Yamada et al. 2005). Together, these studies suggest that instead of being a mere waste product, Aβ may have important roles in regulating synaptic activity; for instance, regulating NMDA receptor trafficking (Snyder, Nong et al. 2005). This concept is further supported by recent studies which showed that overexpression of mutant APP in mice resulted in a global dysregulation of neuronal network activity (Palop, Chin et al. 2006; Palop, Chin et al. 2007). Although the biochemical mechanism by which Aβ peptide alters glutamatergic neurotransmission remains to be fully elucidated, current evidences highly suggest Aβ peptide as a potent physiological regulator of synaptic function.

Apolipoprotein E is the only well-established genetic risk factor for late-onset AD (Corder, Saunders et al. 1993; Schmechel, Saunders et al. 1993; Strittmatter, Saunders et al. 1993). However, the pathogenic mechanisms by which ApoE regulate the susceptibility and age-of-onset of AD *in vivo* are largely unknown. In the brain, ApoE is major apolipoprotein and is important for cholesterol and phospholipids transport (Boyles, Pitas et al. 1985; Mauch, Nagler et al. 2001). However, the neuronal ApoE receptors also transmit kinase signaling events from another ligand Reelin, and serve essential functions in the regulation of glutamatergic synaptic transmission through modulating NMDA receptor tyrosine phosphorylation in the mature CNS (Bock and Herz 2003; Beffert, Weeber et al. 2005; Chen, Beffert et al. 2005; Herz and Chen 2006). Thus, Aβ and ApoE

receptors appear to converge on the same fundamental molecular mechanisms which are essential for synapse formation and maintenance. Here we show that the activation of ApoE receptor signaling can reverse the reduction of NMDA receptor surface expression induced by Aβ peptide. Thus we propose that Aβ and ApoE receptors function as opposing physiological regulator of synaptic activity, which suggests a potential role for ApoE receptors in the pathogenesis of AD.

Results and Discussion

Several independent studies have shown that Aβ oligomers can potently suppress LTP and glutamatergic neurotransmission. On the contrary, activation of ApoE receptor signaling by Reelin potently increases LTP and NMDA receptor-mediated neurotransmission (Weeber, Beffert et al. 2002; Chen, Beffert et al. 2005). Snyder et al. (2005) used cell surface biotinylation to show that Aβ reduces neuronal NMDA receptor functions by accelerating NMDA receptor endocytosis. We decided to investigate whether the activation of Reelin signaling can alter the subcellular distribution of NMDA receptor subunits in the presence of Aβ (Figure 5.1).

A truncated form of Aβ peptide consisting only amino acids 25-35 of $A\beta_{1-42}$ which form the minimal fibrillogenic region ($A\beta_{25-35}$) was used in the biotinylation assay. $A\beta_{25-35}$ has similar neurotoxic effect as $A\beta_{1-40}$ and $A\beta_{1-42}$, and

is able to potently suppress synaptic plasticity *in vivo* (Yankner, Duffy et al. 1990; Holscher, Gengler et al. 2007). To test whether this truncated Aβ peptide, $A\beta_{25\text{-}35}$, alters the subcellular distribution of NMDA receptor similar to what has been reported by Snyder et al. (2005) for $A\beta_{1-42}$, we performed cell surface biotinylation experiments on primary cortical neurons exposed to 0, 0.1 or 1 μM $A\beta_{25\text{-}35}$ (lanes 1-3, Figure 5.1). We found that $A\beta_{25\text{-}35}$ increased the fraction of intracellular NR2A and NR2B subunits in a dose-dependent manner. In addition, this effect of $A\beta_{25\text{-}35}$ was reversed by Reelin (lane 4, Figure 5.1), which resulted in a higher proportion of NMDA receptors at the cell surface.

It has been reported that Aβ peptide activates a tyrosine phosphatase, striatal-enriched phosphatase (STEP), and inhibits the phosphorylation of NR2B at Tyr1472, an important regulatory residue for the endocytosis of NMDA receptor (Snyder, Nong et al. 2005). We have shown in Chapter 3 that Reelin signaling activation potently induces tyrosine phosphorylation of NR2B. We therefore decided to determine how Reelin and Aβ peptide interact when altering the phosphorylation of NR2B. As demonstrated in Chapter 3 and 4, Reelin increased tyrosine phosphorylation of NR2B in wild type neurons (Figure 5.2, lane 2). Reelin-induced tyrosine phosphorylation of NR2B subunits was prevented by either $A\beta_{25\text{-}35}$ or $A\beta_{1\text{-}42}$ (Figure 5.2, lane 4 and 6).

Taken together, we have demonstrated that Reelin and Aβ opposingly regulate the endocytosis and tyrosine phosphorylation of NMDA receptor. Therefore, we propose that synaptic NMDA receptor activity is modulated in opposite directions by Reelin and Aβ, which contributes to the maintaining of the balance of synaptic network (Figure 5.3).

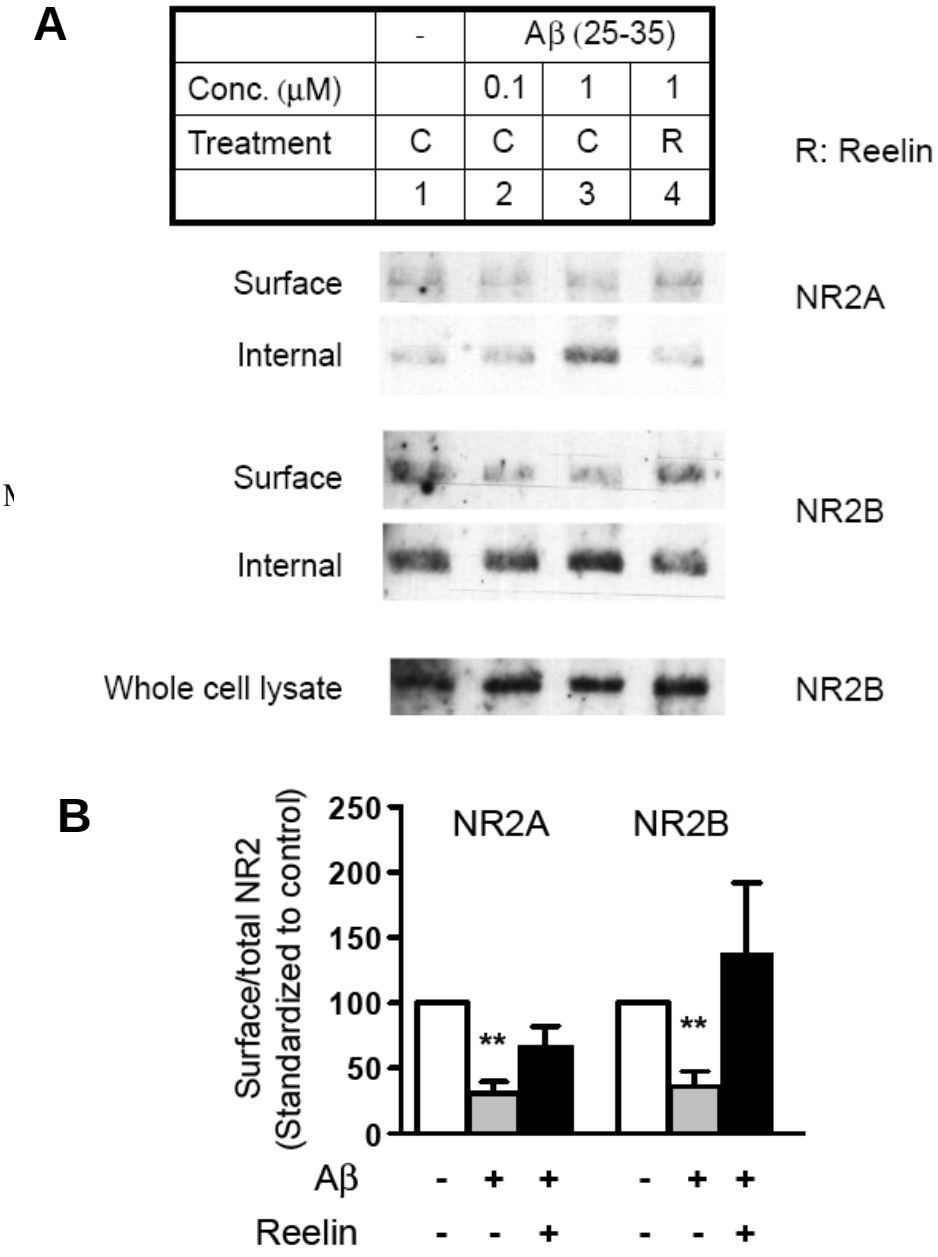

Figure 5.1 Reelin prevents amyloid-β-induced NMDA receptor endocytosis. *A*, neurons were incubated in the presence (*R*) or absence of Reelin (*C*) for 10 minutes before and throughout amyloid-β treatment. Neurons were labeled by sulfo-NHS-LC-biotin and the surface proteins were pulled down from the cell lysates by NeutrAvidin agarose beads. Internal proteins were collected as

the supernatant from NeutrAvidin pull down. The total proteins were detected from the whole cell lysates. The protein levels of NR2A and NR2B in each fraction were analyzed by Western blot. *B*, the intensities of the bands were determined by densitometric scanning. Surface NR2A or NR2B levels were determined as a surface/total ratio through dividing the intensity of surface NR2A or NR2B by the intensity of the corresponding total receptor. Averaged surface NR2A and NR2B levels, which were standardized to control (panel *A*, lane 1) were shown as column graph. ** above individual column indicates significant difference ($p<0.01$) versus control. Paired t test.

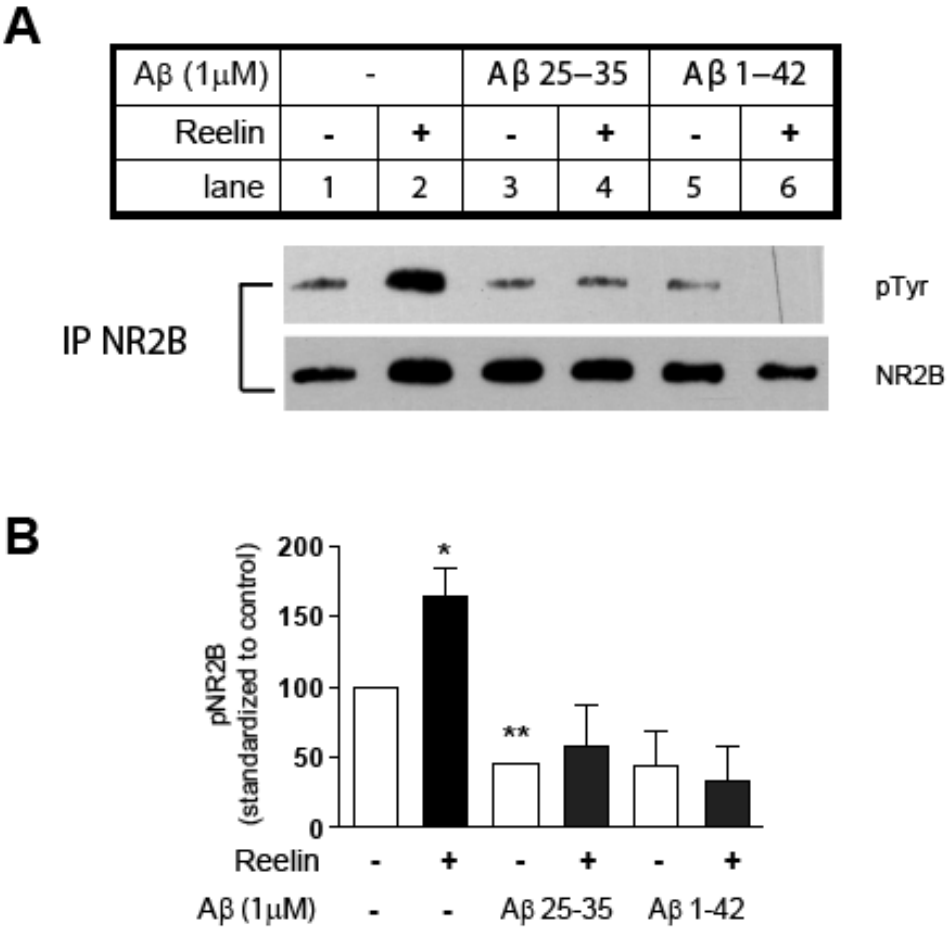

Figure 5.2 Amyloid-β peptide blocks Reelin-enhanced NMDA receptor phosphorylation. *A*, acute hippocampal slices obtained from wild type mice were incubated in the presence or absence of Reelin for 10 minutes before and throughout amyloid-β treatment. NR2B were immunoprecipitated from the homogenized lysates of the slices and analyzed for tyrosine phosphorylation (pTyr, top panel). Total amounts of immunoprecipitated NR2B is also shown (NR2B, bottom panel). *B*, the intensities of the bands were determined by densitometric scanning. Phosphor-NR2B (pNR2B) level was determined as a pTyr/total ratio through dividing the intensity of phosphor-tyrosine (pTyr) by the intensity of total NR2B. Averaged pNR2B levels, which were standardized to control (panel *A*, lane 1), were shown as column graph. * above individual column indicates significant difference versus control (far left column). *$p<0.05$, **$p<0.001$, paired t test.

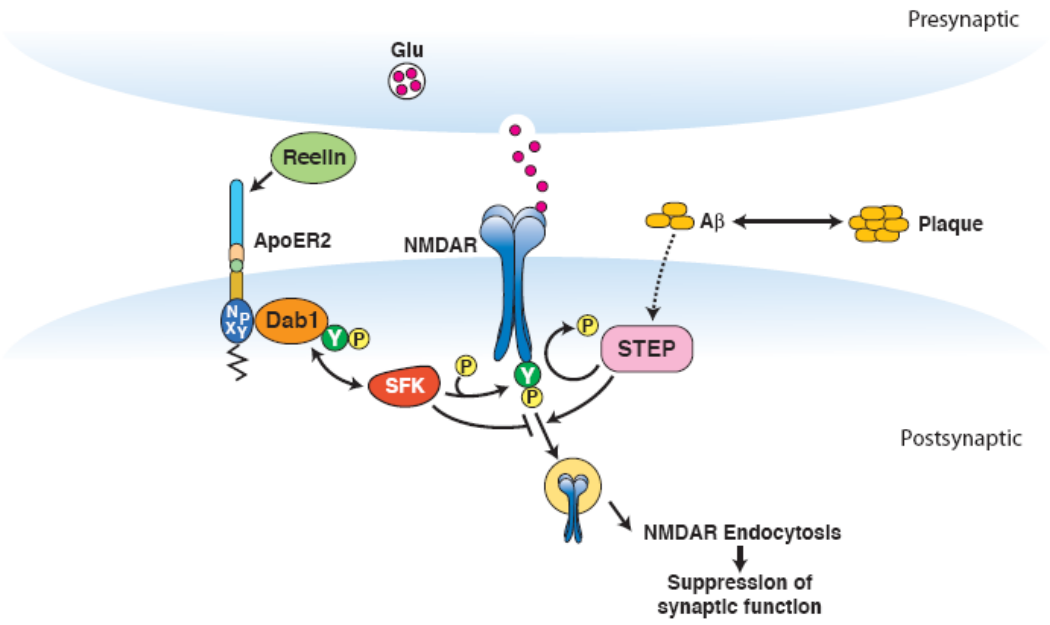

Figure 5.3 Model for Aβ and ApoE receptor-mediated regulation of synaptic function. Amyloid-β activates tyrosine phosphatase STEP, leading to the de-phosphorylation of the tyrosine residues on NMDA receptor, specifically the residue Tyr1472 on NR2B. NMDA receptor endocytosis is promoted presumably by the de-phosphorylation of NR2B subunit, which results in suppressed synaptic function. Reelin signaling activates kinase pathway involving Src tyrosine family kinases (SFK) and enhances the tyrosine phosphorylation of NR2A and NR2B as well as NMDA receptor conductance. Reelin signaling also blocks NMDA receptor endocytosis induced by amyloid-β and maintains the normal synaptic NMDA receptor activity. Thus, in the synapse, Reelin signaling counteracts the suppressive effect of amyloid-β and is important for the maintenance of normal synaptic function.

Material and Methods

Amyloid β preparation

Amyloid β (Aβ) $_{25–35}$ (Tocris) was dissolved in ddH_2O as a 100 μM solution and kept in aliquots at -20°C until use. Upon thawing, aliquots were incubated at 37°C for 1 hour before used in the experiments. $A\beta_{1–42}$ (Biosource) was dissolved in ddH_2O and diluted to 1mg/ml in PBS and kept in aliquots at -20°C until use. Upon thawing, aliquots were incubated at 37°C for two days before used in the experiments.

Surface Biotinylation

Primary cortical neurons were prepared from embryonic day16 (E16) embryos from timed pregnant mice as described in Chapter 2. Reelin was produced and purified as described in Chapter 3. At 12-13 days in vitro (DIV), the neurons were incubated in the presence or absence of Reelin (5 μg/ml) for 10 minutes before and throughout amyloid-β treatment (1 hour, 37°C). Neurons were washed by cold PBS and then incubated in PBS containing 1.5 mg/ml sulfo-NHS-LC-biotin (Pierce) for 30 min at 4°C. Neurons were rinsed in cold PBS following by cold PBS with 1 mM glycine. Then 300 μl lysis buffer (PBS with 0.1% SDS and 1% Triton X-100 and protease inhibitor cocktail (Sigma)) were added to the neurons. After 30 min incubation at 4°C, lysis buffer was collected and

centrifuged at 14,000 rpm for 15 min. 80% of the cell lysate were incubated with 50 μl NeutrAvidin agarose (Pierce) at 4°C for 1 hour. Agarose pellets were washed three times in washing buffer (500 mM NaCl, 15 mM Tris-HCl, 0.5% Triton X-100, pH 8). Proteins were eluted from agarose beads by SDS sample buffer.

NMDA receptor phosphorylation.

Hippocampal slices were prepared as described in Chapter 3. Slices were incubated in oxygenated ACSF in the presence or absence of Reelin (5 μg/ml) for 10 minutes before and throughout amyloid-β treatment (1 μM, 1 hour, 37°C). Slices were then homogenized in 900 μl immunoprecipitation buffer (IP buffer; containing 150 mM NaCl, 50 mM Tris-HCl, pH7.4, 1 mM EDTA, and 1% Nonidet P40) supplemented with protease and phosphotase inhibitor cocktails (Sigma). NR2B were immunoprecipitated from the lysate by an α-NR2B antibody (Santa Cruz Biotechnology) and the tyrosine phosphorylation was detected by Western blot analysis as described in Chapter 3.

CHAPTER SIX

ApoE4 Selectively Impairs ApoE Receptor-Mediated Modulation of NMDA Receptor Function and Synaptic Plasticity

Abstract

Apolipoprotein E (ApoE) is a well-established genetic modifier of Alzheimer's disease (AD). The ApoE4 isoform greatly reduces the mean age-of-onset of AD through unknown mechanisms. Here we show that ApoE4 selectively impairs the enhancement of synaptic plasticity and NMDA receptor activity induced by Reelin, a regulator of both brain development and synaptic strength. ApoE4 impairs the trafficking of Apoer2 and reduces neuronal surface expression of Apoer2, a dual function receptor for ApoE and for Reelin. Therefore ApoE4 critically reduces the ability of Reelin to enhance NMDA receptor-mediated Ca^{2+} influx and the phosphorylation of transcription factor CREB. As a result, the ability of Reelin to enhance theta-burst induced LTP is significantly impaired in hippocampal slices from knockin mice expressing the human ApoE4 isoform. These findings reveal a novel mechanism by which ApoE4 may accelerate the onset of AD and neuronal degeneration by impairing the maintenance of synaptic stability.

Introduction

ApoE is the major apolipoprotein in the brain that participates in the regulation of cholesterol metabolism and the transport of dietary lipids (Mahley, Innerarity et al. 1984). In human population, three ApoE alleles encode three isoforms of ApoE (E2, E3, and E4). They differ from each other by one or two amino acid substitutions at residues 112 and 158, respectively. ApoE3 is the most abundant isoform in human population. ApoE4 is present in approximately 25% of the general population and is associated with a significantly earlier mean age-of-onset of Alzheimer's disease (AD) while the rarer ApoE2 form is protective (Corder, Saunders et al. 1993; Schmechel, Saunders et al. 1993; Strittmatter, Saunders et al. 1993). Differential effects of ApoE isoforms on amyloid-β clearance (Weisgraber and Mahley 1996) and the stability of the cytoskeleton (Mahley and Huang 2006) have been reported, but none of these mechanisms alone can fully explain the molecular basis by which ApoE4 significantly increases the risk for AD.

ApoE receptors are members of an evolutionarily conserved multifunctional gene family and abundantly expressed on the surface of most cell types, including the neurons in the CNS. As endocytic receptors they facilitate the transport of synaptogenic cholesterol from astrocytes to neurons (Mauch, Nagler et al.

2001). In addition, two ApoE receptors, ApoE receptor-2 (Apoer2) and very-low-density lipoprotein receptor (Vldlr) also serve as classic signaling receptors for Reelin (D'Arcangelo, Homayouni et al. 1999; Hiesberger, Trommsdorff et al. 1999; Tissir and Goffinet 2003), a ligand that regulates neuronal migration during embryonic development (Trommsdorff, Gotthardt et al. 1999) as well as neurotransmission in the adult brain (Herz and Chen 2006). Through clustering Apoer2 and Vldlr, Reelin activates Src family non-receptor tyrosine kinases (SFKs) (Arnaud, Ballif et al. 2003; Bock and Herz 2003; Strasser, Fasching et al. 2004). SFKs subsequently phosphorylate NMDA receptor NR2 subunits in a highly regulated manner that requires an alternatively spliced exon 19 in the cytoplasmic domain of Apoer2 (Chapter 4). Reelin thereby potently enhances NMDA receptor activity (Chapter 3) and increases long-term potentiation (LTP) (Weeber, Beffert et al. 2002). By contrast, amyloid-β peptide (Aβ) induces NMDA receptor-dependent synaptic depression by decreasing tyrosine phosphorylation and increasing endocytosis of NMDA receptor (Kamenetz, Tomita et al. 2003; Snyder, Nong et al. 2005). Reelin and ApoE receptors thus function together to reverse this Aβ-induced NMDA receptor-dependent synaptic depression and to decrease NMDA receptor internalization from the neuronal surface (Chapter 5).

The single amino acid by which ApoE4 differs from ApoE3 radically alters its intracellular trafficking properties. While ApoE3 readily retro-endocytosis, ApoE4 remains trapped in endosomes for extended period of time (Heeren, Grewal et al. 2004; Rellin, Heeren et al. 2008), which raises the possibility that neuronal ApoE receptors could also remain sequestered along with ApoE in intracellular compartments so that the ApoE receptors are unable to signal to NMDA receptors. Here we show that ApoE4 preferentially impedes the recycling of Apoer2 and depletes Apoer2 from the neuronal surface. This reduction in signaling competent Apoer2 is accompanied by a reduced ability of Reelin to stimulate NMDA receptor-mediated Ca^{2+} influx into cultured neurons. Hippocampal slices from knockin mice expressing the human ApoE4 isoform also respond poorly to Reelin and therefore fail to enhance LTP. These data show that ApoE4 selectively impairs glutamatergic neurotransmission by reducing Apoer2 and NMDA receptor functions.

Results and Discussion

To determine the recycling efficiency of ApoE isoforms in neurons, we exposed primary cortical neurons from wild type mouse embryos to identical (3 μg/ml) concentrations of recombinant ApoE2, E3 or E4 produced by stably

transfected HEK293 cells. ApoE produced in this manner would be naturally lipidated during export from the ER and thus most closely resemble the small high-density lipoprotein (HDL) like particles that are generated by astrocytes in the intact brain. Neurons were firstly incubated with ApoE for 30 min, which was followed by a chase with fresh media. The cells were the washed with suramin and homogenized. As determined by Western blot analysis of the chase media, there was much less ApoE4 in the chase media than ApoE2 after 30 min and 60 min chase, suggesting that the recycling of ApoE4 is less efficient than ApoE2 (Figure 6.1A, top panel). The amount of re-secreted ApoE3 was between ApoE2 and ApoE4. Consistent with the results obtained from chase media, large amounts of ApoE4 were accumulated intracellularly compared to ApoE2 and ApoE3 even after 2 hour chase (Figure 6.1A, middle panel), further suggesting that the recycling of ApoE4 is impaired in primary neurons.

To test whether ApoE isoforms selectively reduce the surface expression of Apoer2, the primary Reelin receptor in the neocortex and in the hippocampus (Trommsdorff, Gotthardt et al. 1999), we exposed primary cortical neurons to recombinant ApoE2, E3 or E4 for 15 min at 37˚C. Neurons were then chilled to 4˚C and labeled with cell-impermeable sulfo-NHS-SS-biotin as described in 'Material and Methods'. Whereas ApoE2 and ApoE3 did not reduce the ratio of

surface expressed/total cellular Apoer2 significantly, ApoE4 significantly decreased surface expression of this 'dual function' Reelin and ApoE receptor (Figure 6.1B).

To further determine the steady state of Apoer2 expression on the neuronal surface, we incubated primary neurons with ApoE2, E3 or E4 together with Reelin for 2 hours before labeling the surface Apoer2 by biotin. It has been shown that Reelin stimulates the endocytosis of the signaling complex, including receptor Apoer2, and drives the degradation of adaptor protein Dab1 by proteasome (Arnaud, Ballif et al. 2003; Bock, Jossin et al. 2004; Morimura, Hattori et al. 2005). Reelin was incorporated in this assay to speed the turnover of Apoer2 so that the steady state of Apoer2 surface expression was easy to achieve. Under this experimental condition, ApoE4 severely depleted Apoer2 from the surface of neurons, with only about 20% of Apoer2 remaining at the surface (Figure 6.1C). Although ApoE2 and ApoE3 also reduced the surface level of Apoer2 by about 40%, ApoE4 was significantly more efficient to deplete surface Apoer2 than ApoE2 and ApoE3. These data suggest that in the presence of ApoE4, the availability and thus the function of Apoer2 at the cell surface might be impaired.

We next tested whether preincubation with the ApoE isoforms would selectively and with similar relative efficacy impair the Reelin-dependent Ca^{2+} influx into primary cortical neurons that can be evoked by the stimulation of NMDA receptors by glutamate (Chapter 3). In the absence of ApoE preincubation, Reelin robustly increased intracellular Ca^{2+} levels in an NMDA receptor-dependent manner (Figure 6.2A). Comparable, though slightly reduced responses were obtained after preincubation with 3μg/ml ApoE2 (Figure 6.2B) or ApoE3 (Figure 6.2C). However, ApoE4, at 3 μg/ml, almost completely abolished the ability of Reelin to increase NMDA receptor activity in response to glutamate (Figure 6.2D). The ApoE isoform-induced reduction in NMDA receptor-dependent Ca^{2+} influx was dose-dependent (Figure 6.2E). ApoE2 had almost no effect at 1 μg/ml, but at 3 μg/ml it reduced the maximal response (ΔR) to approximately 50% of the control (no ApoE) levels. ApoE3 partially reduced NMDA receptor activity at 1 and 3 μg/ml, whereas ApoE4 substantially decreased intracellular Ca^{2+} levels already at 1 μg/ml and almost completely abolished NMDA receptor-dependent Ca^{2+} influx at 3 μg/ml.

cAMP-response element binding protein (CREB) is a transcription factor that is activated by increased intracellular calcium concentration. It initiates gene transcriptions essential for neuronal survival and development, and synaptic

plasticity (Shaywitz and Greenberg 1999). Phosphorylation of CREB at Ser133 is required for CREB-mediated gene transcription. It has been demonstrated that Reelin-induced enhancement of NMDA receptor activity potently stimulates the phosphorylation of CREB at Ser 133 (Chapter 3). In order to determine whether preincubation with ApoE would impair Reelin-stimulated NMDA receptor-dependent CREB Ser133 phosphorylation, we performed immunofluorescent staining with an anti-pCREB (Ser133) antibody in primary neurons. Microtubule-associated protein 2 (MAP2) was used to identify the neuronal cell population. In the absence of ApoE preincubation, Reelin robustly stimulated CREB Ser133 phosphorylation in an NMDA receptor-dependent manner as described in Chapter 3 (Figure 6.3A, first column). Comparable induction of CREB phosphorylation by Reelin were observed after preincubation with 3 μg/ml ApoE2 (Figure 6.3A, second column) or ApoE3 (Figure 6.3A, third column). Compared with mock treatment (-Reelin), Reelin treatment led to a shift to the right in the frequency distribution of the fluorescent intensity of nucleus phospho-CREB in neurons preincubated with no ApoE, ApoE2, or ApoE3 (Figure 6.3B-D). However, ApoE4 almost completely abolished Reelin-induced NMDA receptor-dependent CREB phosphorylation (Figure 6.3A, fourth column). Consistently, after preincubation with ApoE4, the frequency distribution of phospho-CREB intensity

remained the same after Reelin treatment (Figure 6.3E). These data indicate that the neuronal survival and synaptic enhancing effects induced by Reelin and CREB is selectively prevented by ApoE4.

These results indicate that ApoE4 can substantially impair NMDA receptor function by interfering with Reelin receptor, Apoer2. To determine whether ApoE4 impairs the enhancing effect of Reelin on NMDA receptor-dependent synaptic functions (Weeber, Beffert et al. 2002; Beffert, Weeber et al. 2005) to a similar extent *in vivo*, we measured the ability of Reelin to enhance theta-burst induced LTP in the CA1 region in hippocampal slices from homozygous ApoE3 and ApoE4 knockin mice (Sullivan, Mace et al. 2004). In these animals, the endogenous mouse ApoE gene has been partially replaced with human ApoE coding sequences, resulting in the production of human ApoE isoforms from the endogenous murine regulatory sequences. No exogenous, heterologously produced recombinant ApoE was added in these experiments. Hippocampal slices from mice expressing exclusively the human ApoE3 isoform had normal baseline LTP, which was enhanced by Reelin (Figure 6.4A) to a similar extent as observed in slices from wild type mice which express murine ApoE (Weeber, Beffert et al. 2002; Beffert, Weeber et al. 2005). By contrast, ApoE4 expressing slices showed comparable baseline LTP, which was only slightly increased

following Reelin stimulation (Figure 6.4B). Integrated average responses are shown in Figure 6.4C. These results indicate that ApoE4 significantly impairs the synaptic enhancing function of Apoer2 *in vivo*.

Taken together, we have found that the recycling of internalized ApoE4 is impaired in primary neurons compared to ApoE2 and ApoE3. As a result, ApoE4 significantly reduces the surface expression of Apoer2. Through this mechanism, ApoE isoforms differentially antagonize the stimulation of NMDA receptor-dependent Ca^{2+} influx by Reelin in a dose-dependent manner, with ApoE4 being the most effective. ApoE4 also nearly completely inhibited Reelin-induced stimulation of CREB phosphorylation, an essential transcriptional event for synaptic plasticity and neuronal survival. Consequently, in ApoE4 knockin mice, the ability of Reelin to enhance LTP and thereby increase synaptic plasticity *in vivo* is almost completely abolished.

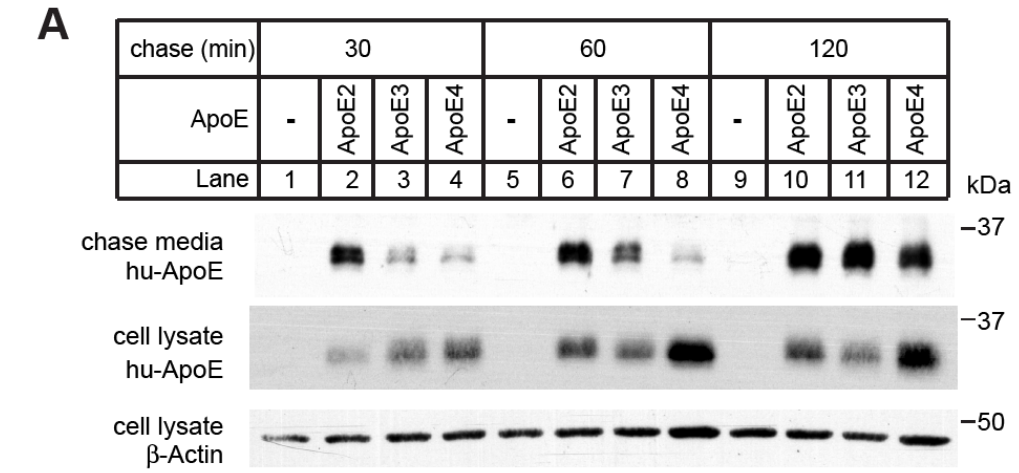
A
chase (min)
30
60
120
ApoE
-
ApoE2
ApoE3
ApoE4
Lane
1
2
3
4
5
6
7
8
9
10
11
12
kDa
chase media hu-ApoE
cell lysate hu-ApoE
cell lysate β-Actin
37
37
50

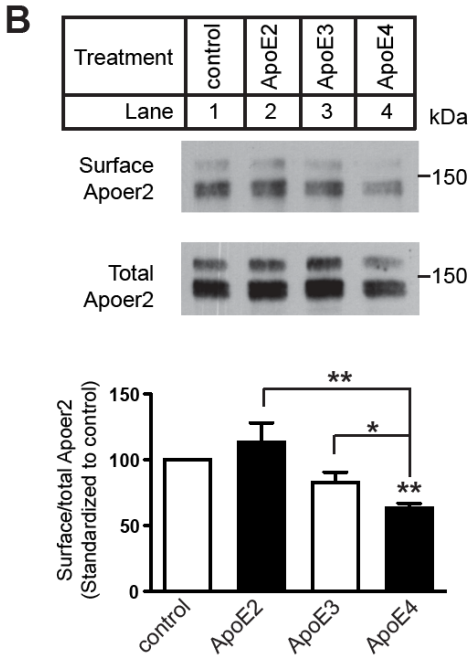
B
Treatment
control
ApoE2
ApoE3
ApoE4
Lane
1
2
3
4
kDa
Surface Apoer2
Total Apoer2
150
150
Surface/total Apoer2 (Standardized to control)
150
100
50
0
**
*
**
control
ApoE2
ApoE3
ApoE4

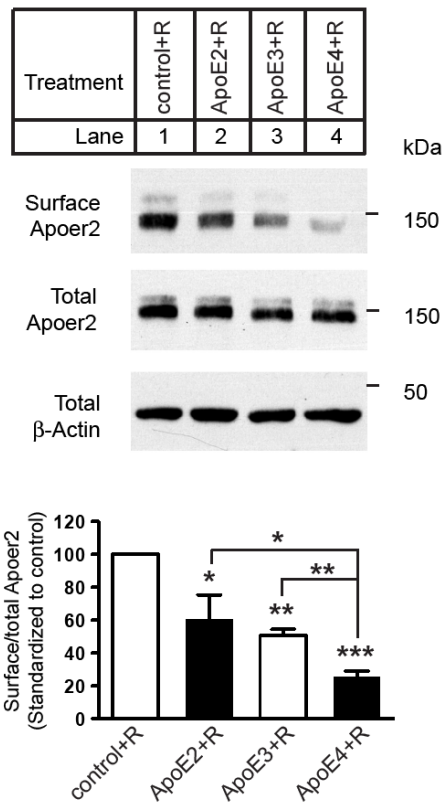
C
Treatment
control+R
ApoE2+R
ApoE3+R
ApoE4+R
Lane
1
2
3
4
kDa
Surface Apoer2
Total Apoer2
Total β-Actin
150
150
50
Surface/total Apoer2 (Standardized to control)
120
100
80
60
40
20
0
*
*
**
**
***
control+R
ApoE2+R
ApoE3+R
ApoE4+R

Figure 6.1 ApoE4 suppresses surface expression of Apoer2 in primary neurons. *A*, primary neurons were incubated with ApoE (3 μg/ml) for 30 min at 37°C. Surface-bound ApoE was removed by suramin, and neurons were incubated with fresh Neurobasal media for an additional 30 min, 1 h, or 2 h at 37°C. The media and neuronal lysates were analyzed by Western blot for human ApoE or β-actin. Molecular weight markers in kDa are given. *B*, after the neurons were incubated with ApoE (3 μg/ml) for 15 min at 37°C, cell surface Apoer2 was labeled by membrane-impermeable biotin and analyzed by Western blot with an anti-Apoer2 antibody (top panel). Total Apoer2 level was analyzed from total cell lysates (bottom panel). The intensities of the Apoer2 signals were determined by densitometric scanning. Surface Apoer2 level was determined by normalizing the intensity of surface Apoer2 to the intensity of total Apoer2. Averaged surface Apoer2 levels, which were standardized to control, from four independent experiments were shown as column graph below. * above individual column indicates significant difference versus control. * on brackets indicates significant difference between treatments. *$p<0.05$, **$p<0.01$, t test. *C*, after neurons were incubated with ApoE (3 μg/ml) and Reelin (2 μg/ml) for 2 hrs at 37°C, cell surface Apoer2 was labeled by membrane-impermeable biotin and analyzed by immunoblotting with an anti-Apoer2 antibody (top panel). Total cell lysates were analyzed for Apoer2 (middle panel) or β-actin (bottom panel). The average surface level of Apoer2 was presented in column graph as described in (*B*). * above individual columns indicates significant difference versus control. * on brackets indicates significant difference between treatments. *$p<0.05$, **$p<0.01$, ***$p<0.0001$, t test.

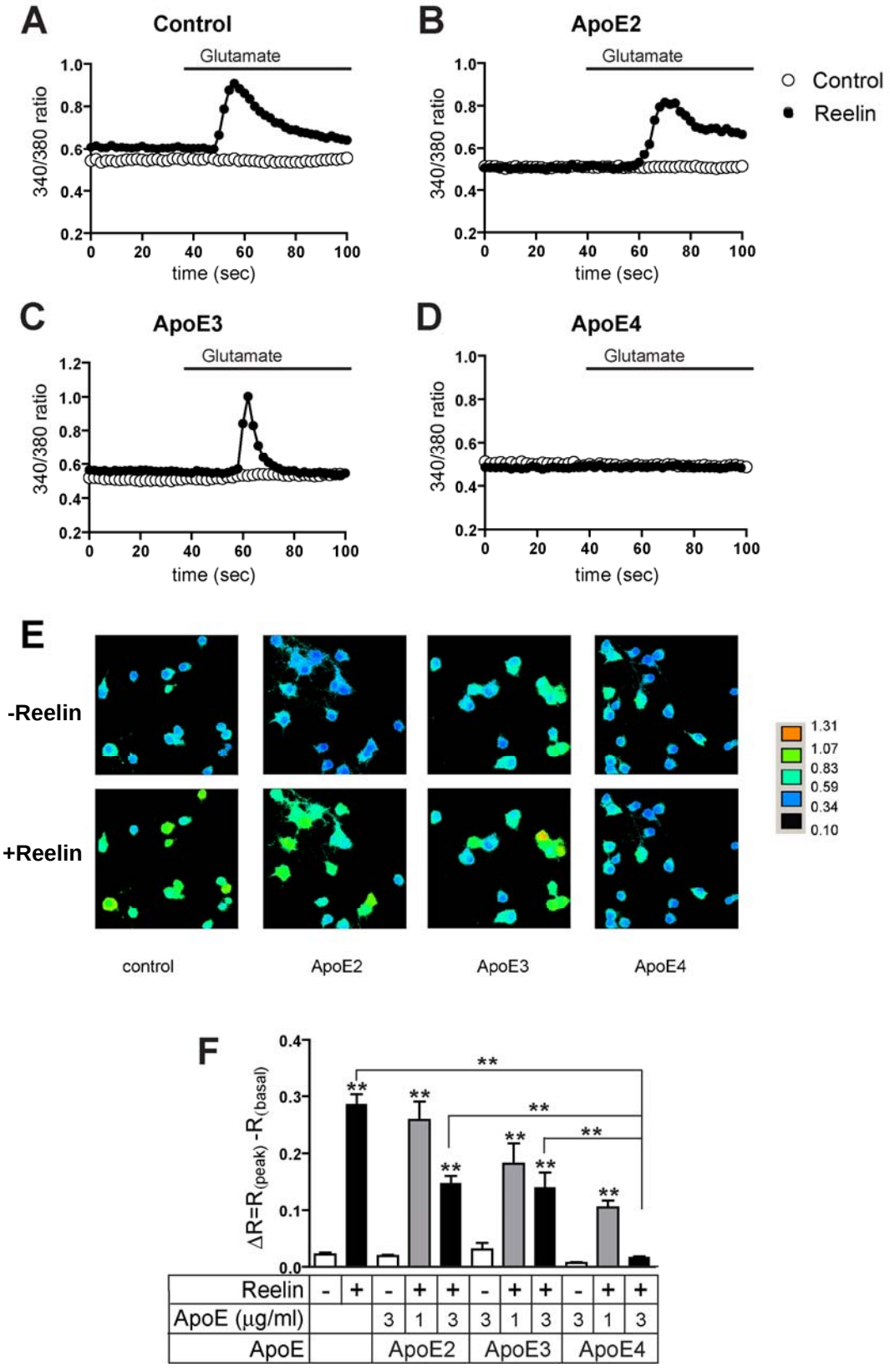
A
Control
Glutamate
340/380 ratio
time (sec)
B
ApoE2
Glutamate
340/380 ratio
time (sec)
Control
Reelin
C
ApoE3
Glutamate
340/380 ratio
time (sec)
D
ApoE4
Glutamate
340/380 ratio
time (sec)
E
-Reelin
+Reelin
1.31
1.07
0.83
0.59
0.34
0.10
control
ApoE2
ApoE3
ApoE4
F
ΔR=R(peak) -R(basal)
Reelin - + - + + - + + - + +
ApoE (μg/ml) 3 1 3 3 1 3 3 1 3
ApoE ApoE2 ApoE3 ApoE4

Figure 6.2 ApoE4 disrupts Reelin-induced enhancement of NMDA receptor-mediated Ca^{2+} influx. Representative traces of fura-2 340/380 ratio recorded from neurons pre-incubated in the conditioned media containing no ApoE (*A*), 3 μg/ml ApoE2 (*B*), 3 μg/ml ApoE3 (*C*), or 3 μg/ml ApoE4 (*D*). *E*, representative images showing fura-2-AM 340/380 ratios of Ca^{2+} transients induced by 20 μM glutamate in cortical neurons are shown. A pseudocolored calibration scale for 340/380 ratios is shown on the right. *F*, averaged ΔR (the maximal difference in 340/380 ratio induced by glutamate) recorded from primary neurons subjected to distinct treatments (n=20-50). ** above individual column indicates significant difference versus neurons with no treatment (the first column from left). ** on brackets indicates significant difference ($p<0.001$) between treatments.

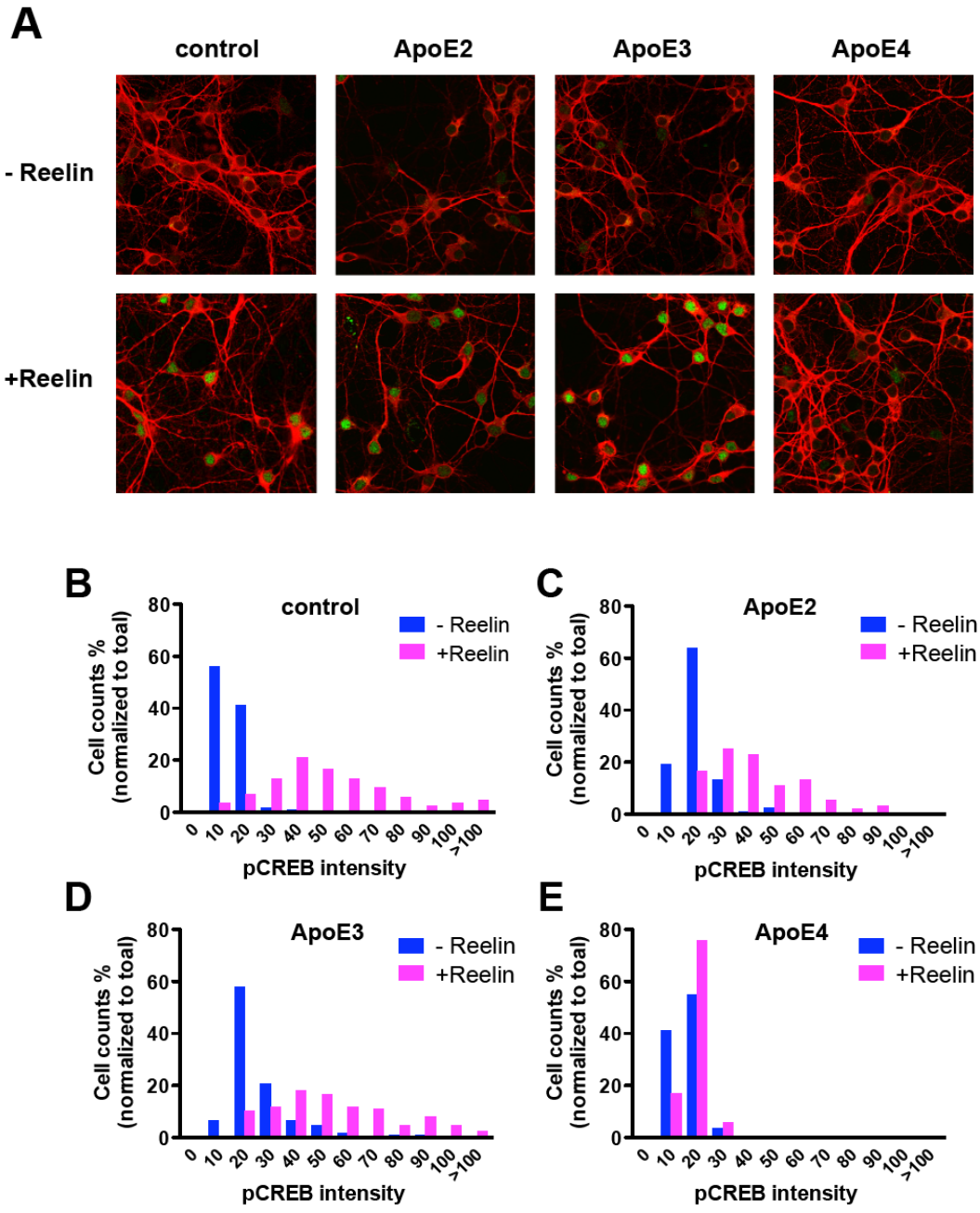
A
control
ApoE2
ApoE3
ApoE4
- Reelin
+Reelin
B
control
C
ApoE2
D
ApoE3
E
ApoE4
- Reelin
+Reelin
Cell counts %
(nomalized to toal)
pCREB intensity
0
10
20
30
40
50
60
70
80
90
100
>100

Figure 6.3 ApoE4 inhibits Reelin-induced CREB Ser133 phosphorylation. *A*, confocal microscopy of primary neurons which were pre-incubated with ApoE-conditioned media (3 μg/ml) and then treated in the presence or absence of Reelin (2 μg/ml) for an additional 30 min at 37°C. The neuronal cells were identified by an anti-MAP2 monoclonal antibody (red). Ser133-phosphorylated CREB was detected by polyclonal antibody (green). *B-E*, fluorescent intensities of phospho-CREB in the nuclei of neurons treated as in (*A*) were quantified by Image J and plotted into frequency distribution histograms as shown.

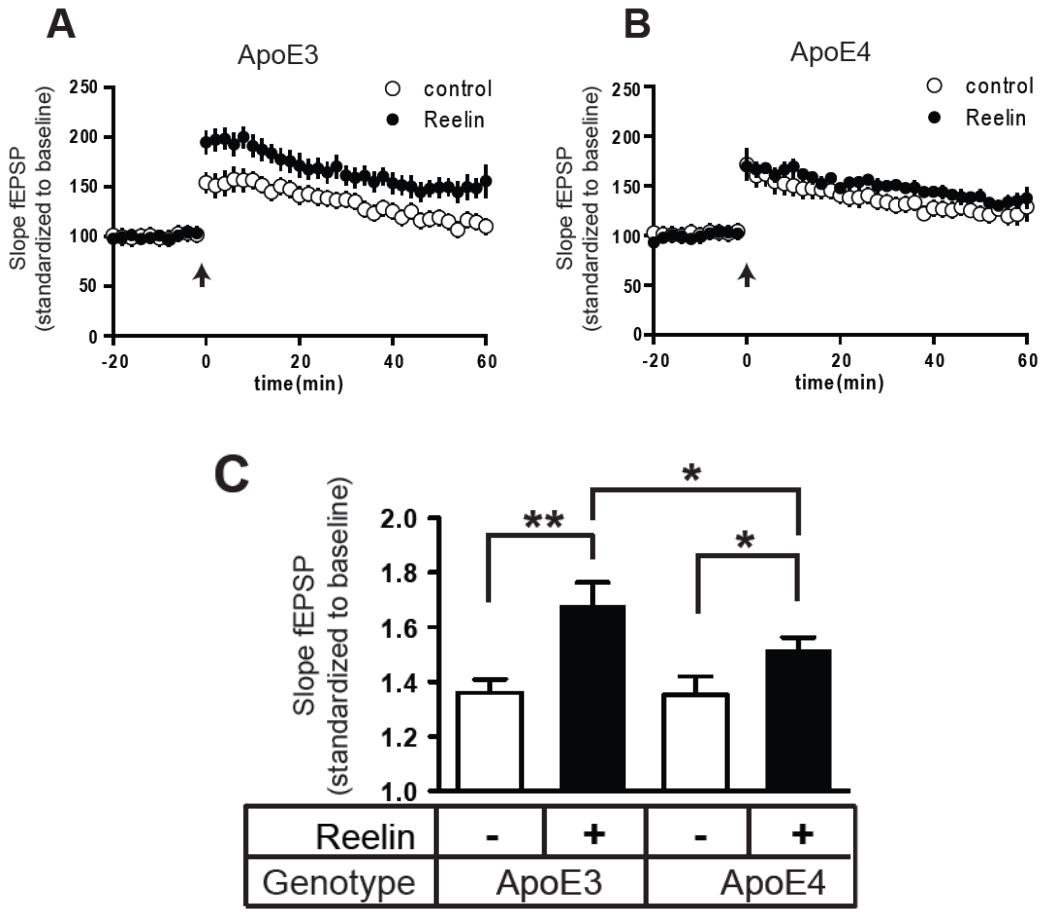

Figure 6.4 ApoE4 inhibits Reelin-induced increase of long-term potentiation. LTP was induced with theta burst stimulation in hippocampal slices expressing human ApoE3 (*A*) or ApoE4 (*B*) prefused with control (○; A, n=15; B, n=12) or Reelin-containing (●; A, n=16; B, n=12) ACSF. *C*, averaged slope fEPSPs recorded from 25 to 30 min after theta burst stimulation. *p<0.1, **p<0.01, t test.

Material and Methods

All animal experiments were performed in compliance with the National Institutes of Health Guide for the Care and Use of Laboratory Animals and the procedures approved by the Institutional Animal Care and Use Committees of the University of Texas Southwestern Medical Center and Baylor College of Medicine.

ApoE Recombinant Protein.

HEK-293 cells (CRL-1573, ATCC) were transfected with pcDNA3.1 zeo(+), or pcDNA3.1 zeo(+) human ApoE2, or pcDNA3.1 zeo(+) human ApoE3, or pcDNA3.1 zeo(+) human ApoE4 constructs. Stably transfected clones were selected by 700 μg/ml zeocin. HEK-293 cells that stably express human ApoE or HEK-293 control cells were plated on 10 cm dishes and grown to 80% confluency in low glucose-DMEM containing 10% fetal calf serum (FCS). Then the media was switched to Neurobasal (Invitrogen) and collected 3 days later. Conditioned media as well as ApoE3 standards (Invitrogen) were separated by SDS-PAGE, transferred to nitrocellulose, blotted with human ApoE antibody (Calbiochem) and IRDye 800CW secondary antibody (Li-Cor). The band intensity was

determined by Odyssey infrared imaging system (Li-Cor), and the concentration of ApoE was calculated accordingly.

ApoE Recycling

Primary cortical neurons were prepared from embryonic day 16 (E16) embryos from timed pregnant wild type mice and grown in 6-well culture dishes as described in Chapter 2. At 12-13 DIV, neurons were treated by control or 3 μg/ml ApoE at 37°C. Surface-bound ApoE was removed by suramin, and neurons were incubated with fresh Neurobasal media for an additional 30 min, 1 h, or 2 h at 37°C. The media was collected and neurons were lysed as described in Chapter 2. The media and neuronal lysates were analyzed by Western blot using a polyclonal α-human ApoE antibody (Calbiochem) and a monoclonal α-β-actin antibody (Sigma).

Surface Biotinylation

At 12-13 DIV, primary neurons were treated by control or 3 μg/ml ApoE at 37°C. Neurons were washed by cold PBS and then incubated in PBS containing 1 mg/ml sulfo-NHS-SS-biotin (Thermo Fisher Scientific) for 30 min at 4°C.

Neurons were rinsed in cold PBS with 1 mM glycine. Then 300 μl lysis buffer (PBS with 0.1% SDS and 1% Triton X-100 and protease inhibitor cocktail (Sigma)) were added to the neurons. After 30 min incubation at 4°C, lysis buffer was collected and centrifuged at 14,000 rpm for 15 min. 200 μl cell lysates were incubated with 50 μl NeutrAvidin agarose (Thermo Fisher Scientific) at 4°C for 1 hour. Agarose pellets were washed three times in washing buffer (500 mM NaCl, 15 mM Tris-HCl, 0.5% Triton X-100, pH 8). Surface proteins were eluted from agarose beads by SDS sample buffer. Proteins were separated by SDS-PAGE, transferred to nitrocellulose and blotted with a polyclonal α-Apoer2 antibody.

Calcium imaging.

At 12-13 DIV, the primary neurons, grown on 12 mm round coverslips, were incubated with ApoE for 10 min at 37°C in artificial cerebrospinal fluid [ACSF; containing (in mM): 140 NaCl, 5 KCl, 2.5 $CaCl_2$, 1.6 $MgCl_2$, 10 HEPES, and 24 D-glucose, pH 7.3] supplemented with 1 μM tetrodotoxin (Sigma), 5 μM nimodipine (Sigma), and 40 μM 6-cyano-7-nitroquinoxaline-2,3-dione (CNQX; Sigma). Then Reelin or mock-conditioned medium and 2 μM fura-2 AM (Molecular Probes) were also applied to neurons and the recording was started 30 min later. Live cell images were acquired every 2 sec and shown as 340/380

ratios as described in Chapter 3. 20 μM glutamate (Sigma) was applied to neurons after baseline measurement. Basal 340/380 ratios [R(basal)] were determined as the average of the 340/380 ratios 15-5 s before glutamate application. Peak 340/380 ratios [R(peak)] were determined as the maximal 340/380 ratios 20-60 s after glutamate application. ΔR [ΔR = R(peak) - R(basal)] was defined to indicate the maximal change in 340/380 ratio induced by glutamate.

Immunocytochemistry.

Primary neurons were subjected to treatment as described in *Calcium imaging*. Then neurons were fixed and processed as described in Chapter 3. Fixed neurons were incubated with anti-phosphorylated CREB (Ser133) antibody (Cell Signaling Technology, 1:100 dilution) and anti-microtubule-associated protein 2 (MAP2) antibody (Sigma, 1:500 dilution) at 4°C over night. Fluorescent images were acquired by a Leica TCS SP5 confocal microscopy with a 40× objective. Fluorescent intensity was quantified using Image J software.

Hippocampal slice preparation and field recording.

Mice that were from 2 to 3 month-old were sacrificed and the brains were rapidly removed. Transverse hippocampal slices (400 μm) were prepared in oxygenated ice-cold dissecting buffer (110 mM sucrose, 3 mM KCl, 1 mM NaH_2PO_4, 26 mM $NaHCO_3$, 0.5 mM $CaCl_2$, 5 mM $MgCl_2$, 5 mM D-glucose) as previously described (Weeber, Beffert et al. 2002). Hippocampal slices were allowed to recover in oxygenated artificial cerebrospinal fluid solution (ACSF) (124 mM NaCl, 5 mM KCl, 1.2 mM NaH_2PO_4, 26 mM $NaHCO_3$, 10 mM D-glucose, 2 mM $CaCl_2$, and 1 mM $MgCl_2$) for a minimum of 1 hour before recording. Long-term potentiation (LTP) was recorded from CA1 stratum radiatum and evoked by theta-burst stimulation (TBS): five trains with an interval of 20 sec, each consisting of ten 100-Hz bursts (four pulses) given at 5 Hz. Stimulus intensity was selected to give 50% of the maximal fEPSPs. For Reelin treatment, slices were exposed to Reelin (2 μg/ml in ACSF) for a minimum of 45 min before TBS application. The 20/80 slopes of the fEPSPs were used to quantify the magnitude of LTP. Potentiation was determined as the mean pEPSP 25 to 30 min following TBS normalized to the mean pEPSP from baseline recording.

CHAPTER SEVEN

Discussion

Role of Reelin/Apoer2 in the regulation of synaptic activity

The LDL receptor gene family consists of seven closely related multifunctional cell surface proteins which share the common structural domains. All the receptors in LDL receptor family are expressed in the brain, and they are well-known endocytic receptors which undergo endocytosis upon ligand binding. The signaling role of the receptor members, Apoer2 and Vldlr, were revealed by a mouse genetic study. Apoer2 and Vldlr connect their ligand Reelin to a cytoplasmic adaptor protein Dab1, which activates Src tyrosine family kinases (SFKs) and PI-3-kinase (PI3K)/Akt pathway. Disruption of this Reelin-initiated signaling has profound impact on the development of embryonic brain, especially neocortex, hippocampus, and cerebellum. Hence, the role of Reelin signaling in the regulation of neuronal migration during brain development has been extensively studied (Tissir and Goffinet 2003). The expression of Reelin and its receptors, Apoer2 and Vldlr, in the brain persist to the adulthood. Reelin is produced by a subset of GABAergic interneurons in cortex and hippocampus (Drakew, Frotscher et al. 1998; Pesold, Impagnatiello et al. 1998), and it has been

found in the vicinity of synapses (Pesold, Liu et al. 1999). Immunoelectron microscopy has confirmed the expression of Apoer2 in the postsynaptic density of the synapses in the CA1 region of mouse hippocampus (Beffert, Weeber et al. 2005). Taken together, these findings suggest that Reelin and its receptors may have distinct roles in the synapse.

Previously our lab discovered that Reelin and its receptors, Apoer2 and Vldlr, are important for the modulation of synaptic plasticity (i.e., LTP, memory, and learning) (Weeber, Beffert et al. 2002). NMDA receptor is a Ca^{2+}-permeable ionotropic postsynaptic glutamate receptor that is essential for the LTP induction, and maintenance in the CA1 region. The activity of NMDA receptor is partly regulated by SFKs, which are activated by Reelin signaling. In Chapter 3, we have investigated the effect of Reelin signaling on the function of NMDA receptors by measuring NMDA receptor-dependent calcium influx in primary cortical neurons. We show that Reelin can potently enhance NMDA receptor activity upon glutamate stimulation in wild type cortical neurons (Figure 3.2) but not in Dab1-deficient neurons (Figure 3.4), which are unable to respond to Reelin. Inhibition of either SFKs activity (Figure 3.5) or of Reelin binding to its receptors Apoer2 and Vldlr by RAP (Figure 3.3) abolishes this modulatory effect of Reelin. Reelin could increase NMDA receptor tyrosine phosphorylation and potentiate

NMDA receptor-mediated currents (Figure 3.6 and 3.7). Reelin-induced increase of Ca^{2+} entry through NMDA receptors increases the phosphorylation of the transcription factor CREB (Figure 3.8). Taken together, these data implicate the Reelin signaling complex, consisting of the lipoprotein receptors Apoer2 and Vldlr, their ligand Reelin, the adaptor protein Dab1, and SFKs, in the physiological regulation of neuronal NMDA receptor activity, memory and learning. Our findings also suggest that Reelin can physiologically modulate LTP through regulation of NMDA receptor activity.

The coupling of Reelin signal complex with NMDA receptor has been suggested through biochemical studies. PSD-95 is a PDZ domain-containing scaffolding protein located in the postsynaptic density (PSD). It anchors numerous synaptic proteins in the PSD, including NMDA receptor. In a yeast two-hybrid screen aiming to identify novel adaptor proteins interacting with the cytoplasmic tails LDL receptor family members, PSD-95 was found to associate with Apoer2, and this association was dependent on the presence of amino acid sequence encoded by the alternatively spliced exon 19 of Apoer2 (Gotthardt, Trommsdorff et al. 2000). Immunoprecipitation from mouse brain lysates has confirmed that Apoer2 interacts with NMDA receptor by a mechanism that is dependent on exon 19 of Apoer2 (Beffert, Weeber et al. 2005). Our findings

indicate that Apoer2/Vldlr and NMDA receptors are functionally coupled *in vivo*. We show that Reelin can potently enhance NMDA receptor-mediated Ca^{2+} influx and tyrosine phosphorylation of NMDA receptor in wild type cortical neurons (Figure 3.2 and 3.6). Blockade of Reelin signaling on any level, either by disrupting binding of Reelin to its receptors (Figure 3.3), by genetic inactivation of Dab1 (Figure 3.4), or by pharmacological inhibition of SFKs (Figure 3.5) prevented the Reelin-enhanced NMDA receptor-mediated Ca^{2+} entry. In addition, Reelin-induced regulation of NMDA receptor phosphorylation and function is completely abolished in primary neurons expressing Apoer2 mutant that constitutively lack exon 19 (Figure 4.6), suggesting that the physical association of Reelin signaling complex with NMDA receptor is necessary for their functional interaction.

To determine the distinct contribution of Reelin receptors, Apoer2 and Vldlr, in the regulation of NMDA receptor, we studied Reelin-stimulated calcium influx and tyrosine phosphorylation of NMDA receptor in Apoer2-deficient and Vldlr-deficient neurons (Figure 4.1 and 4.2). In the absence of Apoer2, Reelin-induced modulation of NMDA receptor activity was completely abolished. However, in Vldlr-knockout neurons, Reelin stimulates NMDA receptor-mediated Ca^{2+} influx to a slightly reduced, though comparable level as observed in wild type neurons.

These data suggest that Apoer2 is the major receptor for Reelin to regulate NMDA receptor activity, whereas Vldlr is dispensable. The difference in Apoer2 and Vldlr may be derived from their relative expression abundance. In human tissues, Apoer2 is mostly expressed in brain and placenta, whereas Vldlr is highly expressed in heart and muscle (Kim, Magoori et al. 1997). In primary neuronal culture, Apoer2 is expressed at higher level than Vldlr (Niu, Renfro et al. 2004). The higher expression of Apoer2 in neurons may account for the more severe defects observed in Apoer2-knockout neurons. Our observation in primary neurons is also consistent with the findings in intact animals. The hippocampal slices from Apoer2-deficient mice displayed a significant decay of late-phase LTP, whereas the LTP in Vldlr-deficient hippocampal slices was only marginally reduced (Weeber, Beffert et al. 2002). On the contrary, Reelin-induced enhancement of LTP was completely abolished in either Apoer2- or Vldlr-deficient hippocampal slices, suggesting the existence of discrepancy between the experimental systems using acute brain slices and primary neuron culture. Nevertheless, all the findings consistently suggest that Apoer2 is the key receptor for Reelin to regulate synaptic NMDA receptor function.

We propose a model for the regulation of NMDA receptor by Reelin signaling complex (Figure 7.1). Exon 19-encoded sequence in the cytoplasmic domain of

Apoer2 associates with PSD-95 which also binds to NMDA receptor. Thereby, PSD-95 may recruit the Reelin signaling complex to the vicinity of NMDA receptor. Reelin binding to its receptor Apoer2 activates SFKs through Dab1. SFKs in turn enhance NMDA receptor activity through the phosphorylation of tyrosine residues in the cytoplasmic domains of NR2 subunits.

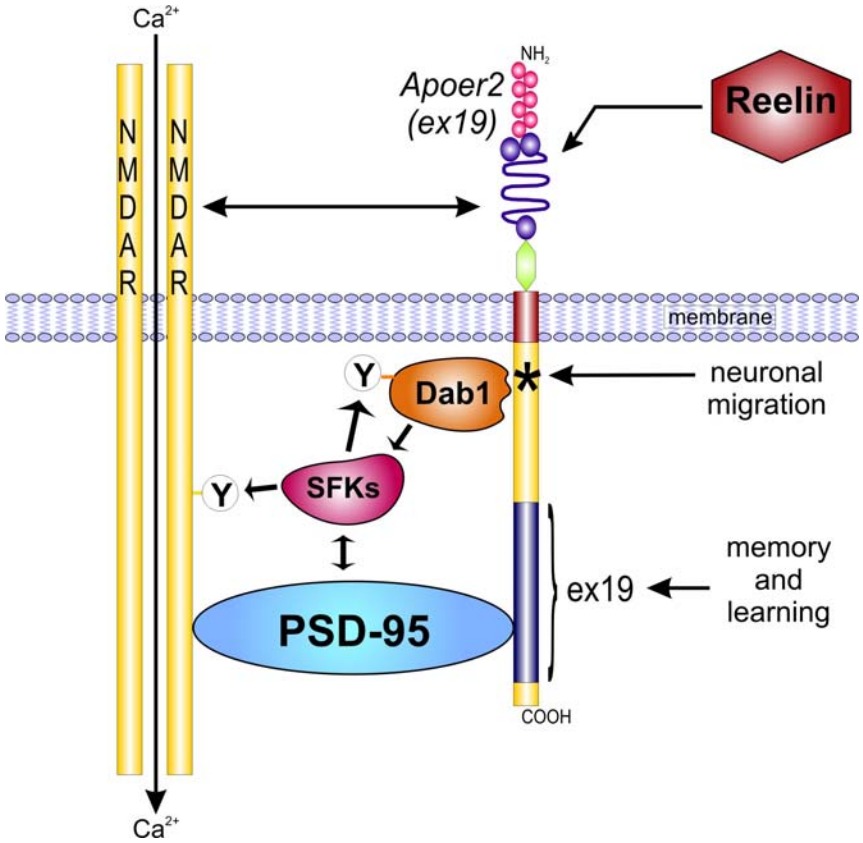

Figure 7.1 Model for the physical and functional coupling of Reelin signaling complex with NMDA receptor at the synapse.

It is well-established that the phosphorylation of tyrosine residues on NR2A and NR2B upregulates NMDA receptor activity, likely through altering the gating or the trafficking of NMDA receptor channel (Salter and Kalia 2004). It has been shown that D1-type dopamine receptor signaling regulates the trafficking of NMDA receptor and promotes its surface insertion by a tyrosine kinase-dependent mechanism in striatal neurons (Hallett, Spoelgen et al. 2006). However, we did not detect any significant change in surface NMDA receptor expression in response to Reelin treatment in primary neurons (data not shown), suggesting that altered NMDA receptor trafficking is not the mechanism underlying Reelin-mediated regulation of NMDA receptor. This conclusion is supported by another study, in which Groc et al found the surface expression of NR2B and NR2A was not significantly affected by the addition of Reelin or CR-50, the function-blocking anti-Reelin antibody (Groc, Choquet et al. 2007). The patch-clamp experiment we performed showed that Reelin increased the amplitude of NMDA currents over the entire voltage range (from -70 to +70 mV) of membrane holding potential (Figure 3.7), which strongly suggested that Reelin-induced phosphorylation of NMDA receptor alters the gating of the channel. Instead of NR2 subunit phosphorylation, phosphorylation of other proteins in the NMDA receptor complex by SFKs might also change the gating of the channel, such as

PSD93. It would be intriguing to identify if Reelin signaling induces phosphorylation of other protein components in the PSD and thereby regulates synaptic activity (Nada, Shima et al. 2003).

The functional interaction between Reelin signaling and NMDA receptor is also suggested by independent studies carried out by other research groups. The expression pattern of NR2A and NR2B is subject to temporal regulation (Monyer, Burnashev et al. 1994; Wenzel, Fritschy et al. 1997). In early developmental stage, NR2B-containing NMDA receptors are predominant. As neurons getting mature, NR2B-containing receptors are replaced by NR2A-containing receptors, so that NR2A is the predominant NR2 subunit in mature neurons. Combining electrophysiological and biochemical approaches, two research groups have demonstrated that blocking the function of Reelin prevents the NR2B to NR2A switch, whereas exogenous Reelin accelerats the NR2B to NR2A switch (Sinagra, Verrier et al. 2005; Qiu and Weeber 2007). The maturation-induced change in NMDA receptor composition was blocked by an inhibitor of SFKs or an antagonist of the LDL receptor family members. Groc et al, taking advantage of single-particle tracking technique, found that inhibition of Reelin reduced the surface mobility of NR2B-containing NMDA receptors and increased their synaptic dwell time (Groc, Choquet et al. 2007). Conversely, exogenous Reelin

significantly decreased the synaptic dwell time of NR2B-containing NMDA receptors. Therefore, besides modulating synaptic NMDA receptor activity, Reelin signaling also facilitates the maturation of synapses by regulating the subunit composition of NMDA receptors in the synapse.

Ca^{2+} influx through synaptic NMDA receptors promotes neuronal survival and synaptic plasticity; however, excess Ca^{2+} flow through NMDA receptors also causes neuronal death in pathological conditions (Hardingham and Bading 2003). Ca^{2+}-activated transcription factor CREB activates transcription of target genes that are essential for the neuron development, survival and synaptic plasticity (Shaywitz and Greenberg 1999). Excess Ca^{2+} triggered cell death pathway generally shuts off CREB activity. Reelin potentiates the phosphorylation event necessary for CREB activity by an NMDA receptor-dependent mechanism (Figure 3.8). This raises the possibility that Reelin can physiologically modulate activity dependent gene transcription *in vivo*, and strongly indicates that Reelin signaling promotes the strength and plasticity of synapses, as well as the survival of neurons. This serves as the molecular mechanism not only for the previously observed Reelin-mediated regulation of synaptic plasticity, learning and memory, but also for the function of Reelin in neuronal development. For example, it has been shown that Reelin can promote the branching of entorhinocortical-

hippocampal projections (Del Rio, Heimrich et al. 1997), and promote dendrite development in the hippocampal neurons through an Apoer2/Vldlr-Dab1 dependent pathway (Niu, Renfro et al. 2004). Since some target genes of CREB participate in neurite outgrowth and dendrite development, Reelin-mediated sensitization of NMDA receptors to the stimulation of glutamate could therefore also contribute to the activity-dependent regulation of neurite outgrowth, dendritogenesis and synapse formation.

Recent findings reveal that the regulatory effect of Reelin signaling complex in synapses is not limited to NMDA receptor regulation. Reelin treatment could enhance the surface expression of AMPA receptor as well as AMPA receptor current in a PI3K dependent manner (Qiu, Zhao et al. 2006). Reeler heterozygous mice (Reelin+/-) display multiple electrophysiological defects in hippocampus, including reduced excitatory postsynaptic potentials, impaired LTP and LTD, reduced spontaneous inhibitory postsynaptic currents (Qiu, Korwek et al. 2006). Although the explanation of the latter study is complicated by the fact that reduced Reelin signal input during developmental stage results in lower synaptic complexity (Del Rio, Heimrich et al. 1997; Borrell, Del Rio et al. 1999), these findings consistently support the pivotal synaptic function of Reelin signaling complex.

Reelin/Apoer2 in synaptic network

Human brain has around 100 billion neurons, each of which form 10 thousand synapses with other neurons. The synapses in the brain use different neurotransmitters, and transmit either excitatory or inhibitory signals. The activity of synapses is subject to the regulation from multiple signals. It is the integration and plasticity of this complex synaptic network that forms the basis of learning, memory and behavior. The function of brain is dependent upon the finely tuned integration of synaptic network and the regulatory signals.

Alzheimer's disease (AD) is the most common neurodegenerative disease and the leading cause of dementia in the elderly. The patients of AD suffer from progressive impairment of cognitive function and memory loss. Besides the massive neuronal loss and decreased brain volume, the brains of AD patients have two hallmarks, deposition of amyloid plaques and neurofibrillary tangles. Current two mainstays of medications for AD are acetylcholinesterase inhibitors, which aim at increasing the level of acetylcholine and cholinergic neurotransmission in the brain; and an NMDA receptor antagonist, which aims at preventing overexcitation-induced neurotoxicity and neuronal death (Lleo, Greenberg et al. 2006). These drugs provide modest benefits on cognitive function to patients, and

none of them can alter the underlying pathophysiology of dementia or prevent the progression of AD.

So as to understand the mechanism underlying the dementia, numerous studies have been carried out to investigate the initial functional alteration involved in the pathogenesis of AD. The results from these studies strongly suggest that altered synaptic function underlies the initial cognitive deficits of AD. In a morphometric study of postmortem brains of AD patients and normal subjects, the density of neocortical synapses has a very powerful correlation with premortem cognitive deficits, whereas the numbers of plaques or tangles, or the degree of neuronal perikaryal loss show only weak correlations with psychometric indices (Terry, Masliah et al. 1991). In another independent study, changes in the presynaptic vesicle protein synaptophysin in hippocampus and association cortices are strongly correlated with the degree of cognitive decline of AD patients (Sze, Troncoso et al. 1997).

Amyloid-β (Aβ) peptide is the well accepted causative factor in AD. Emerging evidences suggest that it also cause synaptic dysfunction. Mice that overexpress Aβ have significantly reduced LTP and glutamatergic synapse transmission (Kamenetz, Tomita et al. 2003). Specifically, Greengard and colleagues have shown that Aβ reduces the surface expression of NMDA receptor

by promoting its endocytosis from the cell surface (Snyder, Nong et al. 2005). As mentioned before, synaptic NMDA receptor activity promotes synaptic plasticity and neuronal survival partly by phosphorylating and activating transcription factor CREB. Reduced CREB phosphorylation has been detected in the brains of AD patients, suggesting the involvement of CREB and NMDA receptor in AD. Inhibition of NMDA receptor impairs learning and memory in rodents (Lisman, Fellous et al. 1998). It is also well indicated that inadequate neuronal stimulation and activity can contribute to neurodegeneration. Therefore, sustained suppression of NMDA receptor activity by Aβ may initiate the pathological changes in AD.

Snyder et al also demonstrated that Aβ activates tyrosine phosphatase STEP, and thereby dephosphorylates NR2B subunit and promotes the endocytosis of NMDA receptors (Snyder, Nong et al. 2005). In Chapter 3 and 4, we have shown that Reelin and Apoer2 regulate the activity of excitatory synapses by increasing the tyrosine phosphorylation and the activity of NMDA receptor. In Chapter 5, we demonstrate that Reelin and Apoer2 reverses Aβ-induced reduction of NMDA receptor surface expression (Figure 5.1). An independent study using electrophysiological technique shows consistent result that Reelin reverses Aβ-induced suppression of synaptic NMDA receptor current (Durakoglugil M., Chen

Y., Kavalali ET., Herz J., unpublished data). Activation of Src family tyrosine kinases (SFKs) is necessary for Reelin to reverse the Aβ-mediated synaptic depression. We propose a model in which synaptic NMDA receptor activity is regulated in opposite directions by Aβ and Reelin (Figure 5.3). In this model, Aβ activates tyrosine phosphotase causing NMDA receptor endocytosis and synaptic depression (Snyder, Nong et al. 2005), whereas Reelin activates SFKs (Bock and Herz 2003), which serves to retain NMDA receptors at the neuronal surface and preserves their synaptic functions.

Aβ peptides spontaneously assemble in aqueous solutions into a variety of structures, including low n-oligomers or ADDLs (amyloid β derived diffusible ligand, a heterogeneous mixture of Aβ oligomers), protofibrils and fibrils (Bitan, Kirkitadze et al. 2003; Bitan, Vollers et al. 2003; Walsh and Selkoe 2007). Oligomeric, but not monomeric Aβ potently suppresses LTP at low and therefore likely physiologically occurring concentrations (Walsh, Klyubin et al. 2002; Townsend, Shankar et al. 2006). ADDLs have been shown to stimulate formation of reactive oxygen species (ROS) through extrasynaptic NMDA receptor activation (De Felice, Velasco et al. 2007). Oligomers are also thought to be responsible for the LTP blocking effect of Aβ and reversible synapse loss by modulating an NMDA receptor-dependent signaling pathway (Townsend,

Shankar et al. 2006; Shankar, Bloodgood et al. 2007). Consistent with a direct effect on synapses, externally added ADDLs have been shown to bind to a subset of synapses where they can induce the expression of protein Arc (Lacor, Buniel et al. 2004). Since Apoer2 is expressed in the postsynaptic densities of excitatory synapses where it interacts with NMDA receptors (Beffert, Weeber et al. 2005), it is likely that the mechanisms that mediate synaptic depression through Aβ and synaptic enhancement through Reelin converge on the same organelle.

It has been shown that Aβ also drives the endocytosis of AMPA receptor and removes it from the cell surface, which results in the loss of dendritic spines and the reduction of synaptic responses (Hsieh, Boehm et al. 2006). Conversely, Reelin signaling promotes the insertion of AMPA receptor into the synaptic membrane by a PI3K dependent mechanism (Qiu, Zhao et al. 2006). Therefore, Reelin may oppose Aβ-induced synaptic depression in part also through stabilizing synaptic AMPA receptors.

Recently, synaptic network dysfunction is emerging as a novel perspective on AD. Patients with AD often show surprising fluctuations in their neurological functions even in a short period of time. These reversible fluctuations cannot be caused by changes in neuronal number. Instead, it may reflect the adjustments in neuronal network. The activity of synapse is maintained at a delicate balance by

strengthening and weakening inputs. The integrity of synaptic network is also maintained by integrating both excitatory and inhibitory inputs. Disruption of one aspect of this dynamic circuit may chronically alter synaptic plasticity and disintegrate neuronal network. Reelin/Apoer2 and Aβ form enhancing and depressing inputs to the synapse. Therefore, Reelin and Apoer2 play critical role in maintaining synaptic integrity by counteracting the suppressive effect of Aβ.

In an intriguing study, Palop et al found that the AD mouse models that overexpress Aβ have aberrant excitatory neuronal activity and spontaneous nonconvulsive seizure in cortical and hippocampal networks (Palop, Chin et al. 2007), which strongly supports the network dysfunction concept described above. However, the synaptic enhancing effect of Reelin does not seem to fit in the over-excitatory situation in AD mouse at the first glance. Reelin is expressed primarily by GABAergic interneurons in the adult brain, and the physiological site of action of Reelin is unsolved. It is possible that Reelin acts locally on the excitatory input synapses on interneurons, and thereby enhance inhibitory synaptic network and antagonize network over-excitation. This idea consistently supports that Reelin and Apoer2 are important synaptic input to maintain the integrity of synaptic network. Disrupting the function of Reelin and Apoer2 may cause alteration of synaptic plasticity and eventually the disintegration of neuronal network.

Apoer2 mediates the pathological effect of ApoE

ApoE4 isoform of ApoE significantly reduces the average age of onset of late-onset AD through unknown mechanisms (Corder, Saunders et al. 1993; Schmechel, Saunders et al. 1993; Strittmatter, Saunders et al. 1993). ApoE is produced and secreted by astrocytes and is the major apolipoprotein in the brain (Xu, Bernardo et al. 2006). ApoE, together with cholesterol and phospholipids, forms HDL-like particles and transports lipids throughout the brain (Boyles, Pitas et al. 1985; Boyles, Zoellner et al. 1989). One type of receptors for ApoE are receptors in LDLR gene family. They are abundantly expressed in the brain where they mediate lipoprotein uptake as well signal transduction (Herz and Bock 2002). We have demonstrated in Chapter 3 to 5 that by modulating the function of NMDA receptor, Apoer2-mediated Reelin signaling is a key enhancing input to synaptic balance. As an endogenous ligand for Apoer2, ApoE isoforms may differentially regulate the function of Apoer2, and thereby differentially accelerate the disintegration of synaptic network and the onset of dementia.

In Chapter 6, we have shown that ApoE4 significantly impedes the recycling of Apoer2 and reduces the surface expression of Apoer2 in primary culture neurons. ApoE isoforms differentially antagonize the stimulation of NMDA receptor-mediated Ca^{2+} influx by Reelin in a dose-dependent manner, with ApoE4

being the most effective. Through this mechanism, ApoE4 prevents Reelin-induced NMDA receptor-dependent CREB phosphorylation. Consequently, in ApoE4 knockin mice, the ability of Reelin to enhance LTP and thereby increase synaptic plasticity *in vivo* is severely compromised.

ApoE might regulate Reelin signaling through two potential mechanisms: direct competing for the binding to Apoer2, or altering subcellular trafficking of Apoer2. Ligand binding interference is an attractive mechanism that could explain the relative protective effect of ApoE2 over ApoE3 and ApoE4 because the receptor binding affinity of ApoE2 is much lower than the other two isoforms (Mahley, Innerarity et al. 1984). However, it can not easily explain the powerful disease promoting effect of ApoE4 over ApoE3, since these two isoforms bind to receptors with equal affinity (Mahley, Innerarity et al. 1984).

ApoE-containing triglyceride-rich lipoprotein (TRL) in the plasma is efficiently internalized into liver after binding of ApoE to LRP1 and LDLR (Beisiegel, Weber et al. 1989). Once internalized, TRLs immediately disintegrate in early endosomes. ApoE is retained in recycling endosomes and form a complex with cholesterol, whereas the majority of lipids are targeted to the lysosomal compartments (Heeren, Weber et al. 1999; Heeren, Grewal et al. 2001). HDL or lipid-poor ApoA-I stimulates the recycling of ApoE, which is

accompanied by cholesterol efflux (Heeren, Grewal et al. 2001; Heeren, Grewal et al. 2003). However, the recycling process of ApoE4 is severely impaired in both hepatoma cells and neuronal cell line HT-22 (Heeren, Grewal et al. 2004; Rellin, Heeren et al. 2008). In contrast to ApoE3, ApoE4 fails to efficiently retroendocytose and accumulates in intracellular compartments following endocytosis in these cell types. These observations raised the possibility that if the recycling of ApoE4 is also impaired in neurons, ApoE4 may also retard the recycling of its receptor Apoer2. Thereby ApoE4 may effectively sequester a fraction of the receptors inside the cell where they would be unable to signal and regulate synaptic activity.

It has been shown that, in neuronal cells, ApoE4 was more susceptible to degradation compared with ApoE3, resulting in the intracellular accumulation of truncated ApoE4 (Huang, Liu et al. 2001). However, we did not detect any truncated ApoE fragments from neuron lysates after ApoE was internalized by neurons (data not shown), indicating that protein degradation and accumulation of truncated ApoE4 do not contribute to the impaired recycling of ApoE4 in primary neurons.

Our findings support this model. Following internalization, exogenously added recombinant ApoE4, but not ApoE2 and ApoE3 lipoproteins, accumulated

in large amount inside the primary neurons and failed to recycle back to the extracellular space (Figure 6.1A). Consequently, ApoE4 significantly decreased surface expression of Apoer2 in primary neurons (Figure 6.1B, 6.1C). This decreased expression would reduce NMDA receptor priming by Reelin and thus increase the threshold at which glutamate can stimulate Ca^{2+} entry through NMDA receptor in primary neurons (Chapter 3). In addition, a less effective direct competition by ApoE2 might also manifest itself through reduced interference and larger Ca^{2+} influx in this assay. The results shown in Figure 6.2 are consistent with both of these proposed mechanisms. This relative effect of the ApoE isoforms on Reelin and glutamate evoked Ca^{2+} influx intriguingly parallels the order of their relative contribution to the age of onset of AD (Corder, Saunders et al. 1993; Schmechel, Saunders et al. 1993; Strittmatter, Saunders et al. 1993). Moreover, these *in vitro* findings also bear direct relevance to the function of the intact CNS, where endogenously produced ApoE4, but not ApoE3 severely impaired the ability of Reelin to enhance theta-burst induced LTP in hippocampal CA1 field recordings (Figure 6.4). ApoE levels in human cerebrospinal fluid (CSF) average approximately 5 μg/ml (Hesse, Larsson et al. 2000). The ApoE concentrations we have used in this study thus lie well within this physiological range. Taken together, these results support two distinct

molecular mechanisms by which ApoE isoforms can interfere with neuronal functions that underlie the modulation of synaptic plasticity.

Several models have been proposed to explain the mechanisms underlying the pathogenic nature of ApoE4 in late-onset AD. First, ApoE4 has been suggested to promote deposition of Aβ into plaques (Holtzman, Bales et al. 2000). Second, ApoE4 increases Aβ production in neuroblastoma cells (Ye, Huang et al. 2005). Third, ApoE4 fragments are toxic to primary neurons (Chang, ran Ma et al. 2005). However, the confirming *in vivo* evidence to support some of these models is still missing. What's more, none of these models demonstrate the effect of ApoE4 on synaptic activity, where the key initial pathological changes occur as discussed in the previous session.

Several studies have been reported trying to identify the effect of ApoE isoforms on synaptic plasticity; however, the results are controversial. Trommer et al showed that LTP in ApoE4 knockin mice was reduced compared with ApoE3 knockin mice, whereas the basal synaptic transmission was normal (Trommer, Shah et al. 2004). In another study, LTP in ApoE4 knockin mice was enhanced at younger age compared to wild type control (Kitamura, Hamanaka et al. 2004). These discrepancies may result from the experiment protocols adopted by different research groups. Still, these results suggest that the effect of ApoE

isoforms on synaptic plasticity may not be significantly different under those experimental conditions, or the basal LTP is not the ideal parameter to distinguish the effect of ApoE isoforms.

The findings in Chapter 6 provide a novel mechanism by which ApoE isoforms differentially affect synaptic network. Our findings together with those of several other groups provide a model in which the trafficking of the amyloid precursor protein (APP) and ApoE receptors (Andersen, Reiche et al. 2005; Cam, Zerbinatti et al. 2005; Liu, Zerbinatti et al. 2007; Schmidt, Sporbert et al. 2007), ApoE receptor and APP expression (Liu, Zerbinatti et al. 2007), APP processing and Aβ production (Kamenetz, Tomita et al. 2003; Cirrito, Yamada et al. 2005), and modulation of synaptic activity by ApoE receptor, Apoer2 (Beffert, Weeber et al. 2005), and Aβ (Kamenetz, Tomita et al. 2003; Hsieh, Boehm et al. 2006) are cornerstones of an integrated signaling network that is critical for maintaining the balance of the synapse and synaptic network. Aβ induces synaptic depression, which is potently counter-regulated by Reelin and Apoer2 (Chapter 5). Disruption of this highly interconnected and ordered process may result in a self-reinforcing, progressive synaptic network dysfunction that might accelerate synapse destabilization and neuronal loss (Palop, Chin et al. 2006). Here, we propose a model in which an ApoE isoform-selective impairment of Apoer2

signaling reduces the couter-regulation of Aβ-induced synaptic depression, and thereby the self-adjustment and compensatory ability of synaptic network, which eventually leads to the failure of synaptic network and neurodegeneration (Figure 7.2). These findings provide a novel mechanism that may explain in part the differential effects of ApoE isoforms on memory, learning and neuronal survival, as well as the pathologic nature of ApoE4 in late onset AD.

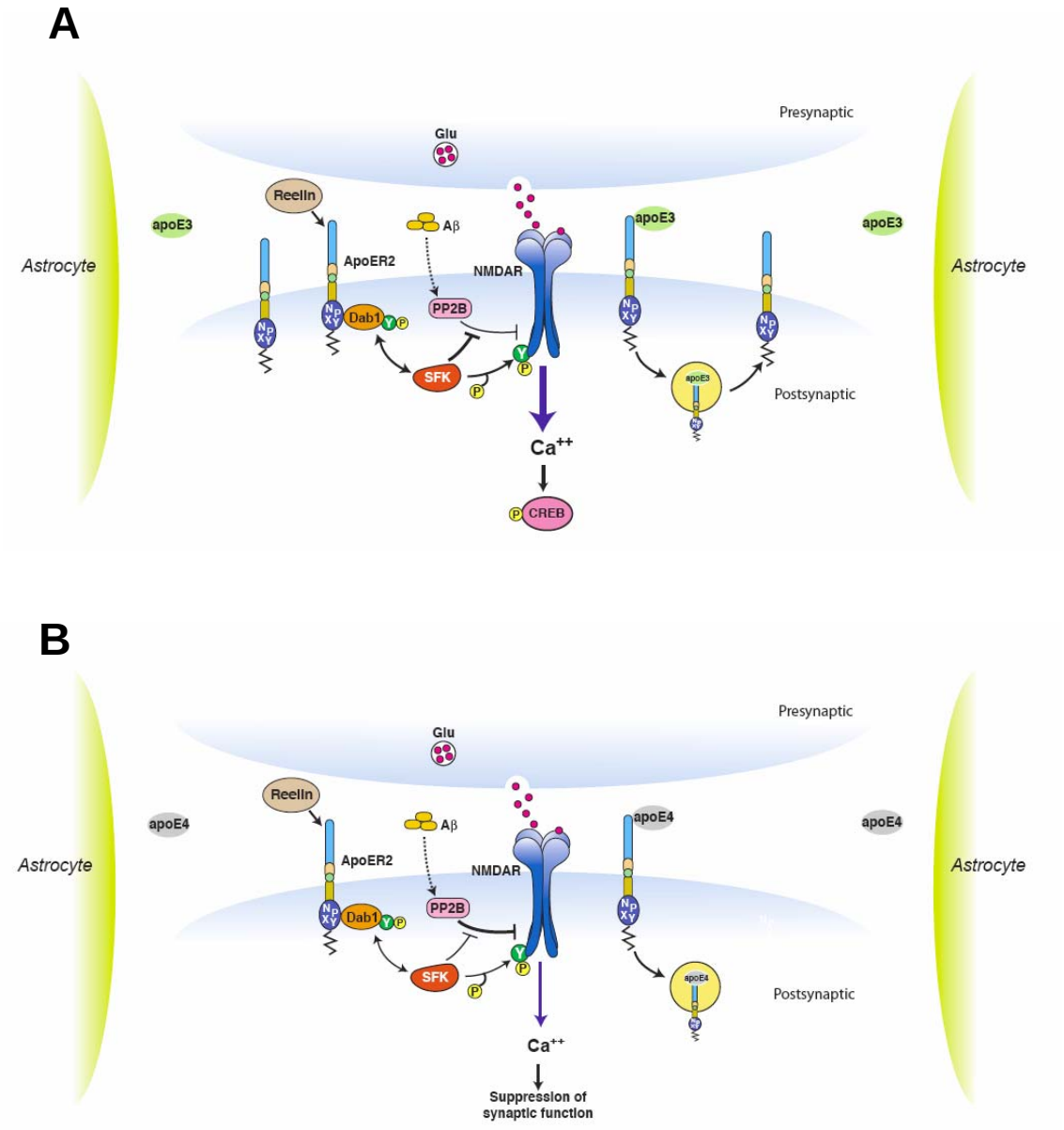

Figure 7.2. Model for ApoE isoform-selective regulation of synaptic function. *A*, at synapses, Apoer2 upregulates NMDA receptor activity and opposes the suppressive effect of Aβ. *B*, by impeding the intracellular trafficking of Apoer2, ApoE4 inhibits the synaptic function of Apoer2, and thereby the self-adjustment ability of synaptic network, which may eventually lead to the failure of synaptic network and neurodegeneration.

BIBLIOGRAPHY

Alcantara, S., M. Ruiz, et al. (1998). "Regional and cellular patterns of reelin mRNA expression in the forebrain of the developing and adult mouse." J Neurosci **18**(19): 7779-99.

Andersen, O. M., J. Reiche, et al. (2005). "Neuronal sorting protein-related receptor sorLA/LR11 regulates processing of the amyloid precursor protein." Proc Natl Acad Sci U S A **102**(38): 13461-6.

Anderson, R., J. C. Barnes, et al. (1998). "Behavioural, physiological and morphological analysis of a line of apolipoprotein E knockout mouse." Neuroscience **85**(1): 93-110.

Arnaud, L., B. A. Ballif, et al. (2003). "Regulation of protein tyrosine kinase signaling by substrate degradation during brain development." Mol Cell Biol **23**(24): 9293-302.

Arnaud, L., B. A. Ballif, et al. (2003). "Fyn tyrosine kinase is a critical regulator of disabled-1 during brain development." Curr Biol **13**(1): 9-17.

Ascher, P. and L. Nowak (1988). "The role of divalent cations in the N-methyl-D-aspartate responses of mouse central neurones in culture." J Physiol **399**: 247-66.

Assadi, A. H., G. Zhang, et al. (2003). "Interaction of reelin signaling and Lis1 in brain development." Nat Genet **35**(3): 270-6.

Bacskai, B. J., M. Q. Xia, et al. (2000). "The endocytic receptor protein LRP also mediates neuronal calcium signaling via N-methyl-D-aspartate receptors." Proc Natl Acad Sci U S A **97**(21): 11551-6.

Ballif, B. A., L. Arnaud, et al. (2004). "Activation of a Dab1/CrkL/C3G/Rap1 pathway in Reelin-stimulated neurons." Curr Biol **14**(7): 606-10.

Barria, A., D. Muller, et al. (1997). "Regulatory phosphorylation of AMPA-type glutamate receptors by CaM-KII during long-term potentiation." Science **276**(5321): 2042-5.

Bayer, K. U., P. De Koninck, et al. (2001). "Interaction with the NMDA receptor locks CaMKII in an active conformation." Nature **411**(6839): 801-5.

Beffert, U., A. Durudas, et al. (2006). "Functional dissection of Reelin signaling by site-directed disruption of Disabled-1 adaptor binding to apolipoprotein E receptor 2: distinct roles in development and synaptic plasticity." J Neurosci **26**(7): 2041-52.

Beffert, U., G. Morfini, et al. (2002). "Reelin-mediated signaling locally regulates protein kinase B/Akt and glycogen synthase kinase 3beta." J Biol Chem **277**(51): 49958-64.

Beffert, U., E. J. Weeber, et al. (2005). "Modulation of synaptic plasticity and memory by Reelin involves differential splicing of the lipoprotein receptor Apoer2." Neuron **47**(4): 567-79.

Beisiegel, U., W. Weber, et al. (1989). "The LDL-receptor-related protein, LRP, is an apolipoprotein E-binding protein." Nature **341**(6238): 162-4.

Bitan, G., M. D. Kirkitadze, et al. (2003). "Amyloid beta -protein (Abeta) assembly: Abeta 40 and Abeta 42 oligomerize through distinct pathways." Proc Natl Acad Sci U S A **100**(1): 330-5.

Bitan, G., S. S. Vollers, et al. (2003). "Elucidation of primary structure elements controlling early amyloid beta-protein oligomerization." J Biol Chem **278**(37): 34882-9.

Bliss, T. V. and G. L. Collingridge (1993). "A synaptic model of memory: long-term potentiation in the hippocampus." Nature **361**(6407): 31-9.

Bock, H. H. and J. Herz (2003). "Reelin activates SRC family tyrosine kinases in neurons." Curr Biol **13**(1): 18-26.

Bock, H. H., Y. Jossin, et al. (2004). "Apolipoprotein E receptors are required for reelin-induced proteasomal degradation of the neuronal adaptor protein Disabled-1." J Biol Chem **279**(32): 33471-9.

Borrell, V., J. A. Del Rio, et al. (1999). "Reelin regulates the development and synaptogenesis of the layer-specific entorhino-hippocampal connections." J Neurosci **19**(4): 1345-58.

Boucher, P., M. Gotthardt, et al. (2003). "LRP: role in vascular wall integrity and protection from atherosclerosis." Science **300**(5617): 329-32.

Boulanger, L. M., P. J. Lombroso, et al. (1995). "Cellular and molecular characterization of a brain-enriched protein tyrosine phosphatase." J Neurosci **15**(2): 1532-44.

Boyles, J. K., R. E. Pitas, et al. (1985). "Apolipoprotein E associated with astrocytic glia of the central nervous system and with nonmyelinating glia of the peripheral nervous system." J Clin Invest **76**(4): 1501-13.

Boyles, J. K., C. D. Zoellner, et al. (1989). "A role for apolipoprotein E, apolipoprotein A-I, and low density lipoprotein receptors in cholesterol transport during regeneration and remyelination of the rat sciatic nerve." J Clin Invest **83**(3): 1015-31.

Brown, M. S. and J. L. Goldstein (1986). "A receptor-mediated pathway for cholesterol homeostasis." Science **232**(4746): 34-47.

Brown, M. T. and J. A. Cooper (1996). "Regulation, substrates and functions of src." Biochim Biophys Acta **1287**(2-3): 121-49.

Bu, G., H. J. Geuze, et al. (1995). "39 kDa receptor-associated protein is an ER resident protein and molecular chaperone for LDL receptor-related protein." Embo J **14**(10): 2269-80.

Cam, J. A., C. V. Zerbinatti, et al. (2005). "Rapid endocytosis of the low density lipoprotein receptor-related protein modulates cell surface distribution and processing of the beta-amyloid precursor protein." J Biol Chem **280**(15): 15464-70.

Chang, S., T. ran Ma, et al. (2005). "Lipid- and receptor-binding regions of apolipoprotein E4 fragments act in concert to cause mitochondrial dysfunction and neurotoxicity." Proc Natl Acad Sci U S A **102**(51): 18694-9.

Chapman, P. F., G. L. White, et al. (1999). "Impaired synaptic plasticity and learning in aged amyloid precursor protein transgenic mice." Nat Neurosci **2**(3): 271-6.

Chen, Y., U. Beffert, et al. (2005). "Reelin modulates NMDA receptor activity in cortical neurons." J Neurosci **25**(36): 8209-16.

Christensen, E. I., J. O. Moskaug, et al. (1999). "Evidence for an essential role of megalin in transepithelial transport of retinol." J Am Soc Nephrol **10**(4): 685-95.

Cirrito, J. R., K. A. Yamada, et al. (2005). "Synaptic activity regulates interstitial fluid amyloid-beta levels in vivo." Neuron **48**(6): 913-22.

Corder, E. H., A. M. Saunders, et al. (1993). "Gene dose of apolipoprotein E type 4 allele and the risk of Alzheimer's disease in late onset families." Science **261**(5123): 921-3.

Cull-Candy, S. G. and D. N. Leszkiewicz (2004). "Role of distinct NMDA receptor subtypes at central synapses." Sci STKE **2004**(255): re16.

D'Arcangelo, G., R. Homayouni, et al. (1999). "Reelin is a ligand for lipoprotein receptors." Neuron **24**(2): 471-9.

D'Arcangelo, G., G. G. Miao, et al. (1995). "A protein related to extracellular matrix proteins deleted in the mouse mutant reeler." Nature **374**(6524): 719-23.

Davies, C. A., D. M. Mann, et al. (1987). "A quantitative morphometric analysis of the neuronal and synaptic content of the frontal and temporal cortex in patients with Alzheimer's disease." J Neurol Sci **78**(2): 151-64.

De Felice, F. G., P. T. Velasco, et al. (2007). "Abeta oligomers induce neuronal oxidative stress through an N-methyl-D-aspartate receptor-dependent mechanism that is blocked by the Alzheimer drug memantine." J Biol Chem **282**(15): 11590-601.

De Strooper, B. (2007). "Loss-of-function presenilin mutations in Alzheimer disease. Talking Point on the role of presenilin mutations in Alzheimer disease." EMBO Rep **8**(2): 141-6.

Del Rio, J. A., B. Heimrich, et al. (1997). "A role for Cajal-Retzius cells and reelin in the development of hippocampal connections." Nature **385**(6611): 70-4.

Dietschy, J. M. and S. D. Turley (2001). "Cholesterol metabolism in the brain." Curr Opin Lipidol **12**(2): 105-12.

Drakew, A., M. Frotscher, et al. (1998). "Developmental distribution of a reeler gene-related antigen in the rat hippocampal formation visualized by CR-50 immunocytochemistry." Neuroscience **82**(4): 1079-86.

Dull, T., R. Zufferey, et al. (1998). "A third-generation lentivirus vector with a conditional packaging system." J Virol **72**(11): 8463-71.

Fitzjohn, S. M., R. A. Morton, et al. (2001). "Age-related impairment of synaptic transmission but normal long-term potentiation in transgenic mice that overexpress the human APP695SWE mutant form of amyloid precursor protein." J Neurosci **21**(13): 4691-8.

Ghosh, A. and M. E. Greenberg (1995). "Calcium signaling in neurons: molecular mechanisms and cellular consequences." Science **268**(5208): 239-47.

Gordon, I., E. Grauer, et al. (1995). "Memory deficits and cholinergic impairments in apolipoprotein E-deficient mice." Neurosci Lett **199**(1): 1-4.

Gotthardt, M., M. Trommsdorff, et al. (2000). "Interactions of the low density lipoprotein receptor gene family with cytosolic adaptor and scaffold proteins suggest diverse biological functions in cellular communication and signal transduction." J Biol Chem **275**(33): 25616-24.

Groc, L., D. Choquet, et al. (2007). "NMDA receptor surface trafficking and synaptic subunit composition are developmentally regulated by the extracellular matrix protein Reelin." J Neurosci **27**(38): 10165-75.

Hallett, P. J., R. Spoelgen, et al. (2006). "Dopamine D1 activation potentiates striatal NMDA receptors by tyrosine phosphorylation-dependent subunit trafficking." J Neurosci **26**(17): 4690-700.

Hardingham, G. E., F. J. Arnold, et al. (2001). "A calcium microdomain near NMDA receptors: on switch for ERK-dependent synapse-to-nucleus communication." Nat Neurosci **4**(6): 565-6.

Hardingham, G. E., F. J. Arnold, et al. (2001). "Nuclear calcium signaling controls CREB-mediated gene expression triggered by synaptic activity." Nat Neurosci **4**(3): 261-7.

Hardingham, G. E. and H. Bading (2003). "The Yin and Yang of NMDA receptor signalling." Trends Neurosci **26**(2): 81-9.

Harris, F. M., W. J. Brecht, et al. (2003). "Carboxyl-terminal-truncated apolipoprotein E4 causes Alzheimer's disease-like neurodegeneration and behavioral deficits in transgenic mice." Proc Natl Acad Sci U S A **100**(19): 10966-71.

Heeren, J., T. Grewal, et al. (2001). "Recycling of apolipoprotein E and lipoprotein lipase through endosomal compartments in vivo." J Biol Chem **276**(45): 42333-8.

Heeren, J., T. Grewal, et al. (2004). "Impaired recycling of apolipoprotein E4 is associated with intracellular cholesterol accumulation." J Biol Chem **279**(53): 55483-92.

Heeren, J., T. Grewal, et al. (2003). "Recycling of apoprotein E is associated with cholesterol efflux and high density lipoprotein internalization." J Biol Chem **278**(16): 14370-8.

Heeren, J., W. Weber, et al. (1999). "Intracellular processing of endocytosed triglyceride-rich lipoproteins comprises both recycling and degradation." J Cell Sci **112 (Pt 3)**: 349-59.

Herz, J. and H. H. Bock (2002). "Lipoprotein receptors in the nervous system." Annu Rev Biochem **71**: 405-34.

Herz, J. and Y. Chen (2006). "Reelin, lipoprotein receptors and synaptic plasticity." Nat Rev Neurosci **7**(11): 850-9.

Herz, J., J. L. Goldstein, et al. (1991). "39-kDa protein modulates binding of ligands to low density lipoprotein receptor-related protein/alpha 2-macroglobulin receptor." J Biol Chem **266**(31): 21232-8.

Hesse, C., H. Larsson, et al. (2000). "Measurement of apolipoprotein E (apoE) in cerebrospinal fluid." Neurochem Res **25**(4): 511-7.

Hiesberger, T., M. Trommsdorff, et al. (1999). "Direct binding of Reelin to VLDL receptor and ApoE receptor 2 induces tyrosine phosphorylation of disabled-1 and modulates tau phosphorylation." Neuron **24**(2): 481-9.

Holscher, C., S. Gengler, et al. (2007). "Soluble beta-amyloid[25-35] reversibly impairs hippocampal synaptic plasticity and spatial learning." Eur J Pharmacol **561**(1-3): 85-90.

Holtzman, D. M., K. R. Bales, et al. (2000). "Apolipoprotein E isoform-dependent amyloid deposition and neuritic degeneration in a mouse model of Alzheimer's disease." Proc Natl Acad Sci U S A **97**(6): 2892-7.

Holtzman, D. M., R. E. Pitas, et al. (1995). "Low density lipoprotein receptor-related protein mediates apolipoprotein E-dependent neurite outgrowth in a central nervous system-derived neuronal cell line." Proc Natl Acad Sci U S A **92**(21): 9480-4.

Howell, B. W., F. B. Gertler, et al. (1997). "Mouse disabled (mDab1): a Src binding protein implicated in neuronal development." Embo J **16**(1): 121-32.

Howell, B. W., R. Hawkes, et al. (1997). "Neuronal position in the developing brain is regulated by mouse disabled-1." Nature **389**(6652): 733-7.

Howell, B. W., T. M. Herrick, et al. (1999). "Reelin-induced tyrosine [corrected] phosphorylation of disabled 1 during neuronal positioning." Genes Dev **13**(6): 643-8.

Howell, B. W., T. M. Herrick, et al. (2000). "Dab1 tyrosine phosphorylation sites relay positional signals during mouse brain development." Curr Biol **10**(15): 877-85.

Howell, B. W., L. M. Lanier, et al. (1999). "The disabled 1 phosphotyrosine-binding domain binds to the internalization signals of transmembrane glycoproteins and to phospholipids." Mol Cell Biol **19**(7): 5179-88.

Hsia, A. Y., E. Masliah, et al. (1999). "Plaque-independent disruption of neural circuits in Alzheimer's disease mouse models." Proc Natl Acad Sci U S A **96**(6): 3228-33.

Hsieh, H., J. Boehm, et al. (2006). "AMPAR removal underlies Abeta-induced synaptic depression and dendritic spine loss." Neuron **52**(5): 831-43.

Huang, Y., X. Q. Liu, et al. (2001). "Apolipoprotein E fragments present in Alzheimer's disease brains induce neurofibrillary tangle-like intracellular inclusions in neurons." Proc Natl Acad Sci U S A **98**(15): 8838-43.

Johnson, E. B., R. E. Hammer, et al. (2005). "Abnormal development of the apical ectodermal ridge and polysyndactyly in Megf7-deficient mice." Hum Mol Genet **14**(22): 3523-38.

Kamenetz, F., T. Tomita, et al. (2003). "APP processing and synaptic function." Neuron **37**(6): 925-37.

Kennedy, M. B. (2000). "Signal-processing machines at the postsynaptic density." Science **290**(5492): 750-4.

Kim, D. H., K. Magoori, et al. (1997). "Exon/intron organization, chromosome localization, alternative splicing, and transcription units of the human apolipoprotein E receptor 2 gene." J Biol Chem **272**(13): 8498-504.

Kitamura, H. W., H. Hamanaka, et al. (2004). "Age-dependent enhancement of hippocampal long-term potentiation in knock-in mice expressing human apolipoprotein E4 instead of mouse apolipoprotein E." Neurosci Lett **369**(3): 173-8.

Kutsuwada, T., N. Kashiwabuchi, et al. (1992). "Molecular diversity of the NMDA receptor channel." Nature **358**(6381): 36-41.

Lacor, P. N., M. C. Buniel, et al. (2004). "Synaptic targeting by Alzheimer's-related amyloid beta oligomers." J Neurosci **24**(45): 10191-200.

Lambert, M. P., A. K. Barlow, et al. (1998). "Diffusible, nonfibrillar ligands derived from Abeta1-42 are potent central nervous system neurotoxins." Proc Natl Acad Sci U S A **95**(11): 6448-53.

Lisman, J., H. Schulman, et al. (2002). "The molecular basis of CaMKII function in synaptic and behavioural memory." Nat Rev Neurosci **3**(3): 175-90.

Lisman, J. E., J. M. Fellous, et al. (1998). "A role for NMDA-receptor channels in working memory." Nat Neurosci **1**(4): 273-5.

Lisman, J. E. and A. M. Zhabotinsky (2001). "A model of synaptic memory: a CaMKII/PP1 switch that potentiates transmission by organizing an AMPA receptor anchoring assembly." Neuron **31**(2): 191-201.

Liu, Q., C. V. Zerbinatti, et al. (2007). "Amyloid precursor protein regulates brain apolipoprotein E and cholesterol metabolism through lipoprotein receptor LRP1." Neuron **56**(1): 66-78.

Lleo, A., S. M. Greenberg, et al. (2006). "Current pharmacotherapy for Alzheimer's disease." Annu Rev Med **57**: 513-33.

Lynch, G., J. Larson, et al. (1983). "Intracellular injections of EGTA block induction of hippocampal long-term potentiation." Nature **305**(5936): 719-21.

Ma, J., A. Yee, et al. (1994). "Amyloid-associated proteins alpha 1-antichymotrypsin and apolipoprotein E promote assembly of Alzheimer beta-protein into filaments." Nature **372**(6501): 92-4.

Mahley, R. W. and Y. Huang (2006). "Apolipoprotein (apo) E4 and Alzheimer's disease: unique conformational and biophysical properties of apoE4 can modulate neuropathology." Acta Neurol Scand Suppl **185**: 8-14.

Mahley, R. W., T. L. Innerarity, et al. (1984). "Plasma lipoproteins: apolipoprotein structure and function." J Lipid Res **25**(12): 1277-94.

Malenka, R. C. (2003). "The long-term potential of LTP." Nat Rev Neurosci **4**(11): 923-6.

Manabe, T., A. Aiba, et al. (2000). "Regulation of long-term potentiation by H-Ras through NMDA receptor phosphorylation." J Neurosci **20**(7): 2504-11.

Marino, M. J., S. T. Rouse, et al. (1998). "Activation of the genetically defined m1 muscarinic receptor potentiates N-methyl-D-aspartate (NMDA) receptor currents in hippocampal pyramidal cells." Proc Natl Acad Sci U S A **95**(19): 11465-70.

Marschang, P., J. Brich, et al. (2004). "Normal development and fertility of knockout mice lacking the tumor suppressor gene LRP1b suggest functional compensation by LRP1." Mol Cell Biol **24**(9): 3782-93.

Masliah, E., M. Mallory, et al. (1995). "Neurodegeneration in the central nervous system of apoE-deficient mice." Exp Neurol **136**(2): 107-22.

Mauch, D. H., K. Nagler, et al. (2001). "CNS synaptogenesis promoted by glia-derived cholesterol." Science **294**(5545): 1354-7.

May, P., A. Rohlmann, et al. (2004). "Neuronal LRP1 functionally associates with postsynaptic proteins and is required for normal motor function in mice." Mol Cell Biol **24**(20): 8872-83.

Mensenkamp, A. R., M. C. Jong, et al. (1999). "Apolipoprotein E participates in the regulation of very low density lipoprotein-triglyceride secretion by the liver." J Biol Chem **274**(50): 35711-8.

Moechars, D., I. Dewachter, et al. (1999). "Early phenotypic changes in transgenic mice that overexpress different mutants of amyloid precursor protein in brain." J Biol Chem **274**(10): 6483-92.

Monyer, H., N. Burnashev, et al. (1994). "Developmental and regional expression in the rat brain and functional properties of four NMDA receptors." Neuron **12**(3): 529-40.

Morimura, T., M. Hattori, et al. (2005). "Disabled1 regulates the intracellular trafficking of reelin receptors." J Biol Chem **280**(17): 16901-8.

Mulkey, R. M. and R. C. Malenka (1992). "Mechanisms underlying induction of homosynaptic long-term depression in area CA1 of the hippocampus." Neuron **9**(5): 967-75.

Nada, S., T. Shima, et al. (2003). "Identification of PSD-93 as a substrate for the Src family tyrosine kinase Fyn." J Biol Chem **278**(48): 47610-21.

Naldini, L., U. Blomer, et al. (1996). "In vivo gene delivery and stable transduction of nondividing cells by a lentiviral vector." Science **272**(5259): 263-7.

Niu, S., A. Renfro, et al. (2004). "Reelin promotes hippocampal dendrite development through the VLDLR/ApoER2-Dab1 pathway." Neuron **41**(1): 71-84.

Nowak, L., P. Bregestovski, et al. (1984). "Magnesium gates glutamate-activated channels in mouse central neurones." Nature **307**(5950): 462-5.

Palop, J. J., J. Chin, et al. (2006). "A network dysfunction perspective on neurodegenerative diseases." Nature **443**(7113): 768-73.

Palop, J. J., J. Chin, et al. (2007). "Aberrant excitatory neuronal activity and compensatory remodeling of inhibitory hippocampal circuits in mouse models of Alzheimer's disease." Neuron **55**(5): 697-711.

Pelkey, K. A., R. Askalan, et al. (2002). "Tyrosine phosphatase STEP is a tonic brake on induction of long-term potentiation." Neuron **34**(1): 127-38.

Pesold, C., F. Impagnatiello, et al. (1998). "Reelin is preferentially expressed in neurons synthesizing gamma-aminobutyric acid in cortex and hippocampus of adult rats." Proc Natl Acad Sci U S A **95**(6): 3221-6.

Pesold, C., W. S. Liu, et al. (1999). "Cortical bitufted, horizontal, and Martinotti cells preferentially express and secrete reelin into perineuronal nets, nonsynaptically modulating gene expression." Proc Natl Acad Sci U S A **96**(6): 3217-22.

Pfrieger, F. W. and B. A. Barres (1997). "Synaptic efficacy enhanced by glial cells in vitro." Science **277**(5332): 1684-7.

Qiu, S., K. M. Korwek, et al. (2006). "Cognitive disruption and altered hippocampus synaptic function in Reelin haploinsufficient mice." Neurobiol Learn Mem **85**(3): 228-42.

Qiu, S. and E. J. Weeber (2007). "Reelin signaling facilitates maturation of CA1 glutamatergic synapses." J Neurophysiol **97**(3): 2312-21.

Qiu, S., L. F. Zhao, et al. (2006). "Differential reelin-induced enhancement of NMDA and AMPA receptor activity in the adult hippocampus." J Neurosci **26**(50): 12943-55.

Ramos-Moreno, T., M. J. Galazo, et al. (2006). "Extracellular matrix molecules and synaptic plasticity: immunomapping of intracellular and secreted Reelin in the adult rat brain." Eur J Neurosci **23**(2): 401-22.

Rellin, L., J. Heeren, et al. (2008). "Recycling of apolipoprotein E is not associated with cholesterol efflux in neuronal cells." Biochim Biophys Acta **1781**(5): 232-8.

Roche, K. W., S. Standley, et al. (2001). "Molecular determinants of NMDA receptor internalization." Nat Neurosci **4**(8): 794-802.

Rubinson, D. A., C. P. Dillon, et al. (2003). "A lentivirus-based system to functionally silence genes in primary mammalian cells, stem cells and transgenic mice by RNA interference." Nat Genet **33**(3): 401-6.

Salter, M. W. and L. V. Kalia (2004). "Src kinases: a hub for NMDA receptor regulation." Nat Rev Neurosci **5**(4): 317-28.

Sanan, D. A., K. H. Weisgraber, et al. (1994). "Apolipoprotein E associates with beta amyloid peptide of Alzheimer's disease to form novel monofibrils. Isoform apoE4 associates more efficiently than apoE3." J Clin Invest **94**(2): 860-9.

Schmechel, D. E., A. M. Saunders, et al. (1993). "Increased amyloid beta-peptide deposition in cerebral cortex as a consequence of apolipoprotein E genotype in late-onset Alzheimer disease." Proc Natl Acad Sci U S A **90**(20): 9649-53.

Schmidt, V., A. Sporbert, et al. (2007). "SorLA/LR11 regulates processing of amyloid precursor protein via interaction with adaptors GGA and PACS-1." J Biol Chem **282**(45): 32956-64.

Selkoe, D. J. (2000). "The origins of Alzheimer disease: a is for amyloid." JAMA **283**(12): 1615-7.

Shankar, G. M., B. L. Bloodgood, et al. (2007). "Natural oligomers of the Alzheimer amyloid-beta protein induce reversible synapse loss by modulating an NMDA-type glutamate receptor-dependent signaling pathway." J Neurosci **27**(11): 2866-75.

Shaywitz, A. J. and M. E. Greenberg (1999). "CREB: a stimulus-induced transcription factor activated by a diverse array of extracellular signals." Annu Rev Biochem **68**: 821-61.

Sheldon, M., D. S. Rice, et al. (1997). "Scrambler and yotari disrupt the disabled gene and produce a reeler-like phenotype in mice." Nature **389**(6652): 730-3.

Sheng, M., J. Cummings, et al. (1994). "Changing subunit composition of heteromeric NMDA receptors during development of rat cortex." Nature **368**(6467): 144-7.

Shieh, P. B., S. C. Hu, et al. (1998). "Identification of a signaling pathway involved in calcium regulation of BDNF expression." Neuron **20**(4): 727-40.

Sinagra, M., D. Verrier, et al. (2005). "Reelin, very-low-density lipoprotein receptor, and apolipoprotein E receptor 2 control somatic NMDA receptor composition during hippocampal maturation in vitro." J Neurosci **25**(26): 6127-36.

Snyder, E. M., Y. Nong, et al. (2005). "Regulation of NMDA receptor trafficking by amyloid-beta." Nat Neurosci **8**(8): 1051-8.

Stockinger, W., C. Brandes, et al. (2000). "The reelin receptor ApoER2 recruits JNK-interacting proteins-1 and -2." J Biol Chem **275**(33): 25625-32.

Stolt, P. C., H. Jeon, et al. (2003). "Origins of peptide selectivity and phosphoinositide binding revealed by structures of disabled-1 PTB domain complexes." Structure **11**(5): 569-79.

Stolt, P. C., D. Vardar, et al. (2004). "The dual-function disabled-1 PTB domain exhibits site independence in binding phosphoinositide and peptide ligands." Biochemistry **43**(34): 10979-87.

Strasser, V., D. Fasching, et al. (2004). "Receptor clustering is involved in Reelin signaling." Mol Cell Biol **24**(3): 1378-86.

Strickland, D. K., J. D. Ashcom, et al. (1990). "Sequence identity between the alpha 2-macroglobulin receptor and low density lipoprotein receptor-related protein suggests that this molecule is a multifunctional receptor." J Biol Chem **265**(29): 17401-4.

Strittmatter, W. J., A. M. Saunders, et al. (1993). "Apolipoprotein E: high-avidity binding to beta-amyloid and increased frequency of type 4 allele in late-onset familial Alzheimer disease." Proc Natl Acad Sci U S A **90**(5): 1977-81.

Sullivan, P. M., B. E. Mace, et al. (2004). "Marked regional differences of brain human apolipoprotein E expression in targeted replacement mice." Neuroscience **124**(4): 725-33.

Sun, Y., S. Wu, et al. (1998). "Glial fibrillary acidic protein-apolipoprotein E (apoE) transgenic mice: astrocyte-specific expression and differing biological effects of astrocyte-secreted apoE3 and apoE4 lipoproteins." J Neurosci **18**(9): 3261-72.

Sze, C. I., J. C. Troncoso, et al. (1997). "Loss of the presynaptic vesicle protein synaptophysin in hippocampus correlates with cognitive decline in Alzheimer disease." J Neuropathol Exp Neurol **56**(8): 933-44.

Takasu, M. A., M. B. Dalva, et al. (2002). "Modulation of NMDA receptor-dependent calcium influx and gene expression through EphB receptors." Science **295**(5554): 491-5.

Tang, T. S., H. Tu, et al. (2003). "Huntingtin and huntingtin-associated protein 1 influence neuronal calcium signaling mediated by inositol-(1,4,5) triphosphate receptor type 1." Neuron **39**(2): 227-39.

Tao, X., S. Finkbeiner, et al. (1998). "Ca2+ influx regulates BDNF transcription by a CREB family transcription factor-dependent mechanism." Neuron **20**(4): 709-26.

Taubenfeld, S. M., M. H. Milekic, et al. (2001). "The consolidation of new but not reactivated memory requires hippocampal C/EBPbeta." Nat Neurosci **4**(8): 813-8.

Terry, R. D., E. Masliah, et al. (1991). "Physical basis of cognitive alterations in Alzheimer's disease: synapse loss is the major correlate of cognitive impairment." Ann Neurol **30**(4): 572-80.

Tissir, F. and A. M. Goffinet (2003). "Reelin and brain development." Nat Rev Neurosci **4**(6): 496-505.

Townsend, M., G. M. Shankar, et al. (2006). "Effects of secreted oligomers of amyloid beta-protein on hippocampal synaptic plasticity: a potent role for trimers." J Physiol **572**(Pt 2): 477-92.

Trommer, B. L., C. Shah, et al. (2004). "ApoE isoform affects LTP in human targeted replacement mice." Neuroreport **15**(17): 2655-8.

Trommsdorff, M., J. P. Borg, et al. (1998). "Interaction of cytosolic adaptor proteins with neuronal apolipoprotein E receptors and the amyloid precursor protein." J Biol Chem **273**(50): 33556-60.

Trommsdorff, M., M. Gotthardt, et al. (1999). "Reeler/Disabled-like disruption of neuronal migration in knockout mice lacking the VLDL receptor and ApoE receptor 2." Cell **97**(6): 689-701.

Valastro, B., O. Ghribi, et al. (2001). "AMPA receptor regulation and LTP in the hippocampus of young and aged apolipoprotein E-deficient mice." Neurobiol Aging **22**(1): 9-15.

Vissel, B., J. J. Krupp, et al. (2001). "A use-dependent tyrosine dephosphorylation of NMDA receptors is independent of ion flux." Nat Neurosci **4**(6): 587-96.

Walsh, D. M., I. Klyubin, et al. (2002). "Naturally secreted oligomers of amyloid beta protein potently inhibit hippocampal long-term potentiation in vivo." Nature **416**(6880): 535-9.

Walsh, D. M. and D. J. Selkoe (2007). "A beta oligomers - a decade of discovery." J Neurochem **101**(5): 1172-84.

Wang, Y. T. and M. W. Salter (1994). "Regulation of NMDA receptors by tyrosine kinases and phosphatases." Nature **369**(6477): 233-5.

Wang, Y. T., X. M. Yu, et al. (1996). "Ca(2+)-independent reduction of N-methyl-D-aspartate channel activity by protein tyrosine phosphatase." Proc Natl Acad Sci U S A **93**(4): 1721-5.

Weeber, E. J., U. Beffert, et al. (2002). "Reelin and ApoE receptors cooperate to enhance hippocampal synaptic plasticity and learning." J Biol Chem **277**(42): 39944-52.

Weisgraber, K. H. and R. W. Mahley (1996). "Human apolipoprotein E: the Alzheimer's disease connection." FASEB J **10**(13): 1485-94.

Wenzel, A., J. M. Fritschy, et al. (1997). "NMDA receptor heterogeneity during postnatal development of the rat brain: differential expression of the NR2A, NR2B, and NR2C subunit proteins." J Neurochem **68**(2): 469-78.

Willnow, T. E. (1998). "Receptor-associated protein (RAP): a specialized chaperone for endocytic receptors." Biol Chem **379**(8-9): 1025-31.

Willnow, T. E., J. Hilpert, et al. (1996). "Defective forebrain development in mice lacking gp330/megalin." Proc Natl Acad Sci U S A **93**(16): 8460-4.

Xu, Q., A. Bernardo, et al. (2006). "Profile and regulation of apolipoprotein E (ApoE) expression in the CNS in mice with targeting of green fluorescent protein gene to the ApoE locus." J Neurosci **26**(19): 4985-94.

Yaka, R., D. Y. He, et al. (2003). "Pituitary adenylate cyclase-activating polypeptide (PACAP(1-38)) enhances N-methyl-D-aspartate receptor function and brain-derived neurotrophic factor expression via RACK1." J Biol Chem **278**(11): 9630-8.

Yankner, B. A., L. K. Duffy, et al. (1990). "Neurotrophic and neurotoxic effects of amyloid beta protein: reversal by tachykinin neuropeptides." Science **250**(4978): 279-82.

Ye, S., Y. Huang, et al. (2005). "Apolipoprotein (apo) E4 enhances amyloid beta peptide production in cultured neuronal cells: apoE structure as a potential therapeutic target." Proc Natl Acad Sci U S A **102**(51): 18700-5.

Yu, X. M., R. Askalan, et al. (1997). "NMDA channel regulation by channel-associated protein tyrosine kinase Src." Science **275**(5300): 674-8.

Yun, M., L. Keshvara, et al. (2003). "Crystal structures of the Dab homology domains of mouse disabled 1 and 2." J Biol Chem **278**(38): 36572-81.

Zhang, S. J., M. N. Steijaert, et al. (2007). "Decoding NMDA receptor signaling: identification of genomic programs specifying neuronal survival and death." Neuron **53**(4): 549-62.

Zheng, G., D. R. Bachinsky, et al. (1994). "Organ distribution in rats of two members of the low-density lipoprotein receptor gene family, gp330 and LRP/alpha 2MR, and the receptor-associated protein (RAP)." J Histochem Cytochem **42**(4): 531-42.

Zola-Morgan, S. and L. R. Squire (1993). "Neuroanatomy of memory." Annu Rev Neurosci **16**: 547-63.